EVALUATION AND REDESIGN OF RADIATION SHIELDING IN A RADIONUCLIDE PRODUCTION FACILITY AT A PARTICLE ACCELERATOR

NORTH WEST UNIVERSITY
A33641200162935C

ONALENNA KEGOPOTSEMANG

NWU
IBRARY

Evaluation and Redesign of Radiation Shielding in a Radionuclide Production Facility at a Particle Accelerator

Onalenna Kegopotsemang

Dissertation submitted in partial fulfillment of the requirements for
the degree of *Magister Scientia* in Applied Radiation Science & Technology
at North West University (NWU).

2004

b11018161
LIBRARY
MAFIKENG CAMPUS
Call No.: TH 539.722 KEG
2005 -05- 09
Acc. No.: 05/5073
NORTH-WEST UNIVERSITY

Supervisor: Mr TJ van Rooyen

Evaluation and Redesign of Radiation Shielding in a Radionuclide Production Facility at a Particle Accelerator

Onalenna Kegopotsemang

Keywords

Hotcell

Hotcell shielding

Ionising radiation

Photon shielding

Radiation

Radiation protection

Radiation shielding

Radioisotope

Radionuclide

Radioisotope production

Radionuclide production

Shielding

Shielding Calculation

1115145 28

Abstract

iThemba LABS is a particle accelerator facility housing a radionuclide production facility that uses a 66 MeV proton beam to produce radionuclides for medical and industrial use. Ionising radiation is produced by a variety of sources at *iThemba LABS.*

Ionising radiation is a health hazard. High doses can cause acute radiation syndrome, i.e. "radiation sickness." Lower doses cannot cause acute symptom, but carry a risk of radiation-related cancer. Ionising radiation is also detrimental to materials, and can damage polymers and lubricants e.g.

Shielding is used to reduce radiation levels to values that should be safe for the intended level of human occupancy. Shield performance is vital to human health and the life expectancy of polymers and lubricants, so that quality management in shield design is very important. However, until 2003, there has been no formal system at *iThemba LABS* to evaluate and approve all radiation shield designs and layouts from a radiation protection perspective.

This study deals with evaluating and redesigning radiation shielding in the radionuclide production facility of *iThemba LABS*. There are several designs and layouts in the radionuclide production building of *iThemba LABS* that lead to unnecessary exposure of personnel to ionising radiation. The shielding in these areas are sub-standard.

Performance criteria for radiation shields are developed. Inadequate radiation shields are identified. The identified inadequate shields are: the processing hotcells, the target store room and the hotcells in the radiopharmaceutical dispensing laboratory. Point-kernel radiation shielding calculations are done to specify materials and material thicknesses that will adequately protect workers against ionising radiation.

Declaration

I hereby declare that the work contained in this dissertation is my own work and has not been submitted for a degree or other qualification in any other university.

Kego

Onalenna Kegopotsemang

Acknowledgements

I would like to express my sincere gratitude to the following people for making it possible for me to complete this thesis:

Mr TJ van Rooyen, my supervisor, for believing in me by giving me a project, for his guidance and support throughout this study.

iThemba LABS and NRF for financial assistance.

The Radiation Safety group—Mr Senoelo Pheto and Mr Patle Mohajane for their helpful and valuable suggestions.

My parents, family and friends for their emotional support and encouragement during my difficult times.

Finally to Almighty God who gave me strength and faith, "Modimo, o nnile le nna go fitlha fa."

NWU
LIBRARY

Abbreviations

ALARA..... As Low As Reasonably Achievable, i.e. the principle that radiation dose must be minimised, even when it is well below regulatory limits

CCC.....Computer Code Collection (of the RSICC)

CG..... Combinatorial Geometry

DNA..... Deoxyribonucleic acid

DR..... Dose rate

GP..... Geometric Progression

ICRP.....International Commission on Radiological Protection

LET..... Linear Energy Transfer

LNT.....Linear, No-Threshold hypothesis, i.e. the assumption that any radiation dose received, carries a health risk, which is linearly dependent on the dose in the low-dose region

MCNP..... Monte Carlo N-Particle Transport Code

ORNL..... Oak Ridge National Laboratories (USA)

QAD-CGGP.....A point-kernel photon transport code using the Geometric Progression (GP) buildup factor formalism, and Combinatorial Geometry (CG)

QM..... Quality Management

PEA..... Photo-electric absorption

PP..... Pair production

PTFE..... Polytetrafluoroethylene

RSICC..... Radiation Safety Information Computational Center (at ORNL, USA)

SSC.....Separated Sector Cyclotron

VBTS.....Vertical Beam Target Station for radionuclide production at *iThemba LABS*. To be completed in 2005.

Contents

Abstract iii

Declaration iv

Acknowledgements v

Abbreviations vi

1. **Introduction** 1
   - 1.1 Introduction to iThemba LABS 1
   - 1.2 Categories of ionising radiation 2
   - 1.3 Ionising radiation at iThemba LABS 4
   - 1.4 Biological effects of ionising radiation 4
   - 1.5 Stochastic and deterministic effects of ionising radiation 6
   - 1.6 Effects of ionising radiation on polymers 9
   - 1.7 Photon shielding mechanisms 10
   - 1.8 Quality management in radiation shield design 13
   - 1.9 Research objectives 14
   - 1.10 Structure of this study 14

2. **Radiation Hazards at the Radionuclide Production Facility at *iThemba LABS*** 15
   - 2.1 The cyclotrons at *iThemba LABS* — overview 15
   - 2.2 The radionuclide production facility at *iThemba LABS* 17
   - 2.3 Radionuclides produced at the Radionuclide Production facility of *iThemba LABS* 23
   - 2.4 Selection of radionuclide and activity for radiation shielding calculations 28

3. **Overview of point-kernel photon shielding calculation methods** 31

4. **Evaluation of existing shields in the Radionuclide Production Facility** 33
   - 4.1 Dose limits 33
   - 4.2 Radiation shielding performance concepts 36

4.3 Evaluation of existing radiation shields with the aim to identify inadequate shields..... 38
4.4 Conclusions..... 60

5. Plan for upgrading the production facilities of the Radionuclide Production Group..... 61
5.1 Introduction..... 61
5.2 Planned upgrade to radionuclide production facilities..... 61
5.3 Methodology for upgrading radiation shielding..... 62
5.4 The processing hotcell facility..... 63
5.5 The target store-room facility..... 63
5.6 The dispensing facility for radioactive pharmaceuticals..... 63
5.7 Summary..... 64

6. Design calculations for improved radiation shielding in the Radionuclide Production Facility..... 65
6.1 Introduction..... 65
6.2 Shield design for the processing hotcells..... 65
6.3 Shield design calculations for the Radio-pharmaceutical dispensing laboratory..... 76
6.4 Shield design calculations for the Target Store room..... 79

7. Conclusions and recommendations..... 85

Appendix A: MathCAD worksheet for simple point-kernel shielding calculations..... 86

Bibliography..... 87

Chapter 1
Introduction

1.1 Introduction to *iThemba LABS*

The *iThemba Laboratory for Accelerator-Based Sciences (iThemba LABS)* is a multi-disciplinary research laboratory near Cape Town in South Africa. It provides facilities for:

- Basic & applied research using accelerated particle beams;
- Radiotherapy for the treatment of cancer;
- The supply of accelerator-produced radioactive isotopes for nuclear medicine and research.

An air photograph of *iThemba LABS* is shown in Figure 1.1.



Figure 1.1: *iThemba LABS from the air. Photograph taken in winter of 1991. The town Somerset West is visible in the distant background, against the Helderberg mountains.*

Figure 1.2 shows the location of *iThemba LABS* relative to neighbouring areas, roads and landmarks in the Western Cape.

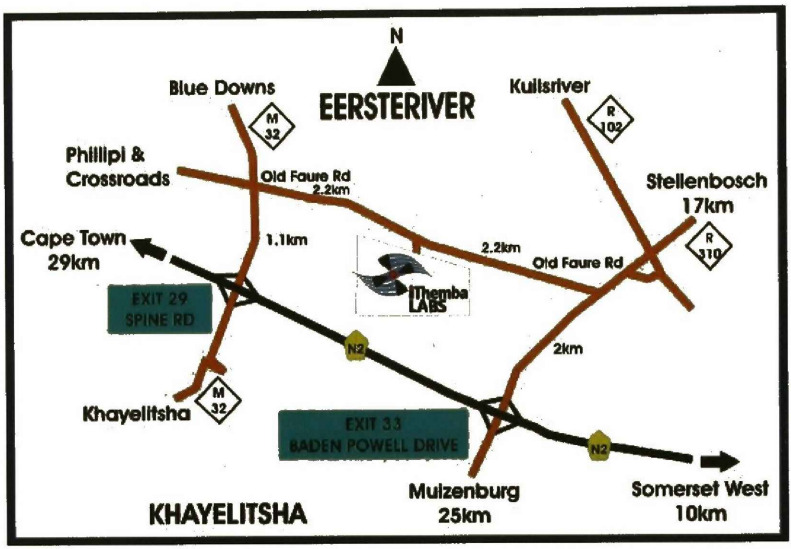


Figure 1.2: *Location of iThemba LABS in Western Cape province of South Africa, near Cape Town, Somerset West, Khayelitsha, Eersterivier and Stellenbosch.*

Activities at *iThemba LABS* are based around four sub-atomic particle accelerators. The large separated sector cyclotron (SSC) accelerates protons to energies up to 200 MeV, and heavier nuclear particles to much higher energies. Charged particles to be accelerated are fed into the SSC via one of two smaller injector cyclotrons, one providing intense beams of light ions, and the other, beams of polarized light ions or heavy ions. The fourth accelerator at *iThemba LABS* is a 6 MV Van de Graaff electrostatic accelerator. *iThemba LABS* brings together scientists working in the physical, medical and biological sciences. The facilities provide for modern research, advanced education, the treatment of cancers, and the production of unique radionuclides.

1.2 Categories of ionising radiation

Ionising radiation is biologically dangerous, and can also damage irradiated materials, especially polymers used in seals, vacuum pipes and coolant water pipes. The following types of ionising radiation of importance are produced at a proton accelerator such as *iThemba LABS.* Each type of ionising radiation has different characteristics and behaviour.

- **Beta particles** come in two types: (1) high speed electrons, denoted as β^--particles, and (2) high speed antiparticles of the electron, i.e. positively charged positrons, symbol: β^+. Nuclei are only stable if they have the correct $\frac{\text{neutron}}{\text{proton}}$ ratio. If the $\frac{\text{neutron}}{\text{proton}}$ ratio is too large for nuclear stability, i.e. if the nucleus is "neutron-rich," it undergoes a β^--transition to gain stability; a β^--particle is emitted in the process. If the $\frac{\text{neutron}}{\text{proton}}$ ratio is too small for nuclear stability, i.e. if the nucleus is

"neutron-poor," it can undergo a β^+-transition to gain stability; a β^+-particle is emitted in the process.

Upon the matter/antimatter annihilation of the β^+-particle with an electron, two 0.511 MeV annihilation photons are produced.

There is a higher inventory of β^+-emitters than β^--emitters at a proton accelerator such as *iThemba LABS,* because neutron-poor, proton-rich isotopes are produced when target nuclei absorb incident protons in nuclear reactions. As a result, 0.511 MeV gamma-rays are emitted by almost all radionuclides produced at a proton accelerator.

A sheet of aluminium a few millimetres thick can stop beta particles. While beta particles are slowed down, *bremsstrahlung* X-rays are emitted. *Bremsstrahlung* are ionising photons emitted when charged particles are slowed down. If a charged particle enters the vicinity of an atomic nucleus, it will be deflected from its original direction, and slowed down, by the electric field of the nucleus. This causes rapid deceleration. When a charged particle is decelerated, it emits ionising photons known as *bremsstrahlung* ("braking radiation"). This process by which charged particles lose energy and slow down, is called ***radiative slowing down***. The faster the deceleration, the more *bremsstrahlung* is produced. The intensity I of bremsstrahlung production is given by

$$I \propto \frac{z^2 Z^2}{m^2} \tag{1.1}$$

where z is the charge of the projectile, m is its mass and Z is the atomic number of the medium. Equation (1.1) contains the following information about *bremsstrahlung* production and radiative slowing down: (1) *Bremsstrahlung* production and radiation slowing down does not play a significant role for heavy charged particles, as a result of the $1/m^2$ term; (2) the slowing down of charged particles in a medium with a high atomic number Z will produce much more *bremsstrahlung* compared to a medium with a low Z, on account of the Z^2 term. This explains why low-Z materials such as aluminium ($Z = 13$) are used to shield beta radiation with minimal *bremsstrahlung* production. Aluminium produces $\left(\frac{82}{13}\right)^2 \approx 40$ times less *bremsstrahlung* than lead ($Z = 82$).

Bremsstrahlung is classified as a type of X-ray; its energy distribution is continuous (unlike the sharp energies at which characteristic X-rays are emitted).

- **Ionising photons** are high energy electromagnetic radiation with high penetrating ability. Dense materials with high atomic numbers (Z) and high mass density (ρ) such as lead can absorb these rays most effectively.

- **Neutrons** are one of the constituents of the nucleus and do not carry any electric charge. They are produced by (p, xn) type nuclear reactions at a proton accelerator facility. Hydrogen-rich materials, such as water or paraffin can shield well against low-energy neutrons ($E \lesssim 3$ MeV), while materials such as iron are required to shield higher-energy neutrons well. In practice, very thick concrete shielding is used to shield neutrons, because concrete is relatively cheap.

1.3 Ionising radiation at *iThemba LABS*

Ionising radiation is produced when the particle beam produced by a cyclotron, strikes materials. When the proton beam produced at *iThemba LABS,* strikes objects such as radionuclide production targets, nuclear reactions will take place. These nuclear reactions will produce unstable, i.e. radioactive nuclides in the material hit by the primary particle beam. Neutrons will also be produced when the particles in the primary beam are involved in nuclear reactions. These neutrons have a large range and will dominate the radiation field when the beam hits the target. A large fraction of these neutrons will escape from the target they are produced in, will travel through materials, and will cause nuclear reactions and, therefore, the production of radioactive nuclides in all materials that they hit. The result is that ionising radiation will not only be present during beam production, but also when the beam is off, because of the radioactive nuclides produced by nuclear reactions of secondary neutrons.

1.4 Biological effects of ionising radiation

Linear Energy Transfer (LET)

The average energy deposited along the track of the particle per unit length depends on the type of particle and its energy and is called the *linear energy transfer* (LET) of the particle,

$$\text{LET} = \frac{dE}{dl}$$

where E is the energy of the radiation and l denotes path length. Thus, a sparsely ionising radiation producing few events per micron of track, is known as a **low-LET** radiation. X-rays and γ-photons are low-LET radiation. Radiations that produce dense ionisations along the track are known as **high-LET** radiation. Alpha particles, heavy ions, protons and recoil nuclei from neutron scattering events are all **high-LET** radiation.

Figure 1.3 illustrates different LET values for different charged particles of the same incident energy.

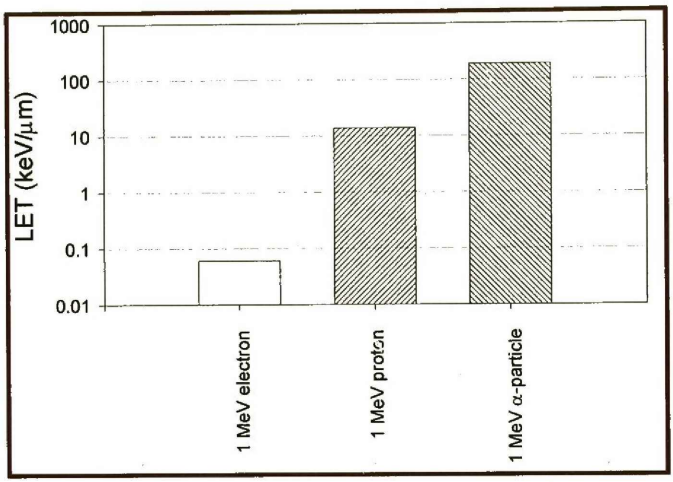


Figure 1.3: *Linear energy transfer (LET) values for different charged particles in human tissue. A 1 MeV electron has a LET of 0.06 keV/µm; a 1 MeV proton has a LET of about 14 keV/µm and a 1 MeV alpha particle has a LET of about 180 keV/µm. Alpha particles are classified as high-LET radiation while electrons are low-LET radiation.*

Direct and indirect damage by ionising radiation

Ionising radiation can damage the DNA in biological cells, produce free radicals and disrupt chemical bonds. Damage to DNA is the most critical effect of low-level ionising radiation. The effect can be direct or indirect. Consider the following example: Water (H_2O) is by far the most common molecule in the human body. Suppose that a photon undergoes scattering off a hydrogen atom in the water medium inside a cell. The electron is dislodged when the photon is absorbed, and the hydrogen atom is ionised. Damage can now take place by the direct effect or the indirect effect:

- **Direct effect:** The dislodged electron itself interacts with the DNA;
- **Indirect effect:** The dislodged electron interacts with a molecule of water to give rise to free radicals, peroxides or singlet-oxygen, which do the damage to the DNA.

As a result of the prevalence of water in cells, the indirect effect is more common than the direct effect for low-LET radiation types such as ionising photons and β-particles. The direct effect is more important for high-LET radiation types such as neutrons and α-particles.

1.5 Stochastic and deterministic effects of ionising radiation

The effects of ionising radiation may be divided into two categories: **deterministic** and **stochastic** effects.

Deterministic effects of ionising radiation occur as a result of the *death of cells*. Cell death occurs by means of necrosis or apoptosis. If the dose and dose rate are large enough, so many cells will die that the tissue can no longer function properly. This type of radiation effect has a dose *threshold:* doses lower than the threshold value have no deterministic effects. For doses above the threshold, the *seriousness of the effects depends on the magnitude of the dose.* The *dose rate* is also important: at low dose rates, cell repair and re-population can keep up with the rate of radiation-induced damage; at high dose rates, repair and repopulation can not keep up with the rate of damage and destruction. As a result, the severity of deterministic effects depends strongly on the *dose rate*. The dose threshold for deterministic effects is much higher than doses met in normal radiation protection practice, so that deterministic effects will only become manifested after accidental massive overexposure. Examples of deterministic effects are *acute radiation syndrome*, i.e. blood disorders, eye disorders, infertility, nausea, loss of hair, reddening of the skin, fatigue and lethargy.

Stochastic effects of ionising radiation occur when radiation does not kill cells, but *modifies* their genetic material. When the cell divides, the modification may be carried over to the daughter cells. A modified cell may, after a so-called period of latency, develop into a *cancer cell,* i.e. a cell that performs no useful function and multiplies unrestrictedly. The term "stochastic" means that the process is governed by the laws of probability. The severity of the cancer is independent of the dose, but the probability of developing cancer is proportional to the dose received. The *linear no threshold* (LNT) assumption states that *no dose threshold* applies to the occurrence of stochastic effects. The rate at which a dose is received, does not influence its stochastic effects significantly. If the damage is manifested in a gamete (i.e. a male sperm cell or a female egg cell), the radiation damage may be transmitted to the descendants of the person who had received the radiation dose. *Radiation induced cancer* and *heritable ill health* are two important classes of the stochastic effects of ionising radiation. It is characteristic of a stochastic effect that it may only become manifested many years after a person has received the dose.

The crucial differences between the deterministic and stochastic effects of ionising radiation are summarised in Table 1.1.

Table 1.1: Deterministic and Stochastic effects of ionising radiation.

Deterministic effects	Stochastic effects
Caused by the death of cells	Caused by changes in cells that do not die
There is a clear, unambiguous causal relationship between exposure and the observed effect. Effect: **injury** — radiation disease & radiation wounds	Effect: 1 **Risk** that cancer may develop, after a period of latency 2 **Risk** of hereditary damage, transferred to progeny
Threshold effect: A certain minimum dose must be exceeded before the particular effect is observed; no injury if dose is below the threshold	No threshold dose for risk
Above the threshold, the seriousness of the **injury is proportional to the magnitude of the dose**	**Seriousness** of cancer is independent of the dose, but the **probability/risk** of cancer is proportional to the dose
Strongly dependent on the dose rate	Practically **independent of the dose rate**

Deterministic effects resulting from exposure to high LET radiation are similar to those from low LET exposure but their frequency and severity are greater per unit absorbed dose of high LET radiation.

The **amount of radiation energy absorbed per unit mass is called the absorbed dose.** The unit for the absorbed radiation dose is the **gray** (symbol Gy; joule.kg^{-1}). Because the Gy is such a large unit, the unit mGy is often used in practice. A given absorbed dose (i.e. amount of energy deposited per unit mass) of different types of ionising radiation will not have the same biological effect. For protons with $E > 2$ MeV, the stochastic effects will be ~ 5 times higher than the same absorbed dose from γ- or X-rays. For neutrons, the stochastic effects of a given absorbed dose will be 5 to 20 times higher than for the same absorbed dose from γ- or X-rays. The reason for this is that the energy of ionising radiation impinging on a living cell is dissipated in different ways, depending on the nature of the radiation. X- and γ-rays generally have a low LET: they penetrate deeply, but generate ions sparsely along their path. Heavy charged particles such as alpha particles, has a higher LET.

High-LET ionising radiation is more detrimental per unit absorbed dose, because the micro-deposition of energy produces a high ionisation density, which can more easily produce **double-strand DNA breaks.** Double-strand DNA breaks are far less repairable than **single-strand DNA breaks,** because there no longer is an intact DNA strand to serve as a "template" for the error-free repair of the broken strand.

Radiation weighting (w_r) factors are employed to quantify the observed differences in the relative abilities of different types of radiation to induce stochastic effects, i.e. cancer and heritable ill health, for identical absorbed doses. Radiation weighting factor gives an indication of the relative biological potential of different types of radiation to produce

stochastic effects. They quantify the carcinogenic potential of the microdistribution of ionisation in the cell by the ionising radiation.

The quantity absorbed dose, i.e. the energy deposited per unit mass in tissue, is not sufficient to quantify the health risk. Epidemiological studies and radiobiological studies indicate the necessity to introduce radiation weighting factors, and to weigh the absorbed dose with these factors to present a more accurate picture of the effects of radiation on an organ. This *weighted sum* is called the *equivalent dose*.

Let:

$D_{T,r}$	$\equiv$	Average absorbed dose deposited in organ or tissue T by radiation of type r;
w_r	$\equiv$	Radiation weighting factor for ionising radiation type r;
H_T	$\equiv$	Average equivalent dose in organ or tissue T;

Then

$$H_T = \sum_r \omega_r \, D_{T,r}$$

This expression should be understood as follows:

$$\underbrace{H_T}_{\substack{\text{Equivalent} \\ \text{dose to tissue } T}} = \underbrace{\sum_r}_{\substack{\text{Sum over all types} \\ \text{of radiation absorbed} \\ \text{in tissue } T}} \underbrace{\omega_r}_{\substack{\text{Radiation weighting} \\ \text{factor for radiation} \\ \text{type } r}} \underbrace{D_{T,r}}_{\substack{\text{Absorbed dose} \\ \text{deposited by radiation } r \\ \text{in tissue } T}}$$

The unit of the equivalent dose is the sievert (Sv) and it expresses radiation detriment or risk to humans. It encapsulates physics plus radiobiology and radiogenic cancer epidemiology. In everyday radiation protection problems, doses far smaller than the sievert are encountered, so that the units millisievert (mSv) and microsievert (μSv) are used as practical units for day-to-day radiation protection practice.

The **effective dose** (symbol E) is the sum of all equivalent doses received by different organs in the human body, taking into account the fact that some organs are more susceptible to the stochastic effects of ionising radiation than others. It is, in other words, a weighted sum for the entire human body. The effective dose is a quantity intended to express the overall risk to humans when several types of organs and tissues in the body are irradiated by several types of ionising radiation.

The effective dose to the entire human body is defined as

$$E = \sum_T \omega_T H_T$$
$$= \sum_T \omega_T \sum_r \omega_r D_{T,r} .$$

This expression should be understood as

$$\underbrace{E}_{\text{Effective dose (Sv)}} = \underbrace{\sum_T \omega_T}_{\substack{\text{Sum over all tissues} \\ \text{in the human body,} \\ \text{each weighted with the} \\ \text{tissue weighting factor}}} \quad \underbrace{\sum_r \omega_r D_{T,r}}_{\substack{\text{Equivalent dose} \\ \text{to organ/tissue } T}}$$

Organs have different radiosensitivities, because they contain different cell types. Immature, undifferentiated, fast-dividing cells are much more radiosensitive than mature, differentiated cells which divide very seldomly. Tissue weighting factors quantify empirical knowledge about the susceptibility of different organs to radiogenic cancer.

The dose units sievert (Sv) and gray (Gy)

The dose quantity gray (Gy), is a purely physics unit and it expresses radiation damage to non-living organic materials such as polymers. The dose quantity sievert (Sv), which is not a physics unit, combines physics with radiobiology and radiogenic cancer epidemiology, and quantifies ionising radiation detriment to humans. Essentially, the unit Sv is used to express radiation damage to humans, because (1) human cells contain DNA, and DNA damage is carcinogenic and (2) because different organs contain different cell types, with different radiosensitivities.

1.6 Effects of ionising radiation on polymers

The following information are summarised from Clough & Shalaby (1991).

Polymers degrade if they are irradiated with ionising radiation and receive a sufficiently high dose. During degradation, physical properties of polymers are changed e.g. electrical optical and mechanical properties. Each polymer reacts differently to ionising radiation.

Ionising radiation reacts with polymers in two basic ways: chain scission and cross-linking. Chain scission is a random rupturing of bonds, which reduces the molecular weight (i.e. strength) of the polymer while cross-linking results in reduced elongation of the polymer. The influence of ionising radiation on the properties and performance of a polymer differs according to whether the material degrades or cross-links, and this in turn depends on specific sensitivities or susceptibilities inherent in the polymer backbone. All materials have been found to break down at very high radiation doses, however, the

range of the dose under which a given plastic will maintain its desirable properties depends on the chemical properties of the polymer.

The effects of ionising radiation depend greatly on polymer chemical structure, and it has been found that the dose necessary to produce similar significant effects in two different materials can vary from values as low as 4 kGy in polytetrafluoroethylene (PTFE; registered trade name TEFLON) to 4000 kGy or more in polystyrene or polyimide. The effects of ionising radiation on the properties of a polymer can also be difficult to predict, especially in the presence of certain additives that can help to prevent radiation damage to plastics. Polymers containing aromatic (ring-structure) molecules generally are much more resistant to radiation degradation than are aliphatic (chain-structure) polymers.

Radiation shielding is not only there to protect people but also to minimise damage to polymers. Good shielding will minimise the need for equipment maintenance and the need to replace polymer seals and pipes.

1.7 Photon shielding mechanisms

This study is concerned with the shielding of ionising photons, so that photon attenuation mechanisms will now be reviewed.

1.7.1 Photo-electric absorption (PEA)

Photo-electric absorption (PEA) involves the total absorption of the incident photon by the electrons of the atomic shell. The atomic electrons do not interact with the incident photon as free electrons, but as bound electrons. PEA is a reaction between the incident ionising photon and the entire atom (Marmier & Sheldon, 1969: 114).

The incident photon is absorbed, and the energy that is imparted to the atom causes the emission of a so-called photo-electron. The name "photo-electron" derives from the fact that the atom releases the electron after having absorbed a photon. Because the recoil energy of the atom is negligible, the kinetic energy T of the ejected electron is related to the energy E'_γ of the incident photon and the binding energy E_b of the ejected electron by the relationship

$$T = E'_\gamma - E_b \,.$$

The release of the photo-electron is followed by the emission of one or more characteristic X-rays and/or Auger electrons, as a result of the rearrangement of orbital electrons.

PEA is the dominant attenuation mechanism for photons having low energies. The microscopic cross-section $\sigma_{\mathrm{PEA}}(E')$ for the PEA of a photon with an incident energy E', by an atom with atomic number Z, follows the following approximate relationship

(Marmier & Sheldon, 1969: 117):

$$\sigma_{\text{PEA}} \propto \frac{Z^{4.5}}{\left(E'_{\gamma}\right)^{3.5}} \cdot \tag{1.2}$$

The large exponential power to which the atomic number Z is raised in Eq. (1.2), indicates why high-Z materials like lead, tungsten and depleted uranium are such excellent absorbers of low energy photons. The large exponential power to which the variable E' is raised, indicates why the contribution of PEA to the attenuation of photons diminishes sharply with increasing photon energy.

Because secondary particles are emitted when PEA takes place, it is not a pure absorption process. However, energy conservation considerations imply that the energies of all individual secondary photons will be far less than the energy of the original incident photon. From Eq. (1.2), it follows that the cross-section for the photo-electric absorption of these less energetic photons will be considerably larger than the cross-section for the photo-electric absorption of the original photon. It is clear that a series of successive reactions will take place, and that every PEA reaction will further decrease the photon energy. Eventually, photon energies will become so low that it will be below the threshold for ionisation. At such low energies, the photons are, for all practical purposes, not biologically dangerous any more.

1.7.2 Compton or incoherent scattering

Incoherent or Compton scattering takes place when an incident photon interacts with an *individual* electron in an atom (as distinguished from the coherent interaction of a photon with all the electrons of an atom). In the energy range where incoherent scattering dominates, bound electrons may be assumed to interact as free particles (Marmier & Sheldon, 1969: 110).

In the energy region of interest, incoherent scattering may be treated as the elastic scattering of a photon from a free electron that is initially at rest.

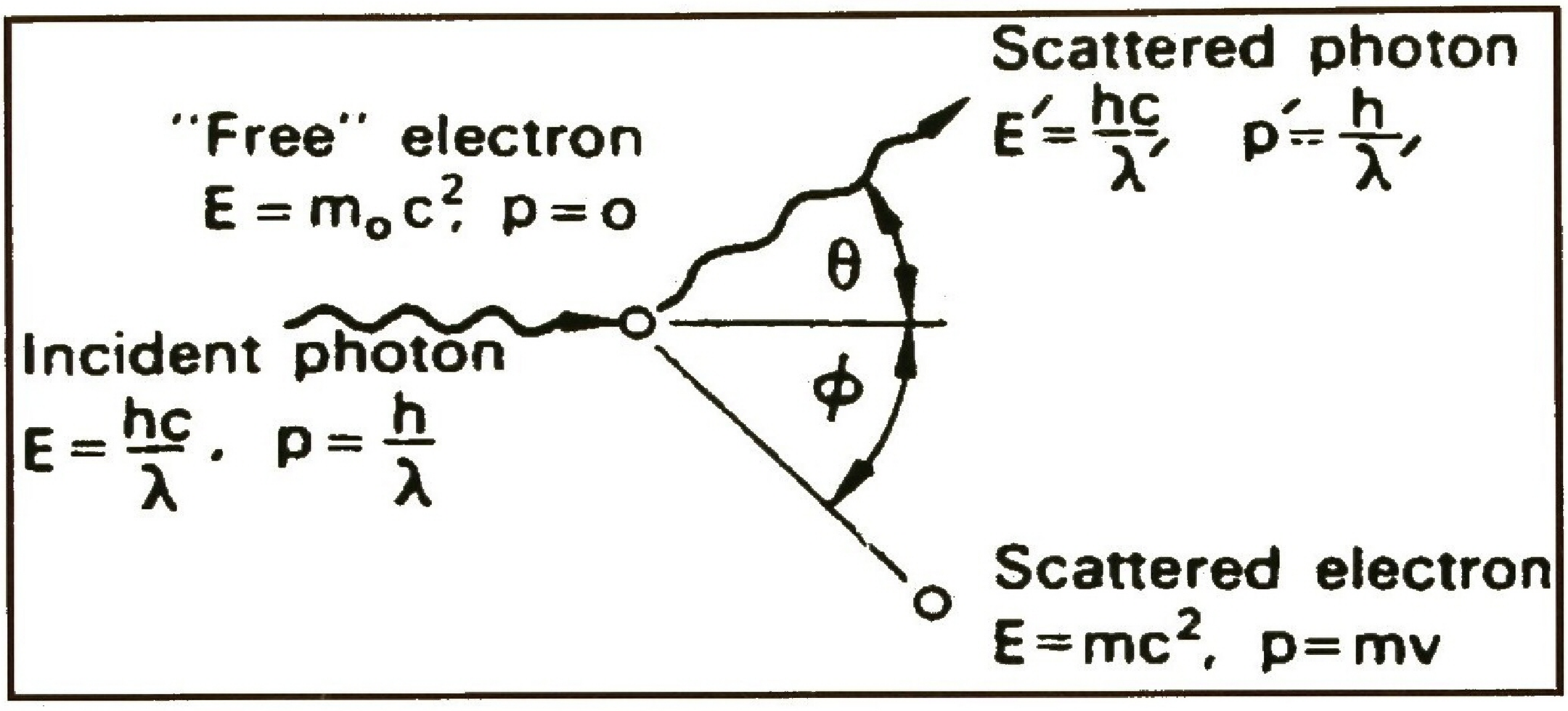


Figure 1.4: *Compton scattering: an elastic collision between a photon and an electron*

By starting from a mathematical statement of the conservation of energy and momentum, the following relationship between the energy E of the scattered photon and the energy E' of the incident photon and the scattering angle θ, can be deduced (Knoll, 2000):

$$E(E', \theta) = E' \left(\frac{m_e c^2}{m_e c^2 + E'(1 - \cos(\theta))} \right). \tag{1.3}$$

In Eq. (1.3), m_e represents the rest mass of the electron, while c is the speed of light in a vacuum; the product $m_e c^2$ is the rest mass energy of the electron, namely 0.511 MeV.

1.7.3 Pair production

The third of the three important reactions that make the dominant contribution to photon attenuation, is pair production (PP):

$$\gamma \longrightarrow e^+ + e^-.$$

Pair production is treated in some detail in Marmier & Sheldon (1969: 122 — 146).

When the energy of a photon is more than twice the rest-mass energy $m_e c^2$ (0.511 MeV) of an electron, i.e. in excess of 1.02 MeV, the formation of an electron-positron pair becomes energetically possible. As a result of the law on the conservation of linear momentum, pair production can only take place in the vicinity of a third particle that can recoil to take up linear momentum. This particle must have an electrical charge. This third particle is usually an atomic nucleus. As a result of the kinetic energy absorbed by the recoil particle, the threshold for pair production is not $2m_e c^2$ any more, but:

$$E'_{\text{PP_threshold}} = 2m_e c^2 \left[1 + \frac{m_e}{M} \right], \tag{1.4}$$

where M is the mass of the recoil particle (Marmier & Sheldon, 1969: 123).

Pair production does not specifically have to take place in the vicinity of an atomic nucleus. There exists a very small probability that it will take place in the Coulomb-field of an electron, with the electron serving as the recoil particle. Because the experimentalist will observe three particle tracks in a cloud chamber, this process is called *triplet formation.* From Eq. (1.4) it follows that the threshold energy for triplet formation in the Coulomb field of an electron, is $4m_{\mathrm{e}}c^2$, i.e. 2.044 MeV.

The electron and positron are charged particles. They are slowed down by continuous Coulomb interactions in matter. *Bremsstrahlung* photons, with energies far lower than that of the incident photon, are produced in the process. When the positron has lost most of its energy, it recombines with a negatively charged electron (negatron). Both leptons disappear, and two *annihilation photons,* each of which has an energy equal to the rest-mass of the leptons, i.e. 0.511 MeV, are produced:

$$\mathrm{e}^+ + \mathrm{e}^- \longrightarrow 2\gamma\,(0.511\ \mathrm{MeV}).$$

The two annihilation photons move in opposite directions, at an angle of approximately 180°. In less than 10% of cases, the positron reacts with a strongly bound atomic electron, with the production of only one annihilation photon.

The cross-section for pair production dominates both PEA and Compton scattering in the high energy region. As a result, it is the dominant photon attenuation mechanism for photons with energy $E'_\gamma \gtrsim 5\,\mathrm{MeV}$. Pair production can easily lower photon energies by an order of magnitude (e.g. from 5 MeV to 0.511 MeV). This final energy (0.511 MeV) falls right in the energy region where PEA dominates photon attenuation. In this fashion, pair production can serve as the first event in the chain of interactions that will eventually degrade photon energy to a value below the threshold for ionisation. When photons reach such a low energy, they are not biologically hazardous any more.

Above the threshold energy for pair production, the cross-section for pair production, $\sigma_{\mathrm{pp}}(E', Z)$, is a function of the incident energy E' and the atomic number Z of the attenuating medium. If the incident energy E' is kept constant, it is found that,

$$\sigma_{\mathrm{pp}}(Z) \propto Z^2. \tag{1.5}$$

If the variable Z is kept constant, it is found that $\sigma_{\mathrm{pp}}(E')$ is zero below the threshold energy, then rises monotonically with E', tending to a plateau (Shultis & Faw, 1996).

1.8 Quality management in radiation shield design

In the nuclear and radiation industry, there are many sources of ionising radiation. One of the ways to reduce radiation levels to safe levels, is to use radiation shielding. The purpose of shielding is to reduce the dose rates to levels that are much safer than it would be without a shield. Lead is a very good shield against ionising photons while thick concrete is normally used to shield neutrons.

NWU LIBRARY

Over the past decades, it has become standard practice in the nuclear and radiation industry, that all radiation shield designs should be evaluated and approved by an expert group. Any facility modification that can effect on personnel exposure to ionising radiation, should be evaluated and approved by such an expert group.

This formal methodology has not been followed at *iThemba LABS* until the end of 2002, as a result of a lack of a Quality Management system in Radiation Protection.

During 2002, it became clear that the informal and rather *ad hoc* way of radiation protection management at *iThemba LABS* was a failure, and the facility's executive management tasked the Radiation Protection Division to introduce a formal Quality Management system in Radiation Protection. This entails, *inter alia,* that all radiation shielding designs must be evaluated and approved by the Radiation Protection Division. No modifications to existing shields may be made without the approval of Radiation Protection.

1.9 Research objectives

The objectives of this study are:

- To identify inadequate radiation shield designs in the radionuclide production facility of *iThemba LABS*, i.e. shields that do not adequately protect workers (and polymers) against ionising radiation.
- To re-design these shields for adequate protection.

This dissertation is the fruit of the first year of implementing a Quality Management system for radiation shields. All important radiation shields in the Radionuclide Production facility will be subjected to evaluation, and inadequate shields that need to be redesigned and rebuilt will be identified. Improved designs will be proposed. Because detailed mechanical design is always done in a team with a mechanical designer, only shielding materials and their thicknesses have been specified.

1.10 Structure of this study

The logical flow in this dissertation is as follows. In Chapter 2 (page 15), the ionising radiation hazards found at the Radionuclide Production facility of *iThemba LABS* are reviewed. Shield design to protect workers against ionising radiation, requires shielding calculations, and Chapter 3 (page 31) briefly deals with the methodology used in simple point-kernel radiation shielding methods for shield design against ionising photons. In Chapter 4 (page 33), measured dose rates as well as dose rate calculation will be used to identify inadequate radiation shield designs in the Radionuclide Production facility — shields which do not adequately protect workers against ionising radiation. Chapter 5 (page 61) deals with plans to upgrade the Radionuclide Production facilities. Chapter 6 (page 65) will set forth the improved shield designs for the inadequate shields that have been identified. The aim, methodology, results and findings of this study will be summarised in Chapter 7 (page 85).

Chapter 2
Radiation hazards at the Radionuclide Production Facility at *iThemba LABS*

2.1 The cyclotrons at *iThemba LABS* — an overview

iThemba LABS is a science laboratory for accelerator-based studies; its full name is *iThemba Laboratory for Accelerator Based Sciences;* the word *"iThemba"* means "hope."

A cyclotron is a machine that accelerates subatomic particles to high speeds, so that the accelerated particle beam can be used in different applications. At present (2004) the cyclotron facility at *iThemba LABS* consists of two injector cyclotrons — SPC1 and SPC2 — and the main cyclotron, SSC. The three cyclotrons can be described as follows:

- **SPC1** is a Solid Pole injector Cyclotron that supplies partly accelerated light positive ions (mainly protons) to the main cyclotron.
- **SPC2** is the second Solid Pole injector Cyclotron which supplies partly accelerated heavy positive ions to the main cyclotron; polarised beams can also be supplied.
- **SSC** is the main, Separated Sector Cyclotron that accelerates positive nuclear particles to the desired final energy.

The ions that will be accelerated in the cyclotrons, are produced in one of several ion sources and are then accelerated to a relatively low energy (about 3 – 8 MeV in case of protons) by one of the injector cyclotrons. Then they are transported to the main cyclotron, by means of a beamline, for further acceleration to higher energies, normally between 66 and 200 MeV in the case of protons. A proton with an energy of 66 MeV can travel more than 2.6 times around the entire circumference of the earth in 1 second. At an energy of 200 MeV, a proton can travel around the earth about 4.2 times in 1 second.

The beam produced by the separated sector cyclotron (SSC) is used for three purposes:

- **Radiotherapy.** Patients can be treated at an isocentric **neutron therapy** unit. *iThemba LABS* is also the centre of the first **proton therapy** facility in the Southern hemisphere.
- **The production of radionuclides.** Radionuclide production has been undertaken on a routine basis since November 1988 and the programme is still expanding. *iThemba LABS* dispatches more than 1000 consignments of radionuclides per year

to more than 20 hospitals and clinics. These radionuclides are administered to more than 5000 patients per year. The radionuclides are used in several nuclear medicine procedures, which entails, inter alia, the localisation of tumours, organs, infections and inflammation, as well as flow studies, lung studies and absorption studies.

- **Nuclear physics and biophysics experiments**. *iThemba LABS* staff as well as scientists from South African and overseas universities utilise the accelerated particles and experimental facilities to conduct a variety of research projects.

Figure 2.1 indicates the positioning of the cyclotrons, the beamlines and important vaults on the ground level of the cyclotron complex.

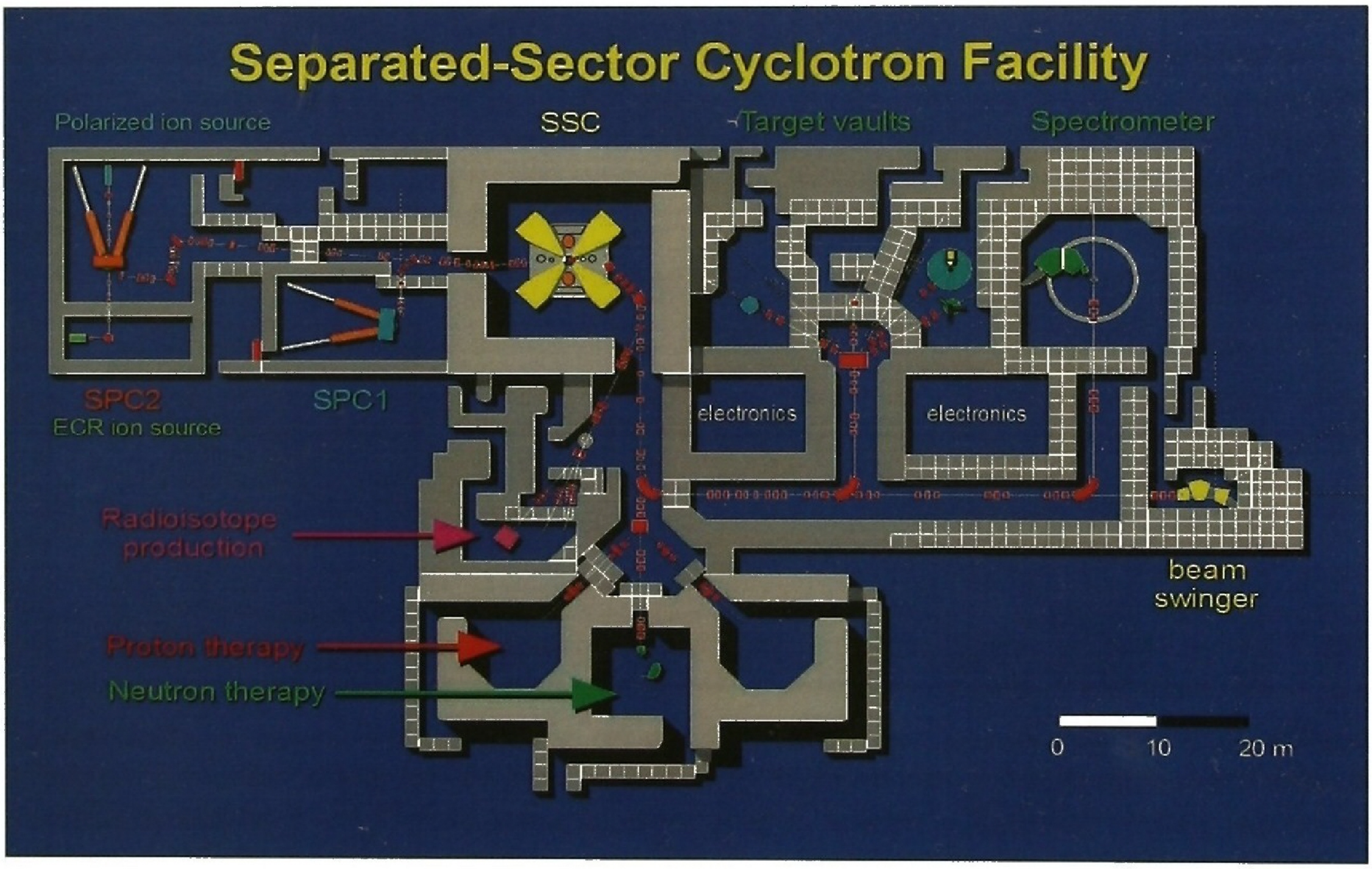


Figure 2.1: *The layout of the ground level of the cyclotron hall of iThemba LABS. The focus of this dissertation is radiation protection against the radionuclides produced at the Radioisotope Production facility, at centre-left in the above diagram.*

2.2 The radionuclide production facility at *iThemba LABS*

Beams and Targets

The backbone of the Radionuclide Production facility at *iThemba LABS* is two vaults where a 66 MeV proton beam falls on specially prepared targets inside target bombardment stations.

The radionuclides are produced with an accelerator by bombarding appropriate target nuclei with nuclei of, usually, hydrogen or helium, accelerated to high velocities by means of the accelerator. The target nuclei are contained in a so-called target, consisting of a material — solid, liquid or gaseous — having the specific stable nuclide of choice as one of its constituents and which is irradiated with the accelerator beam. Collisions then take place between the incident nuclei and the target nuclei, leading to nuclear reactions which have as the reaction product the radionuclide of interest. Figure 2.2 shows a typical radionuclide production target holder used at *iThemba LABS*.

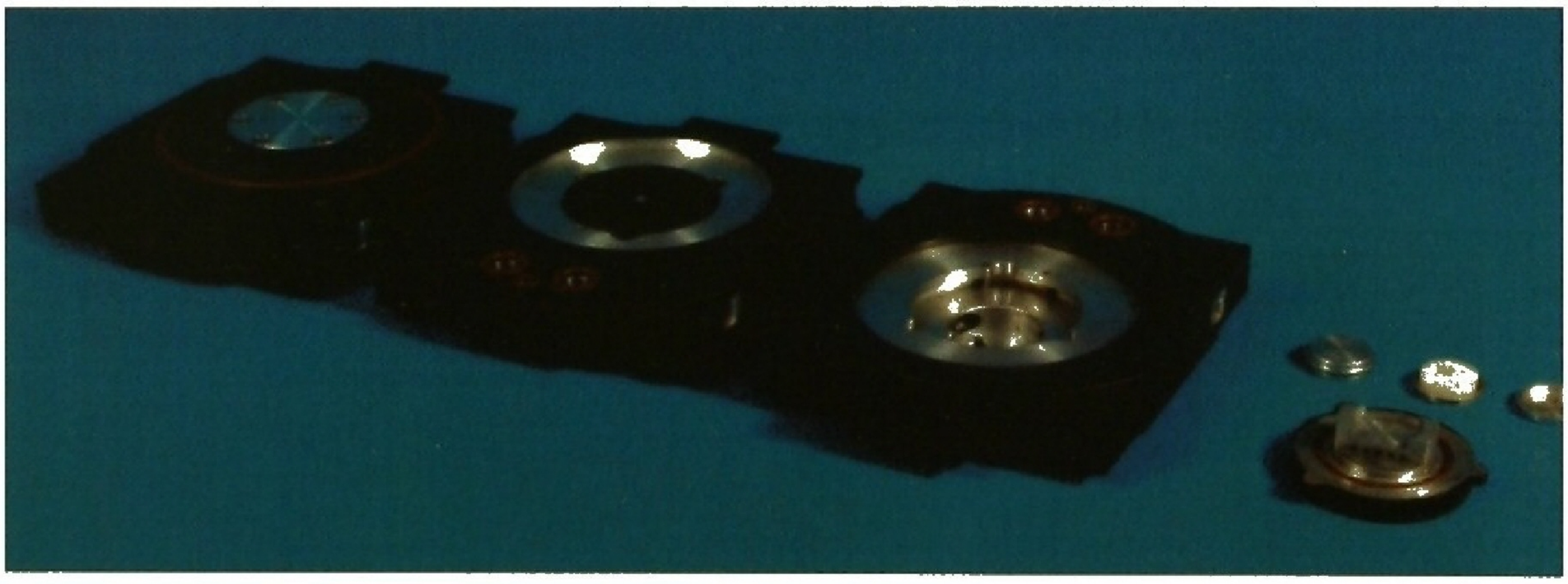


Figure 2.2: *A typical radionuclide production target holder, shown from 3 different perspectives. The small target shown near the right of the picture, is welded into an aluminium canister and inserted into the target holder. Cooling water pipes are connected to the target holder when the latter is mounted in the target bombardment station.*

The target holders are transported by a remotely-controlled trolley & track system, as shown in Figure 2.3. This automated system makes it unnecessary for people to come near the radioactive targets while they are taken from one place to another place.



Figure 2.3: *Target transporter trolley on tracks. A target holder is mounted on the trolley in the foreground.*

Figure 2.4 shows the local shield around the horizontal-beam target bombardment station.

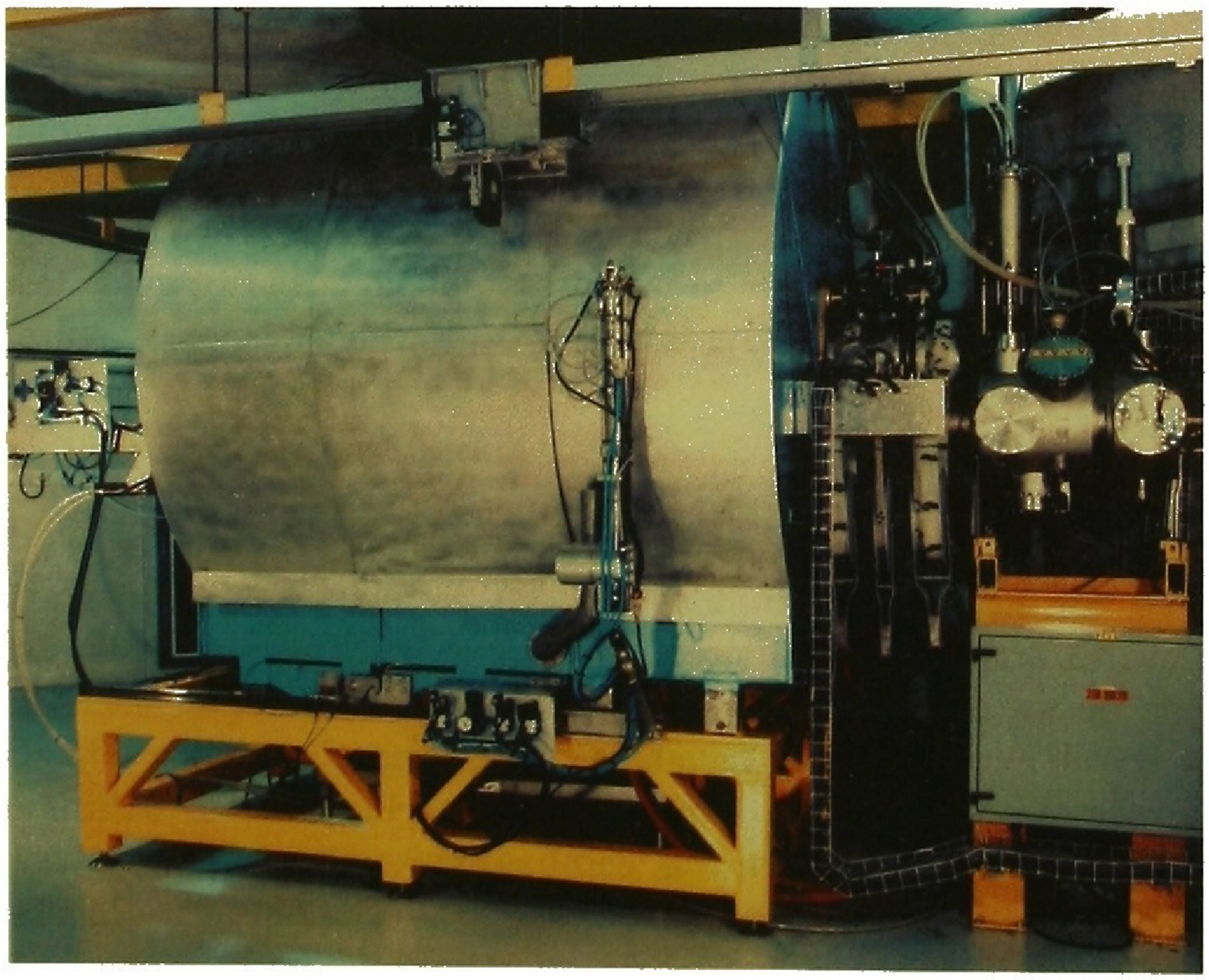


Figure 2.4: *The local shield around the main horizontal-beam target bombardment station. This shield was professionally designed using the radiation transport code ANISN and the cross-section library HILO (RSICC DLC-119). This shield is colloquially referred to as the "elephant," for obvious reasons.*

The accelerator production of radionuclides is done with intense beams of light ions. At *iThemba LABS,* routine radionuclide production is performed with 66 MeV protons. This is dictated by the fact that the 66 MeV proton beam required for neutron therapy is the only suitable one available on a routine basis. Basing the routine radionuclide production programme on this beam, therefore enables production runs to be carried out without having to generate a new beam energy especially for this purpose — a process which consumes, on average, about three hours of valuable accelerator time. Furthermore, it also allows the neutron therapy beam which is idle during the setting up of patients, to be used for radionuclide production, instead of letting this beam time go to waste.

Proton beams have a long range in matter compared with other heavier charged particles, resulting, in effect, in thicker targets and therefore, generally, higher yields of the product radionuclides. Furthermore, a proton energy of 66 MeV is high enough to enable one to make use of an appropriate nuclear reaction to produce nearly every radionuclide of interest which can be produced by means of a particle accelerator; all required energies lower than 66 MeV can, of course, be obtained by degrading the 66 MeV beam by means of a suitable energy degrader. Every effort is being made to effect any degradation needed by means of one or more other production targets, each using an appropriate energy slice in the range 0-66 MeV. A number of targets in series can then be bombarded simultaneously, in this way making use of beam time more effectively and minimising the cost of the radionuclides produced.

Targets are irradiated outside the vacuum system of the beam lines, from which they are isolated by a double metal-foil system. These foils are thin enough to cause little degradation of the beam and the heat dissipated in them by the beam is removed by blowing helium gas through the space between them. Since all types of targets — solid (metal or pressed metal salts), liquid and gaseous — can conveniently be irradiated in this way, any stable nuclide can, if required, be employed as target material. Since more than 10 kW of heat is dissipated in the targets during irradiation, targets are water-cooled and of special design.

Target handling and processing

In view of the radiation hazards existing during and after irradiation of radionuclide production targets, shielded and/or remotely controlled facilities for the irradiation, transport and processing of these targets are essential. At *iThemba LABS,* a remotely-controlled shielded target magazine system makes it possible to set up many different combinations of a variety of targets, to be irradiated, in series, from the control room. A remotely-controlled electric rail system is used to transport the targets between the irradiation vaults and the processing facilities, loading onto and unloading of the targets from the electric transporters is done by means of remotely-controlled transfer mechanisms. Processing of the targets is carried out in remotely operated processing "hotcells," consisting of ventilated boxes shielded with lead bricks.

The processing of the activated targets involves various procedures necessary to isolate and purify the desired radionuclide, and get it in a form suitable for converting it to the

NWU LIBRARY

required radiochemical or labeled compound. Chemical purification of nuclides is normally done by using ion-exchange resins. Microgram quantities of radioactive material have to be separated from a few grams of inactive target material, and *iThemba LABS* has been a pioneer in this field for many years.

Figure 2.5 shows one of 2 rows of these processing hotcells.



Figure 2.5: *View of processing hotcells from the side where chemical technologists control the radiochemical processing of radionuclides. The present (2004) hotcells are shielded by 10 cm of Pb on the front, and 5 cm of Pb on all other sides. Thick glass protects the operators' eyes while enabling them to see into the hotcell. An air extraction system keeps the air pressure inside the hotcells lower than on the outside, so that radioactive gasses will not normally "leak out" of the hotcell. Note the remote tongs used by the technologist.*
(Note: the term "hotcell" simply refers to the fact that the inside of the cell is very radioactive—radioactively "hot." The term has nothing to do with temperature.)

Radiochemistry

The final product obtained after completion of the radiochemical procedures can be either the primary radionuclide in a simple chemical form or, if required by the user, a more complex compound labeled with this radionuclide. A labeled compound is formed by introducing a radionuclide into a molecule by means of chemical synthesis. Two main types of labeled compounds can be synthesised: In isotopically labeled compounds, a stable nuclide of an element is replaced by a radionuclide of the same element in the same molecular site without any change in the structure of the molecule, while in non-

isotopically labeled compounds a stable nuclide of an element in a molecule is replaced by a radionuclide of another element.

Generators

A special type of primary radioisotopic product is the radionuclide generator system, or a "radioactive cow." Such a generator comprises a moderately long-lived parent radionuclide which decays to produce a short-lived daughter radionuclide. The parent radionuclide is usually absorbed on a support material, such as an ion exchange resin, which is packed in a small, lead-shielded column. The short-lived radionuclide is then eluted from the support material whenever required. This "milking" operation involves separating the daughter radionuclide from the parent. Since the activity of the system decreases with the half-life of the parent radionuclide, a radionuclide generator is a convenient means of making a short-lived radionuclide available to users at long distances from the production site.

The target store

In the basement of the Radionuclide Production facility, there is a target store. Targets — mostly irradiated targets — are stored there, awaiting either processing, further irradiation or future use. Concrete bricks are stacked around the target carousel to serve as radiation shielding. Figure 2.6 shows a photograph of the target store *before* the shielding walls were built.



Figure 2.6: *The interior of the target store room in the basement of the Radionuclide Production building, before the shielding walls were built. Many irradiated targets can be stored in this facility. Target holders are stored in the wheel-like target carousel, which is clearly visible in the above picture. Note the trolley rail in the background. These rails require frequent cleaning. Because the target holders may still contain high-activity irradiated targets, activities and dose rates can be very high and very effective shielding is required to make it safe for decontamination workers and technicians to work inside the target store room.*

2.3 Radionuclides produced at the Radionuclide Production facility of *iThemba LABS*

Introduction

The high-purity radionuclides produced at *iThemba LABS,* satisfy the entire country's demand for certain important radio-pharmaceuticals. More than 1000 consignments are supplied to more than twenty provincial hospitals, private nuclear medicine practices and research institutions throughout South Africa, and are used in diagnostic procedures on about 10 000 patients each year. The routine production of radionuclides is supported by an active research and development programme at *iThemba LABS,* the main aim of which is the development of new products and production procedures. This programme covers all aspects relevant to radionuclide production, namely targetry, target handling, determination of excitation functions, chemical recovery and purification of radionuclides from targets after bombardment and the preparation and quality control of the radio-pharmaceuticals. A number of long-lived, non-medical radionuclides, mainly ^{22}Na, are produced, on request, for use in research and industry. The export of ^{22}Na earns *iThemba LABS* a significant income and ensures optimal use of cyclotron beam time. Most of the radionuclides listed in Tables 2.2 and 2.3 cannot be produced anywhere else in South Africa, and cannot be imported cost-effectively from abroad because of their short half-lives. In many instances they also cannot be replaced satisfactorily with alternative reactor-produced or imported radionuclides.

Important radionuclides produced at *iThemba LABS*

Radionuclides are produced by specific nuclear reactions taking place within the irradiated target. The nuclides and nuclear reactions are listed in Table 2.1.

Table 2.1: *Nuclear reactions utilised to produce radionuclides at iThemba LABS. The symbol X denotes "any" particle in the exit channel of the reaction; it designates so-called "inclusive" reactions.*
(Information supplied by Radionuclide Production Group (RPG), iThemba LABS, August 2003).

Radionuclide	Production route
^{18}F	Ne (p, X) ^{18}F
^{22}Na	Mg(p, X)
^{67}Ga	Zn (p, xn) ^{67}Ga Ge (p, X) ^{67}Ga
^{68}Ge	Ga (p, xn) ^{68}Ge
^{81}Rb/^{81m}Kr	Kr (p, xn) ^{81}Rb
^{82}Sr	Rb (p, xn) ^{82}Sr
^{111}In	In (p, xn) ^{111}Sn $\rightarrow$ ^{111}In
^{123}I	^{127}I $(p, 5n)$ ^{123}Xe $\rightarrow$ ^{123}I
^{139}Ce	^{141}Pr(p, X)
^{201}Tl	^{203}Tl $(p, 3n)$ ^{201}Pb $\rightarrow$ ^{201}Tl

The important radionuclides produced at *iThemba LABS* as commercial products, are listed in Table 2.2.

Table 2.2*: Useful radionuclides produced at iThemba LABS.*
(Abbreviations: a ≡ year; d ≡ day; h ≡ hour; m ≡ minute; s ≡ second.)

Nuclide	Symbol	Half-life	Application
Gallium-67	^{67}Ga	78 h	Medical
Cerium-139	^{139}Ce	138 d	Medical/Industrial
Strontium-82	^{82}Sr	25.5 d	Medical/Industrial
Rubidium-81	^{81}Rb	4.6 h	Medical: Production of ^{81m}Kr in Rb-Kr-generator
Iodine-123	^{123}I	13 h	Medical
Sodium-22	^{22}Na	2.6 a	Industrial
Germanium-68	^{68}Ge	288 d	Medical/Industrial

Table 2.3 lists radionuclides produced as waste products.

***Table 2.3**: Radionuclides produced as waste products at iThemba LABS.*

Nuclide	Symbol	Half-life
Sodium-22	^{22}Na	2.6 a
Sodium-24	^{24}Na	15 h
Manganese-54	^{54}Mn	312 d
Zinc-65	^{65}Zn	244 d
Gallium-66	^{66}Ga	9.4 h
Rubidium-83	^{83}Rb	86 d
Rubidium-84	^{84}Rb	33 d
Cobalt-57	^{57}Co	271 d
Cobalt-58	^{58}Co	71 d
Strontium-83	^{83}Sr	32 d
Strontium-85	^{85}Sr	65 d

Besides these listed radionuclides, many other nuclides with short half-lives are produced in the targets.

Photon emission characteristics for the radiologically dominant radionuclides

Operational experience has shown that the radionuclides that contribute the highest external dose rates, after about a day of decay time, are ^{66}Ga, ^{65}Zn, ^{83}Rb and ^{22}Na. The ^{66}Ga will have decayed practically completely after about 5 days, but can still present a problem in the first 2 days after bombardment.

The radiation emission characteristics of these most important radionuclides are as follows (ICRP-38, 1983).

^{22}Na

***Table 2.4:** Energies and yields of ionising photons produced by the radioactive transformation of ^{22}Na (ICRP-38, 1983).*

Photon energy (MeV)	Fractional emission yield
0.511	1.8292
1.27	0.999

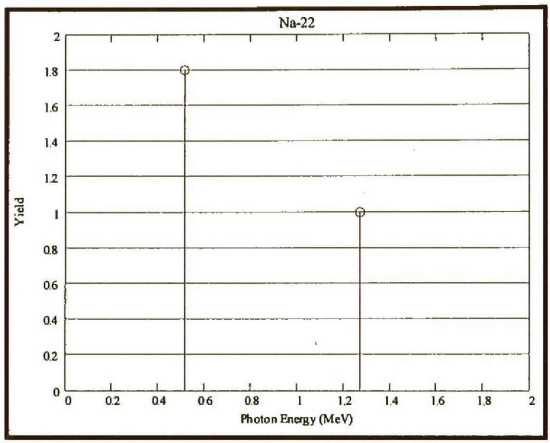


Figure 2.7: *Energies and yields of ionising photons produced by the radioactive transformation of ^{22}Na (ICRP-38, 1983).*

^{66}Ga

The radionuclide ^{66}Ga emits 30 ionising photons, and they will not be listed, but only portrayed graphically.

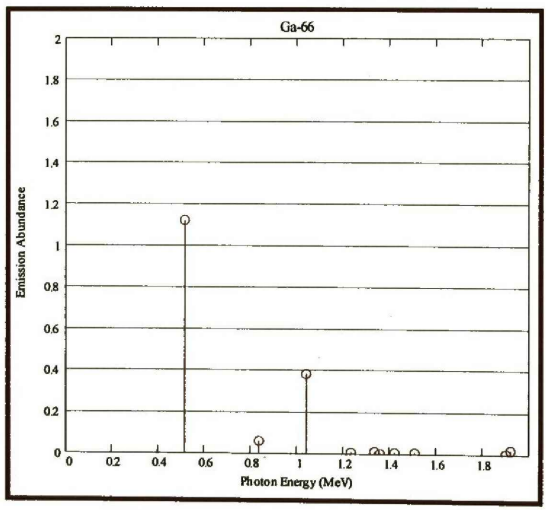


Figure 2.8: *Energies and yields of ionising photons produced by the radioactive transformation of ^{66}Ga (ICRP-38, 1983).*

^{65}Zn

Table 2.5: *Energies and yields of ionising photons produced by the radioactive transformation of ^{65}Zn (ICRP-38, 1983).*

Photon energy (MeV)	Fractional emission yield
0.511	2.92×10^{-2}
1.116	5.07×10^{-1}

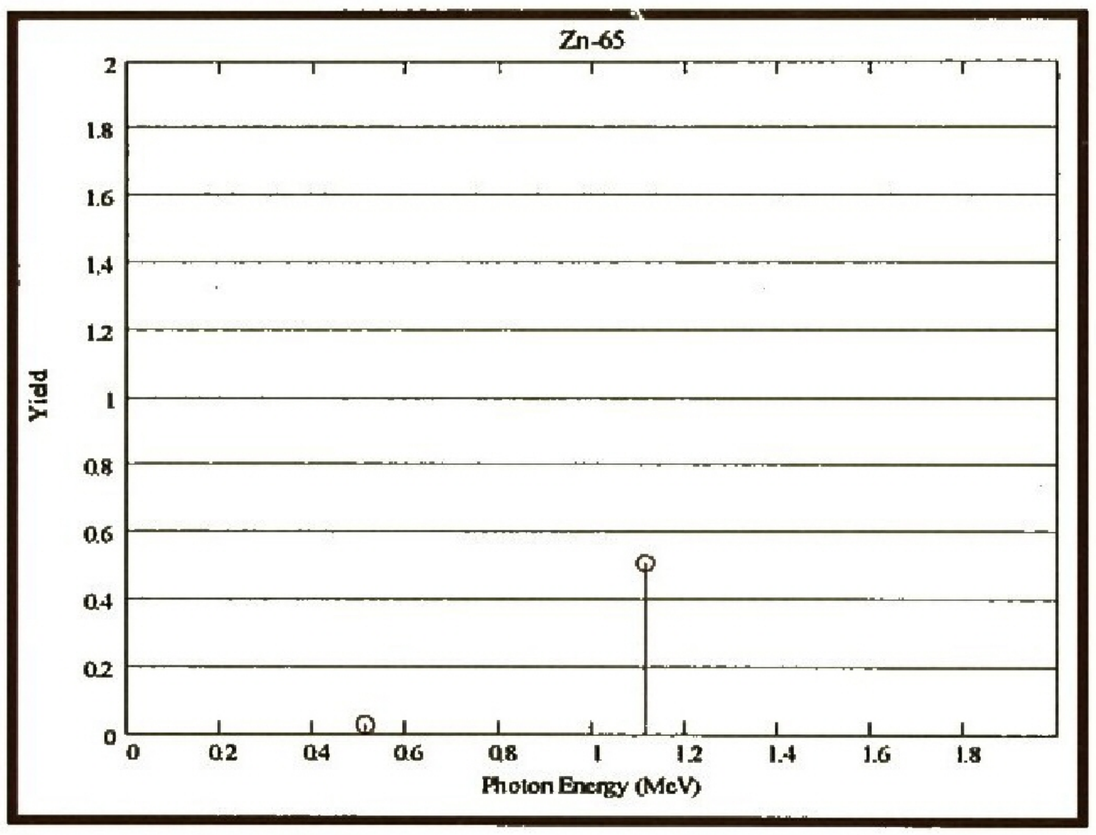


Figure 2.9: *Ionising photon emission characteristics of ^{65}Zn—photon energies and fractional yields (ICRP-38, 1983).*

^{83}Rb

The radionuclide ^{83}Rb emits 9 ionising photons, and they will not be listed, but only portrayed graphically.

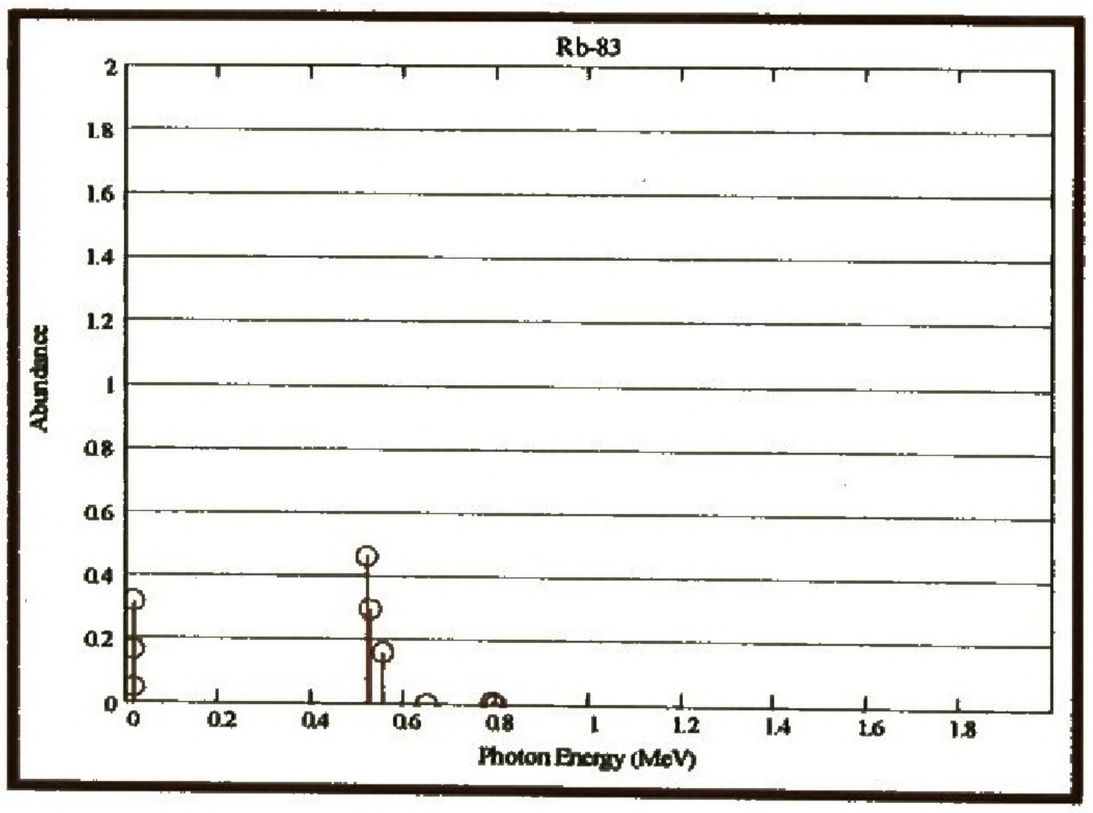


Figure 2.10: *Ionising photon emission characteristics of ^{83}Rb—photon energies and fractional yields (ICRP-38, 1983).*

2.4 Selection of radionuclide and activity for radiation shielding calculations

2.4.1 Fundamental simplification

High-energy ionising photons are more difficult to shield than low-energy photons, because photon attenuation coefficients generally decrease with increasing photon energy. From an inspection of Figures 2.7 to 2.10, it is evident that the spectrum of ionising photons radiated by ^{22}Na generally is higher in photon energy and photon yield than the other radionuclides formed in the targets that will be processed in the hotcells.

The following fundamental simplification can be made: Shield design calculations in this study were performed under the assumption that all the radionuclides present in the object that is to be shielded, can be represented by an ***equivalent activity*** of ^{22}Na. Radiation shields were designed to be adequate for this *equivalent activity* of ^{22}Na. It was assumed that a shield that is effective in shielding the equivalent ^{22}Na activity, will be adequate against the complex mixture of nuclides that will be present in practical situations.

This simplification was necessary, because when a senior Radionuclide Production physicist was approached for information about activities that will be present in targets, the following reply was received (Steyn, 2003b):

> We can provide a list of the activities that we produce per week; however, this is for the "wanted" isotopes, which is a small fraction of the total activities induced in our targets. Our reactions are of the type $(p, xnyp)$, where $x + y$ is an integer with a value up to 7, which means that we typically produce about 30 to 40 different radionuclides in a target when we bombard it. We have never tried to quantify all the activities of the "unwanted" nuclides, which will be a daunting task. In principle one can make estimates based on the GDH nuclear model (Alice IPPA) and perform point-kernel calculations of the gamma emissions to arrive at dose rate values, but this will be an enormous task. Rather, anybody who is interested can take a sample of waste and measure its dose rate.

The decision to use an equivalent amount of ^{22}Na as the equivalent of the complex mixture of radionuclides that is present in reality, is supported by the following reasoning:

Calculate the dose rates from the following 1 Ci (3.7×10^{10} Bq) point sources,

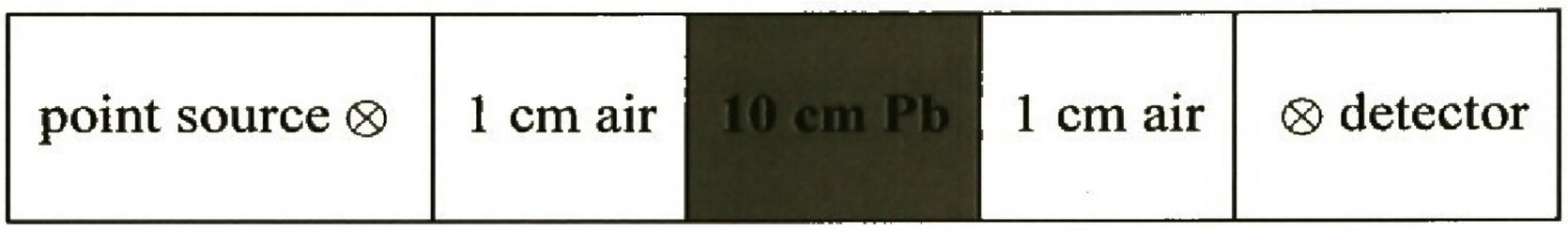
^{66}Ga

^{65}Zn

^{83}Rb

^{22}Na

shielded behind 10 cm Pb in the following source-shield-detector geometry,



using a point-kernel technique. The results are summarised in Table 2.6.

Table 2.6: *Dose rates from four 1 Ci point sources shielded behind 10 cm Pb.*

Nuclide	Half-life	Dose rate (mSv/h)
^{66}Ga	9.4 h	7.3
^{65}Zn	244 d	0.3
^{83}Rb	86.2 d	3.1×10^{-4}
^{22}Na	2.602 a	1.3

The only nuclide that results in higher dose rates than ^{22}Na is ^{66}Ga, but its half-life is quite short (9.4 h) and it will decay away within a few days.

It may thus be concluded that an ***equivalent activity*** of ^{22}Na for shield design calculation in the radionuclide production facility of *iThemba LABS,* may be used.

2.4.2 Selection of maximum realistic activities for each shielding problem

To do radiation shielding calculations, one needs to know the maximum realistic activity of the radionuclides on the source-side of the shield. The shields whose adequacy are in doubt, are now investigated one by one.

Maximum realistic activity in a processing hotcell

When prompted, the Radionuclide Production Group stated that the maximum expected activity of ^{22}Na per hotcell will be about 4 Ci, following the planned upgrades (Steyn, 2003a):

> The worst case I can think about, is 4 Ci ^{22}Na per hotcell. The total amount of activity in such a target at the end of bombardment is, of course, significantly higher as a result of all the other radionuclides which are still present in the target, and which will be separated chemically & dumped as waste.

The 4 Ci of activity that will be present does not include all the other radionuclides produced in an irradiated target. However, ^{22}Na production is always done as follows: The target is irradiated in the proton beam, and then left in the target store room for at least 4 weeks to allow the shorter-lived radionuclides to decay. It is therefore assumed

that the maximum activity of ^{22}Na that will be present in a hotcell, is 10 Ci, i.e. 0.37 TBq. This is 2.5 times higher than the activity stipulated by the Radionuclide Production Group, and therefore represents a conservative assumption to account for the additional radionuclides that will still be present when the target is brought into the reception hotcell for the first processing steps.

Decision: Processing hotcells must be able to shield 10 Ci, i.e. 370 GBq, of ^{22}Na adequately.

Maximum realistic activity in the target store

The wheel-like carousel in the target store can house up to 36 targets holders (Steyn, 2003b). Some of these targets will be "fresh," non-irradiated targets awaiting irradiation, while others will be irradiated targets. Only the irradiated targets will be highly radioactive. Normally, the target carousel is about 50% full. Assume 60% of the targets are irradiated targets awaiting chemical processing. Suppose therefore that about $50\% \times 60\% = 30\%$ of the places in the carousel are occupied by irradiated target holders. Suppose further that the ^{22}Na equivalent activity per irradiated target is 10 Ci. This means that the total activity housed in targets in the carousel, will be about

$$\begin{aligned} 30\% \times 36 \times 10 \text{ Ci} &\approx 100 \text{ Ci} \\ &= 3.7 \text{ TBq} \\ &= 3.7 \times 10^{12} \text{ Bq} \end{aligned}$$

Decision: The shielding in the target store must be able to shield 100 Ci, i.e. 3.7 TBq, of ^{22}Na adequately.

Maximum realistic activity in the radio-pharmaceutical laboratory

The amount of activity handled in the radio-pharmaceutical laboratory, is about 5 times less than the activity handled in a processing hotcell (Steyn, 2003b). In the processing hotcells, the radionuclide that is needed, is purified while the unwanted radionuclides are pumped to the basement as radioactive waste. This leads to a lowering of activity.

Decision: The radio-pharmaceutical laboratory must be safe for an activity of 1 Ci, i.e. 37 GBq, of ^{22}Na per hotcell.

2.4.3 Summary

Processing hotcells must be able to shield 10 Ci, i.e. 370 GBq, of ^{22}Na adequately.

The shielding in the target store must be able to adequately shield 100 Ci, i.e. 3.7 TBq of ^{22}Na.

The radio-pharmaceutical lab and the areas around it must be safe for an activity of 1 Ci, i.e. 37 GBq, of ^{22}Na.

Chapter 3
Point-kernel photon shielding calculation methods

Because this is a practical and not a theoretical work, a detailed mathematical treatment will not be done.

Consider a point source of ionising photons with source strength S, and a single shield layer with thickness t. Initially ignore scattering of radiation. Then the effective dose rate D_{eff} at a point r on the personnel side of the shield, will be given by

$$D_{\text{eff}} = \frac{S\,\mathfrak{R}\exp(-\mu t)}{4\pi r^2} \tag{3.1}$$

The $\left(\frac{1}{4\pi r^2}\right)$ term represents the "geometrical attenuation," i.e. the lowering of dose rate that is purely the result of the distance away from the point source. The symbol S stands for the source strength, i.e. activity times the emission yield. The $\mathfrak{R}$ is the fluence-to-dose conversion factor for the type and energy of the radiation (obtained from e.g. (ANS, 1991)). The $\{\exp(-\mu t)\}$ term represents the attenuation of the radiation in the shield of thickness t. The symbol μ denotes the linear attenuation coefficient; μ is also known as the "macroscopic cross-section," because it is product of the "microscopic cross-section" σ multiplied by the nuclide number density of the chemical elements in the shield.

It is not correct to leave out the contribution of scattered radiation to the dose rate behind a radiation shield. However, to take it into account in a rigorous manner, is quite difficult; to do it properly, one must use Monte Carlo codes, which are not easy to use and can also take many days to simulate, especially if the shield is thick.

The point-kernel method is an approximate method that leads to fast calculations, even though the answers are not as accurate as those obtained from Monte Carlo codes such as the code MCNP.

How does the point-kernel method work? The volume of the source is divided into many small sub-volumes. Each of these is now seen as a little point-source. All the activity in every small subvolume is assumed to be concentrated at its midpoint. Eq. (3.1) is used to determine the contribution of this small sub-volume of the source, to the dose rate at the detector point. However, the result is multiplied by a buildup factor to correct for the neglect of scattering. This process is repeated for all the sub-parts of the source, to obtain the total dose rate at the detector point and all results are summed.

The point-kernel methodology is implemented in the code QAD-CGGP (RSICC code CCC-493). A simple implementation of the point kernel method is version, is presented in the MathCAD worksheet, shown in Appendix A, page 86. This MathCAD worksheet

is handy for simple scoping calculations. It can only model point sources and extremely simple shield geometries. The accuracy of all shield design specifications arrived at using this worksheet, must always be verified by a QAD-CGGP calculation — the latter code is an internationally accepted shield design code.

There are several ways to handle buildup factors, i.e. the correction for the contribution of scattered ionising photons to the dose rate. The Geometrical Progression (GP) method is used in QAD-CGGP and also in the MathCAD Worksheet used for simple calculations. The GP method for handling buildup is the most accurate method.

MathCAD worksheet

A simple implementation of point-kernel photon shielding method was performed, using MathCAD. The MathCAD worksheet is very easy to use, but it has a tendency of underpredicting dose rates behind thick shields by about a factor of about 2. This MathCAD worksheet is shown in Appendix A on page 86.

QAD-CGGP

The FORTRAN code, QAD-CGGP, is a full and comprehensive implementation of the point-kernel method of photon shielding. This method can handle complex source and shield geometries.

Chapter 4

Evaluation of existing shields at the Radionuclide Production Facility

4.1 Dose limits

The present legal limits on exposure to ionising radiation, are summarised in Table 4.1.

Table 4.1: *Dose limits for occupational exposure to external ionising radiation. These limits were recommended by the International Commission on Radiological Protection (ICRP) in 1991 (ICRP-60, 1991) and were promulgated in South African Law in 1994.*

Type of dose	Maximum permissible dose
Effective dose (excluding pregnant women)	20 mSv per year
Dose to the skin, hands & feet	500 mSv per year
Dose to lens of eye	150 mSv per year
Pregnant women: Effective dose to conceptus	1 mSv from diagnosis of pregnancy to its end (ICRP-75, 1997)

Facilities may make internal rules for radiation protection, that are stricter than legal dose limits. *iThemba LABS* has a very pro-active approach to occupational health and safety matters, including radiation protection. *iThemba LABS'* radiation protection management plans to adopt a dose limit of 12 mSv per year from 2004, and a limit of 10 mSv per year from 2005. The administrative monthly dose limit will be lowered to 2 mSv. This means that there will be an internal investigation if a radiation worker exceeds a dose of 2 mSv in any 4-week period.

iThemba LABS' 2005 dose limit values for the occupational dose limits and maximum permitted staytimes in a radiation area, where specific dose rates are measured at the place where a radiation worker must work, are given below, in the same format in which they will appear on the facility's notice boards.

aximum permissible doses for occupational radiation exposure

Type of dose	Maximum permissible dose
Effective dose (excluding pregnant women)	10 mSv per year
Dose to skin, hands & feet	250 mSv per year
Effective dose to a pregnant woman	1 mSv from diagnosis of pregnancy to its end

me ra a on wor

Important: Choose the more restrictive of the two worktimes.

Dose rate @ chest & abdomen	Maximum worktime per day	Dose rate @ hands	Maximum worktime per day
10 µSv/h	10 hours	200 µSv/h	6 hour 15 min
20 µSv/h	5 hours	400 µSv/h	3 hours
30 µSv/h	3 hour 20 min	600 µSv/h	2 hours
40 µSv/h	2 hour 30 min	800 µSv/h	1 hour 30 min
50 µSv/h	2 hours	1 mSv/h	1 hour 15 min
70 µSv/h	1 hour 25 min	2 mSv/h	40 minutes
100 µSv/h	60 minutes	3 mSv/h	25 minutes
200 µSv/h	30 minutes	4 mSv/h	20 minutes
300 µSv/h	20 minutes	5 mSv/h	15 minutes
400 µSv/h	15 minutes	7 mSv/h	10 minutes
500 µSv/h	12 minutes	10 mSv/h	7.5 minutes
1 mSv/h	6 minutes	15 mSv/h	5 minutes
$\geq$ 2 mSv/h	RS Div to decide	$>$ 20 mSv/h	RS Div to decide

Important: This table does **NOT** apply to **PREGNANT WOMEN.**
Pregnant women may **NOT** work where dose rates exceed $\sim$ 10 µSv/h.

4.2 Radiation shielding performance concepts:

- **Design-base dose**
- **Maximum tolerable dose rate**
- **Projected annual dose**
- **Dose-rate reduction factors**

4.2.1 Design-base dose

Jobs involving exposure to ionising radiation must be planned, and shielding must be designed, to ensure that workers are not exposed over the dose limits. In the case of *iThemba LABS,* shields must be designed with a yearly limit of 10 mSv for the effective dose, in mind.

Because the radiation workers in the Radionuclide Production Group typically have more than one major routine task, any single major routine job should not expose them to a *fraction* of the dose limit. Suppose e.g. that a decontamination worker has 4 specific major routine tasks. Then a typical single task should not expose a decontamination worker to about $\left(\frac{1}{4} \times \text{dose limit}\right)$. The same principle will apply to chemical technologists, mechanical technicians, etc.

If the maximum activities of radionuclides present in a source are known, and the typical times that radiation workers will spend performing specific jobs are known too, it is possible to design shields that are effective enough to maintain the total annual exposure of a radiation worker below a chosen "target dose" value—the ***design-base dose.*** The design-base dose at the radionuclide production facility of *iThemba LABS* will typically be 2–3 mSv per year for major routine task, because (1) radiation protection management at *iThemba LABS* plans to lower the in-house annual dose limit to 10 mSv, and (2) most radiation workers typically have 2 to 4 major routine tasks.

Example 1: A typical radiochemical technologist has a job description to perform chemical separations in hotcells, and to perform development work in a low-activity laboratory. If the annual dose of every major routine job category is restricted to a value lower than about 3 mSv, the total yearly dose will normally be safely below 10 mSv.

Example 2: Decontamination workers have more than 5 routine tasks, so the design-base dose for each task category should be about 2 mSv per year.

In summary: The design-base dose is a *realistic fraction of the individual annual dose limit* applying to radiation workers.

4.2.2 Maximum tolerable dose rate

Shields must be designed with the design-base doses in mind.

If the dose-budget is a design-base effective dose of D_{eff}, and the radiation worker must spend a time t in a certain area, the maximum permissible dose rate that can be tolerated, is $\frac{D_{\text{eff}}}{t}$. In other words, shielding must be designed to ensure that dose rates on the personnel-side of shields are lower than the value

$$\text{Maximum tolerable dose rate} = \frac{\text{Annual design-base dose}}{\text{Annual staytime}} \tag{4.1}$$

4.2.3 Projected annual dose

Suppose that a radiation worker has to work a maximum realistic annual staytime t_{yr} in a radiation area where the maximum realistic average dose rate will be $\dot{D}_{\text{av}}$. Then the projected annual dose that the radiation worker will receive, will be

$$\begin{pmatrix}\text{Projected}\\ \text{annual dose}\end{pmatrix} = \begin{pmatrix}\text{Maximum realistic}\\ \text{dose rate}\end{pmatrix} \times \begin{pmatrix}\text{Maximum realistic}\\ \text{annual staytime}\end{pmatrix} \tag{4.2}$$

$$= \dot{D}_{\text{av}} \times t_{\text{yr}}$$

4.2.4 Dose-rate reduction factors

For a given application, a radiation shield has a dose-rate reduction factor of

$$\text{DRF} = \frac{\text{Transmitted dose rate without shield in place}}{\text{Transmitted dose rate with shield in place}} \tag{4.3}$$

If a shield has a DRF of 15, it means that the dose rate is lowered by a factor 15—the transmitted dose rate is lowered by a factor 15 by the shield, compared to what the dose rate would be if there was no shield at all.

4.3 Evaluation of existing radiation shields with the aim to identify inadequate shields

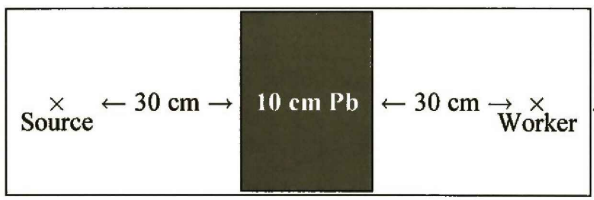
4.3.1 Introduction

The logic behind Eq. (4.1) is applied to see whether existing shields at the Radionuclide Production facility of *iThemba LABS* meet the required standards. The processing hotcells will be investigated first, then the target store room and then the radio-pharmaceutical dispensing laboratory.

4.3.2 Processing hotcells

Maximum realistic dose rate with present shielding

On an arbitrarily chosen day in September 2003, a radiation level of almost 200 μSv/h was measured in front of a hotcell in which a radiochemical separation was being performed. This indicates that dose rates in front of hotcells may be excessively high. As argued above, 10 Ci ^{22}Na is the maximum realistic activity inside a hotcell. The dose rate in front of a hotcell with this activity inside it, is now calculated. It is assumed that the 10 Ci ^{22}Na source is at a point 30 cm from the inside surface of the 10 cm thick lead wall, and that the body of the chemical technologist is 30 cm away from the outside of the lead wall of the hotcell:



The calculated dose rate is 375 μSv/h at the body-position of the worker. According to the table of maximum staytimes for radiation work on page 35, a radiation worker may only work in front of such a hotcell for 15 minutes per day or shift. This is too restrictive, because cutting open the target and then doing the chemical processing will take much longer than this.

Conclusion: The maximum realistic dose rate in front of a processing hotcell is about 375 μSv/h.

Maximum tolerable dose rate

The following realistic assumptions are made:

- Design-base dose for hotcell work: 2 mSv per year

NWU LIBRARY

- Maximum realistic staytime for hotcell work: 200 hours per year in front of the processing hotcells.
- Maximum realistic activity inside a hotcell: equivalent to 10 Ci ^{22}Na.

According to Eq. (4.1), the maximum tolerable dose rate will be

$$\begin{aligned}\text{Maximum tolerable dose rate} &= \frac{\text{Design-base dose}}{\text{Annual staytime}} \\ &= \frac{2\ \text{mSv}}{200\ \text{h}} \\ &= 10\ \mu\text{Sv/h}. \end{aligned} \tag{4.4}$$

This value is far lower than the maximum realistic dose rate. This means that the shield is wholly inadequate, and that personnel doses may be unnecessarily high, so that the shield needs to be redesigned.

Projected annual dose for the present shield

It is very clear that the present shield thickness is inadequate. According to Eq. (4.2) the projected annual dose with the present thickness of lead of the hotcells will be as high as

$$\begin{aligned}\begin{pmatrix}\text{Projected} \\ \text{annual dose}\end{pmatrix} &= \begin{pmatrix}\text{Maximum realistic} \\ \text{dose rate}\end{pmatrix} \times \begin{pmatrix}\text{Maximum realistic} \\ \text{annual staytime}\end{pmatrix} \\ &= \dot{D}_{\text{av}} \times t_{\text{yr}} \\ &\approx 375\ \mu\text{Sv/h} \times 200\ \text{hours} \\ &\approx 75\ \text{mSv}\end{aligned}$$

which is far above the legal dose limit and the design-base dose.

Conclusion

The lead thickness of the present processing hotcells is not adequate at all. These hotcells must be redesigned with thicker lead walls.

Dose-rate reduction factor

The decrease of the dose rate through the existing 10 cm lead shield, calculated with the MathCAD worksheet, is shown in Figure 4.1.

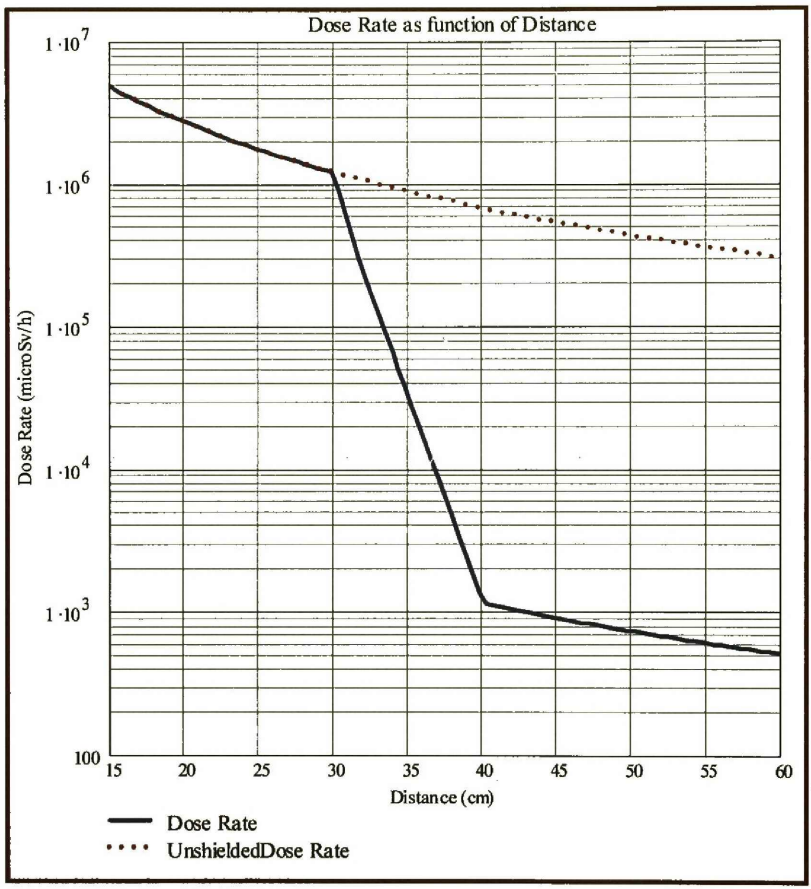


Figure 4.1: *Dose rate reduction by the 10 cm Pb shield of the processing hotcells. The shield starts at 30 cm in the above graph and stops at 40 cm. The solid line shows how the Pb shield lowers the dose rate coming through the lead. The dotted line shows what the dose rate would have been if there was no shield at all. The dose reduction or dose attenuation factor is about 590, i.e. the shield makes the dose rate 590 times less than it would have been without the shield. This is inadequate, because the dose rate on the side of the shield where workers do their work, is far too high and may easily overexpose radiation workers.*

4.3.3 Target store room

Background

After bombardment by the particle beam, the targets are driven to a target store room, on the transporter system. The target transport system consists of a trolley driving on tracks.

Figure 2.3 on page 18 shows a trolley on tracks, while Figure 2.6 on page 22 shows the target store-room, before the existing shield was built.

This transporter system (trolleys & tracks) was obtained from a financial institution in the Gauteng province of South Africa. It was not designed for the purpose *iThemba LABS* uses it for. The air in the Radionuclide Production facility contains moisture and corrosive chemical vapours. The bronze electrical contact strips on the tracks are not well suited to this corrosive chemical environment. As a result, the tracks of the transporter system must be cleaned on a regular maintenance schedule. The decontamination workers have to clean and rub the electrical contact strips until they are clean. This job can not always be done fast. The trolley tracks run through areas of the Radionuclide Production facility where high dose rates are regularly encountered. Cleaning of transporter tracks is therefore a major cause of exposure for decontamination workers.

The photographs in Figure 4.2 to Figure 4.8 will make the current situation clear.

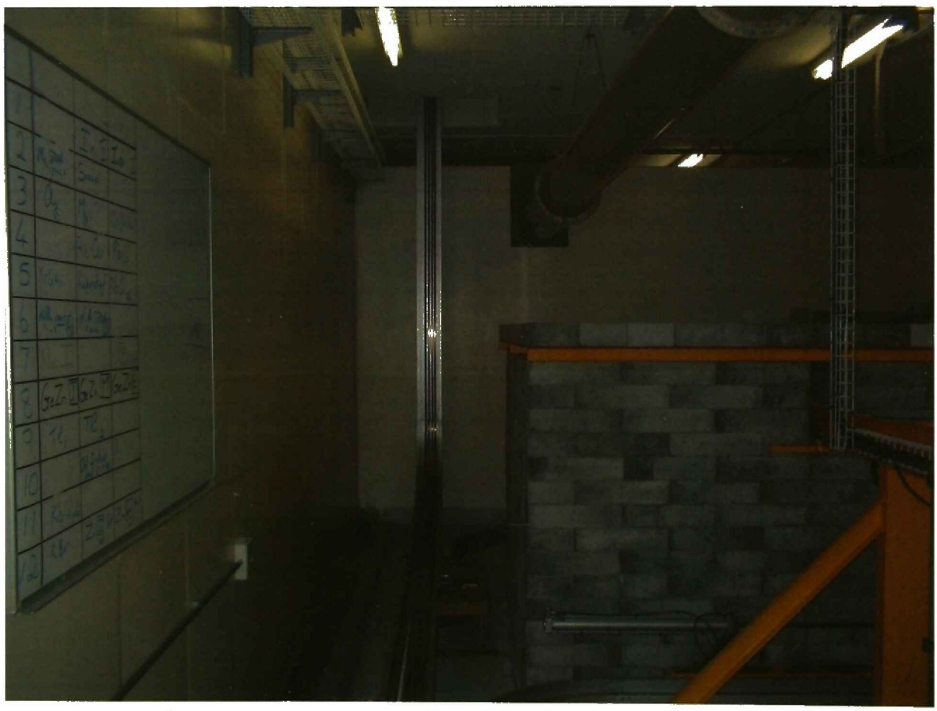


Figure 4.2: *The track for the target-transporting trolleys runs next to a shielding wall around the target storage carousel and then goes up through the roof to the hotcells. The stacked concrete shielding bricks can easily be seen. Every brick is about 10 cm high × 20 cm wide × 40 cm long. The stacked concrete shielding wall facing the horizontal track section in the foreground, is 40 cm thick.*



Figure 4.3: *Another view of a track for the target-transporting trolleys running next to a shielding wall around the target storage carousel. This is the rear shield and it is only 20 cm thick because there is simply not enough space to build a thicker wall—note the small gap between the track and the shielding wall.*



Figure 4.4: *Same track & wall as Figure 4.3, photographed from opposite side.*

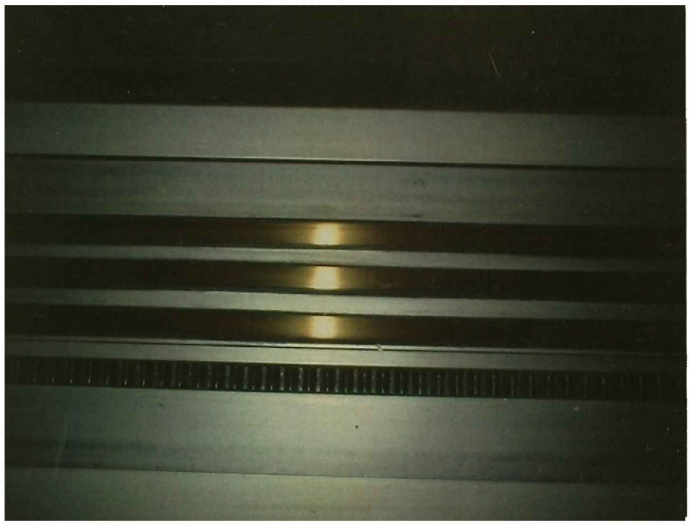


Figure 4.5: *Close-up view of the electrical contact strips that corrode easily and require regular scrubbing and vacuuming to enable the target transporter trolley system to work with high reliability. This cleaning work takes time and can not be mechanised and automated. The only way to make it safer to do the maintenance work, is to improve the shielding.*

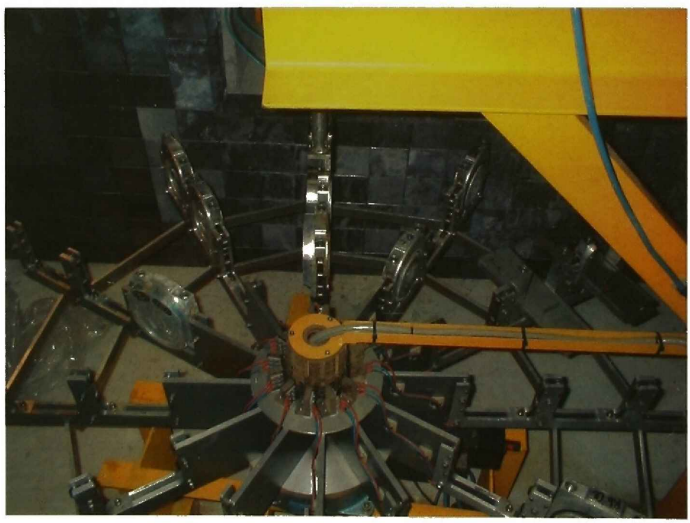


Figure 4.6: *The wheel-like target-storage carousel. The lead inner wall inside the concrete outer wall is stacked on some sides only, because there is no space on other sides.*
The maximum realistic total activity in all the targets stored here in this wheel, is estimated to be radiologically equivalent to approximately 100 Ci ^{22}Na.



Figure 4.7: *View of the stacked concrete shielding in the target store room. Directly above the wheel-like target storage carousel, is a shielding roof constructed of steel blocks and concrete bricks.*



Figure 4.8: *Remote manipulator for loading new targets into target holders. The 10 cm lead and thick glass protect the radiation workers. Trolley-tracks can be seen in the background. This gives an idea of the high dose rates around the target holders, even before the targets are irradiated. The target holders are very radioactive because radionuclides were produced in them during previous irradiations.*

Design-base dose

Decontamination workers have many routine tasks. To stay within dose limits, no single routine task may contribute more than about 1 mSv per year to their dose, and is termed the design-base dose.

Measured dose rates

A floor-plan of the target store room, is shown in Figure 4.9. This is a rough sketch and is not to scale. On a specific date in August 2003, dose rates were measured in the target storage room in the positions where decontamination workers have to clean the tracks of the transporter system. The measured dose rates are also shown in Figure 4.9.

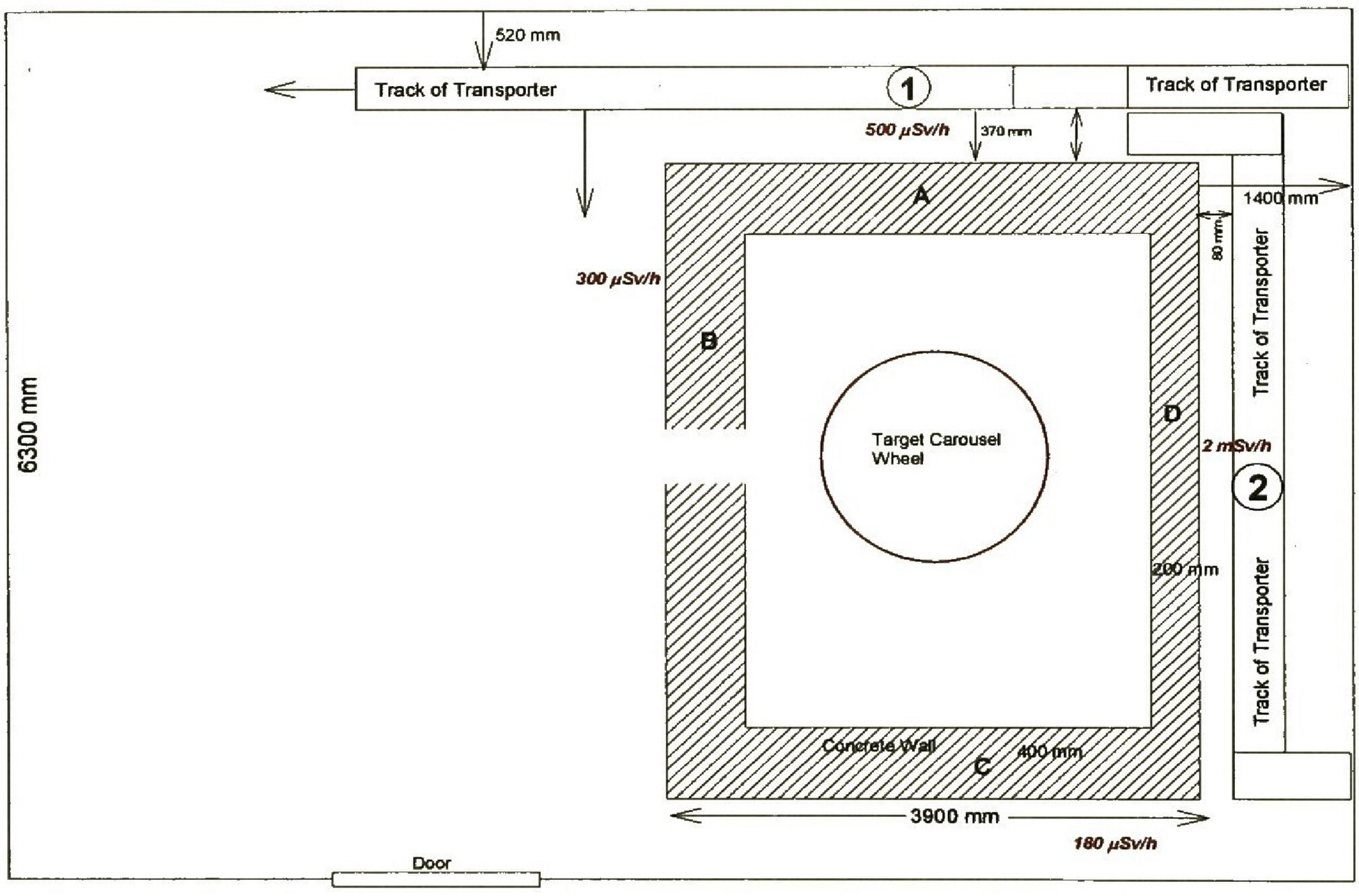


Figure 4.9: *The target store room in the Radionuclide Production facility. This room is located in the basement of the building. Irradiated targets are stored in a wheel-like carousel, surrounded by stacked concrete brick shielding. Decontamination workers have to clean the transporter system tracks regularly to ensure the reliable operation of the transporter trolley system. The dose rates in the diagram were measured on an arbitrarily chosen day in August 2003.*
As a result of space restrictions, concrete shielding wall D is only 20 cm thick. Therefore dose rates at position ② can be dangerously high.

Projected annual dose for measured dose rates

Decontamination workers have to spend about 1 hour per month cleaning the tracks in this room (Mackriel, 2003). The highest measured dose rate at the position of the transporter tracks, on the specific day in August 2003, was 2 mSv/h. This means that a year of cleaning of the tracks will cause a yearly dose of

$$12 \text{ months} \times 1 \text{ hour.month}^{-1} \times 2 \text{ mSv/h} = 24 \text{ mSv}.$$

This dose is excessively high, and exceeds the annual dose limit. As a result of the inadequate shielding, this single routine task may consume the whole dose budget of the decontamination workers, and will leave no room for other jobs to be done. The shielding in the target store is clearly inadequate and should be re-designed.

Calculated maximum realistic dose rates

The target store room was visited on an arbitrary day in 2003, and dose rates were measured at positions ① and ②, shown in Figure 4.9. However, the maximum activity that can be present in that room, may be higher — equivalent to about 3.7 TBq or 100 Ci of ^{22}Na. With the assumptions that,

- all the activity in the different targets in the target carousel is concentrated at a point source 1.5 m from the inside surface of every shielding wall around the wheel-like carousel;
- the maximum total activity in the targets is equivalent to 100 Ci ^{22}Na;
- the body of the radiation worker is 0.5 m outside the outer surface of the shielding walls;

dose rates have been calculated using a MathCAD worksheet. The calculated results are summarised in Table 4.2.

Table 4.2: *Maximum realistic dose rates at selected positions in the target store room. Calculated dose rates with 100 Ci ^{22}Na stored in target carousel.*

Position	Dose rate
Position ①	3.2 mSv/h
Position ②	28 mSv/h

As a result of space restrictions, concrete shielding wall D in Figure 4.9 is only 20 cm thick. Therefore the dose rate at position ② is very high. The dose rate at position ① is lower than at position ② because the concrete shielding wall is thicker. Both dose rates are, nevertheless, far too high to be considered safe.

Projected annual dose for calculated maximum realistic dose rates

At Position ① in Figure 4.9, i.e. at the transporter track opposite shielding wall A, the calculated maximum realistic dose rate is 3.2 mSv per hour. If a worker has to work there 1 hour per month, 12 months per year, the total exposure time will be 12 hours, and the total yearly dose will be about 38 mSv, which is unacceptably high, and exceeds the annual dose limit of *iThemba LABS* by far. As a result of the inadequate shielding, this single routine task will consume the whole dose budget of the decontamination workers, and will leave no room for other jobs to be done.

At Position ② in Figure 4.9, i.e. at the transporter track opposite shielding wall B, the calculated maximum realistic dose rate is 28 mSv per hour. If a worker has to work there 1 hour per month, 12 months per year, the total exposure time will be 12 hours, and the total yearly dose will be above 300 mSv. This is far too high to be unacceptable, and is far above legal dose limits. As a result of the inadequate shielding, this single routine task can potentially consume the whole dose budget of the decontamination workers in less than 1 month, and this will leave no room for other jobs to be done during the rest of the year.

Maximum tolerable dose rate in the target store room

If Eq. (4.1) is applied, the maximum tolerable dose rate in the target store room at the positions of the transporter track, is found to be in the order of

$$\begin{aligned}\text{Maximum tolerable dose rate} &= \frac{\text{Design-base dose}}{\text{Annual staytime}} \\ &= \frac{1\ \text{mSv}}{12 \times 1\ \text{hour}} \\ &\approx 80\ \mu\text{Sv/h}\end{aligned}$$

The shielding in the target store room must be designed for a maximum tolerable dose rate of $\sim 80\ \mu$Sv/h.

Dose reduction factors of existing shields

The decrease of the dose rate through 20 cm and 40 cm concrete shields, calculated with the MathCAD worksheet, is shown in Figure 4.10

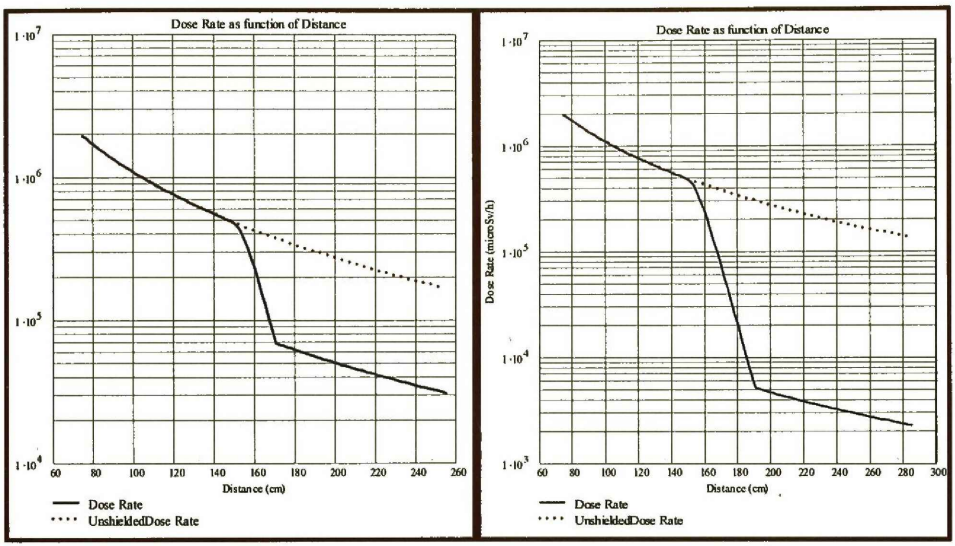


Figure 4.10: *Dose rate reduction by the 20 cm thick concrete shield (left) and by the 40 cm concrete shield (right). The dose reduction factor of the 20 cm concrete shield is only 5.4 (very low) and for the 40 cm thick shield it is better at 58. It is evident that thin concrete shields are very inefficient!*
The solid lines show how the concrete shields lowers the dose rates coming through the concrete. The dotted lines show what the dose rates would be if there was no shield at all.

Conclusion

The shielding in the target store room is clearly inadequate and should be re-designed.

4.3.4 Radio-pharmaceutical dispensing laboratory

There are two well-known problems with shielding in the present radio-pharmaceutical dispensing laboratory:

1. An important problem with the design of the hotcells in the present radio-pharmaceutical dispensing laboratory is that there are large potential gaps between the 10 cm thick steel shield doors. These doors slide from side to side, but there are almost always big gaps between the sliding panels. Radiation can radiate through these gaps.

2. The walls of the present Radio-pharmaceutical dispensing laboratory are made from thin, pre-fabricated material, with walls only about 1 cm thick. On one side of the laboratory, a radionuclide transport trolley containing a radioactive object can drive into this room, and there will only be about 2 mm of shielding between a worker inside this laboratory and the source. There will be 5 cm of Pb between workers outside this laboratory and the source. The other side of the laboratory is

potentially more problematic — if a transport trolley drives in here and carries a strong source, there will be only a few millimetres of shielding between the trolley and people standing inside or outside the laboratory.

The above two problems are illustrated in Figure 4.11 to Figure 4.18.



Figure 4.11: *Front view of the sliding shielding doors in the Radio-pharmaceutical dispensing laboratory. The shielding is 10 cm steel. Note the gaps between the sliding shielding doors. Radiation can "stream" through these gaps.*

NWU LIBRARY



Figure 4.12: *Angled view of the sliding shielding doors in the Radio-pharmaceutical dispensing laboratory. The shielding is 10 cm steel. Note the gaps between the sliding shielding doors.*

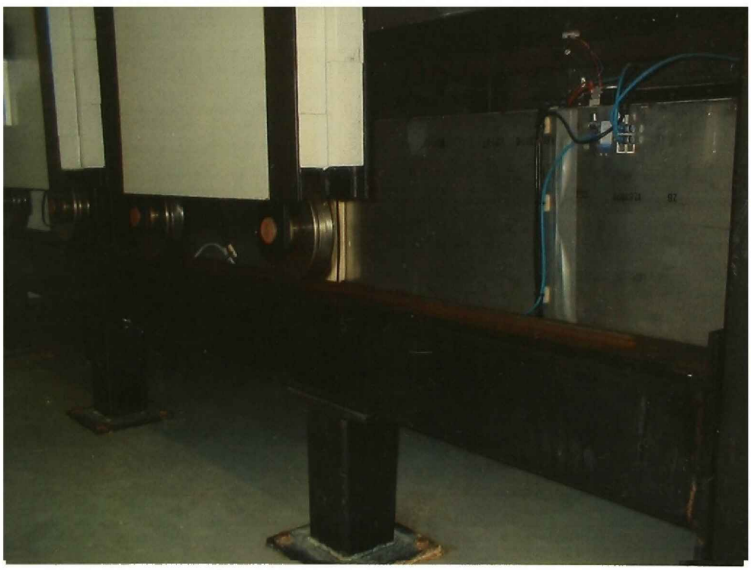


Figure 4.13: *Track-section 1. The transport trolley runs on a track inside the stainless steel box below the hotcells in the Radio-pharmaceutical dispensing laboratory. The stainless steel is less than 2 mm thick. Behind this track, there is a high 5 cm thick lead wall to shield personnel outside this room against radiation. Workers inside this laboratory are not shielded against sources transported by the trolley.*

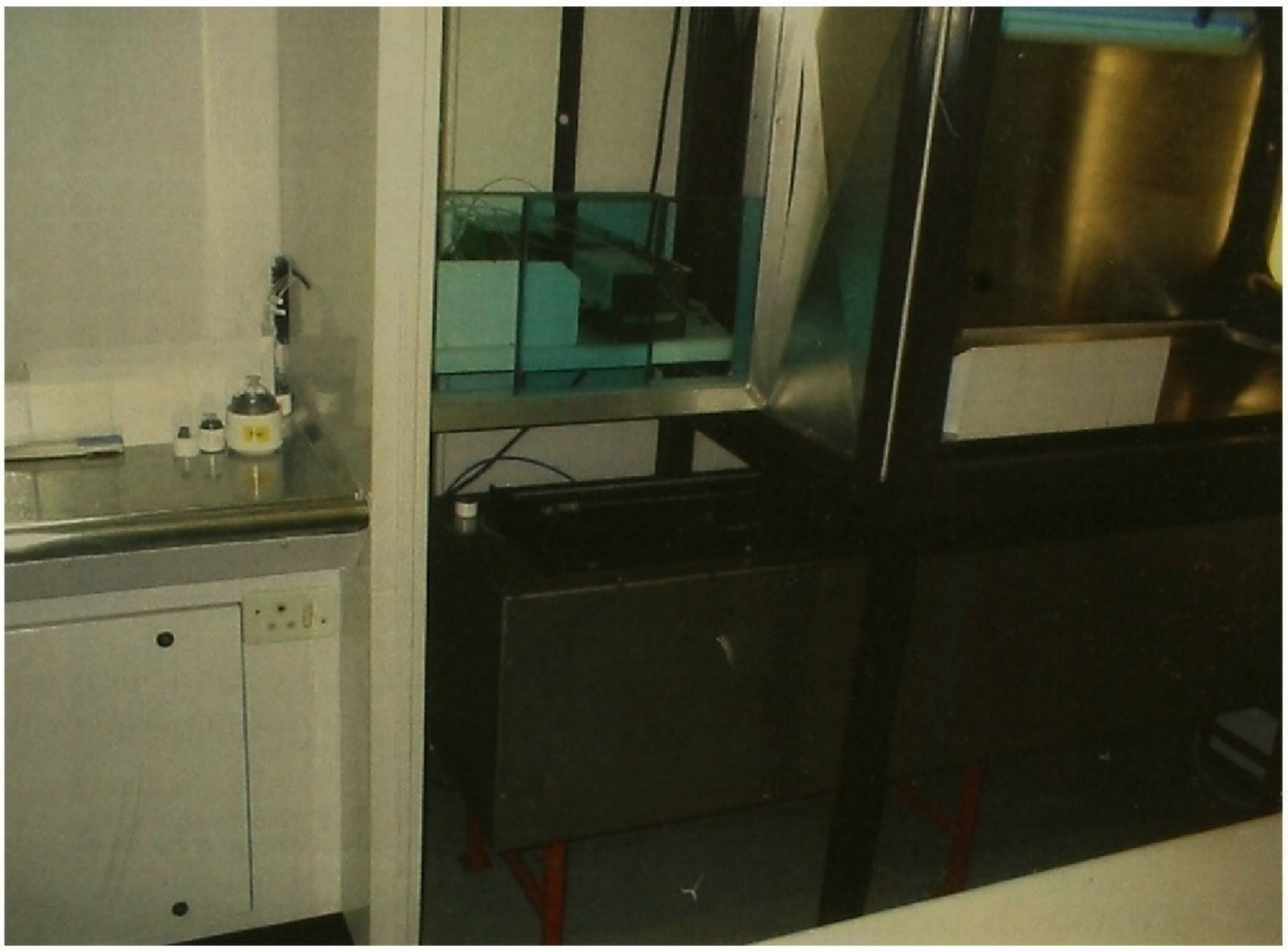


Figure 4.14: *Track-section 2. The other side of the Radio-pharmaceutical dispensing laboratory where the transport trolley can also run on a track inside the stainless steel box below the cabinets in the Radio-pharmaceutical dispensing laboratory. The stainless steel is less than 2 mm thick. There is no extra shielding around this section of the track. People inside and outside the Radio-pharmaceutical dispensing laboratory are not shielded against sources transported by the trolley in this section of track.*



Figure 4.15: *View of the lead shield behind track section 1 in the Radio-pharmaceutical dispensing laboratory. The lead thickness is 5 cm and it reaches to a height of about 180 cm. It shields persons outside the laboratory. Shielding for workers inside the laboratory is inadequate, however.*

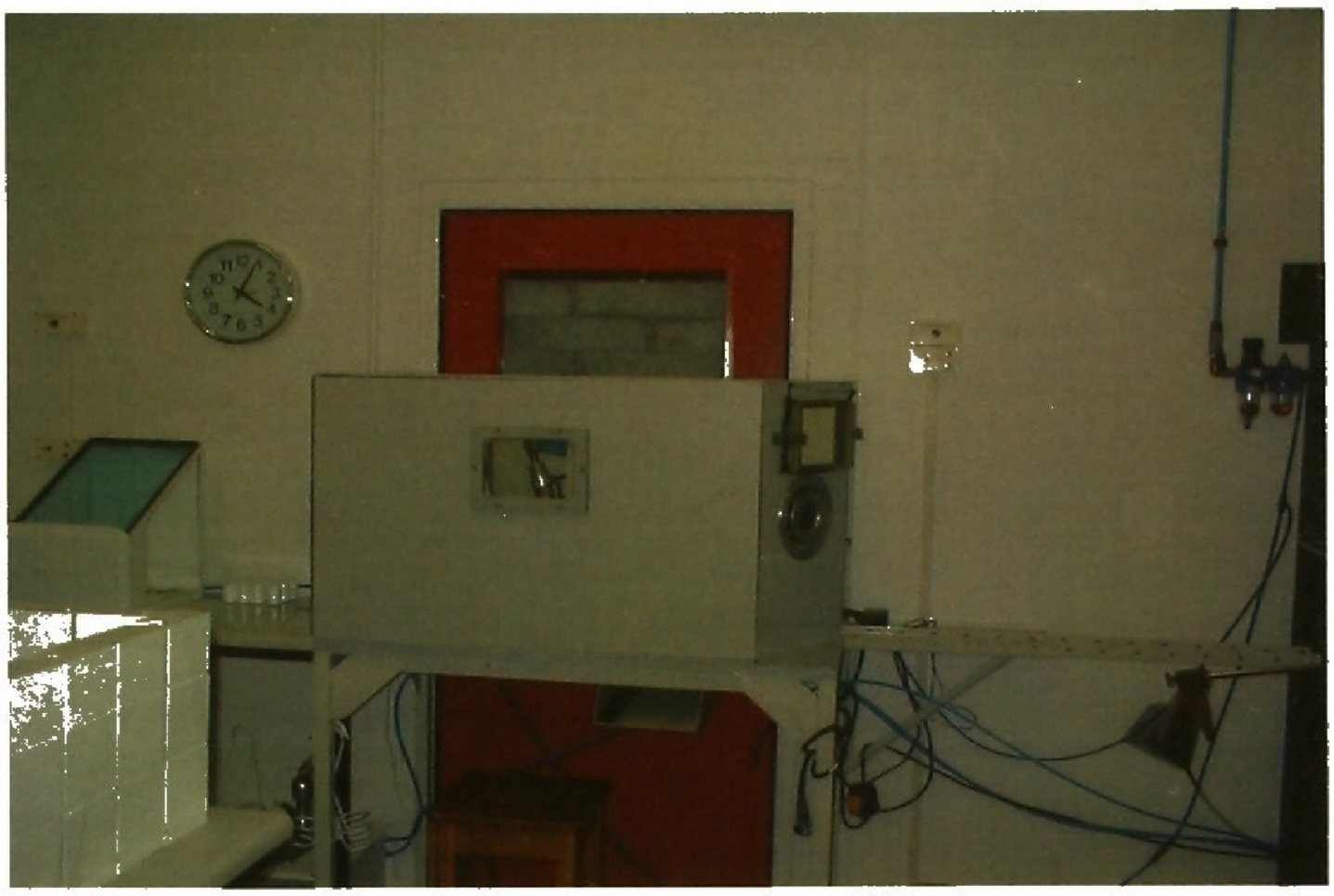


Figure 4.16: *The back wall of the Radio-pharmaceutical dispensing laboratory. Note the red door, which tells that this is an entry into the Red Area of the Radionuclide Production building. Only a thin "prefab" wall separates this laboratory from the Red Area. High dose rates and strong sources are handled in the Red Area. Because the "prefab" wall does not provide shielding against ionising photons, a concrete wall was stacked inside the Red Area. This wall is only 20 cm thick, and its shielding efficiency is only about a factor 5.4 for ^{22}Na. The concrete wall stacked inside the Red Area is visible through the window in the red door.*



Figure 4.17: *Entrance door to the Radio-pharmaceutical dispensing laboratory. This wall is opposite track section 1, so that persons standing here will be shielded by 5 cm lead. In the background, the one row of 6 hotcells is visible.*
In June 2002, a trolley carrying an irradiated target, was sent to a hotcell, but did not stop at the hotcell but drove all the way into the Radio-pharmaceutical dispensing laboratory, causing dose rates to reach dangerously high levels — above 10 mSv/h.

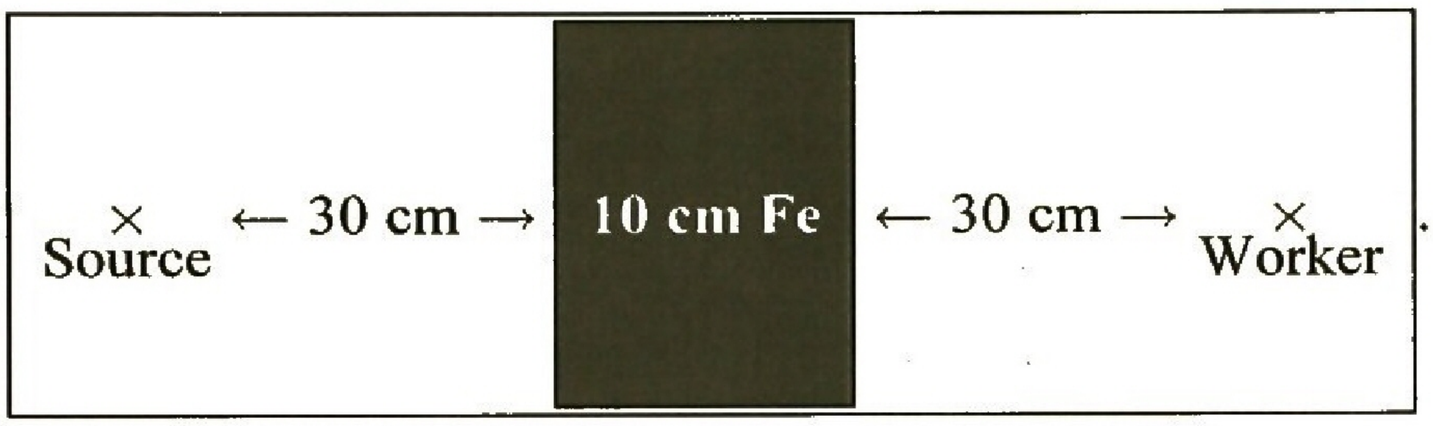


Figure 4.18: *The radio-pharmaceutical dispensing laboratory opposite track section 2, seen in Figure 4.14.* ***Less than 2 mm of steel and only a few millimetres of "prefab" wall is between a potential source inside the laboratory and people standing around the posters at the display area*** *shown here.*
Until July 2002, tour groups, including school tours, gathered here for information sessions lasting about 15 to 30 minutes. There is no radiation monitor or radiation alarm here. Dose rates are not measured and not logged. There is no way to know whether or not high dose rates prevailed here and in other parts of the Radionuclide Production building.
Because there is no Area Radiation Monitoring System (ARMS) in the Radionuclide Production building, it is impossible to go back and look at historical dose rate records to identify bad designs, inadequate shields and dangerous areas. It is also very difficult to, e.g. refute claims of overexposures to tour groups where radiation dosimetry was not worn.

A number of calculations are now presented to prove that dangerously high radiation levels can be encountered inside and outside the radiopharmaceutical dispensing laboratory.

Scenario 1: Source inside pharmaceutical dispensing hotcell and 10 cm thick sliding steel doors closed — dose rate inside radio-pharmaceutical dispensing laboratory

With the following source-shield-worker configuration,



and a 1 Ci ^{22}Na source inside the pharmaceutical dispensing hotcell, the maximum realistic dose rate at the body-position of a worker inside the radio-pharmaceutical dispensing laboratory, is calculated to be 1.1 mSv/h with the MathCAD worksheet.

Figure 4.19 shows how the dose rate is lowered by the shield.

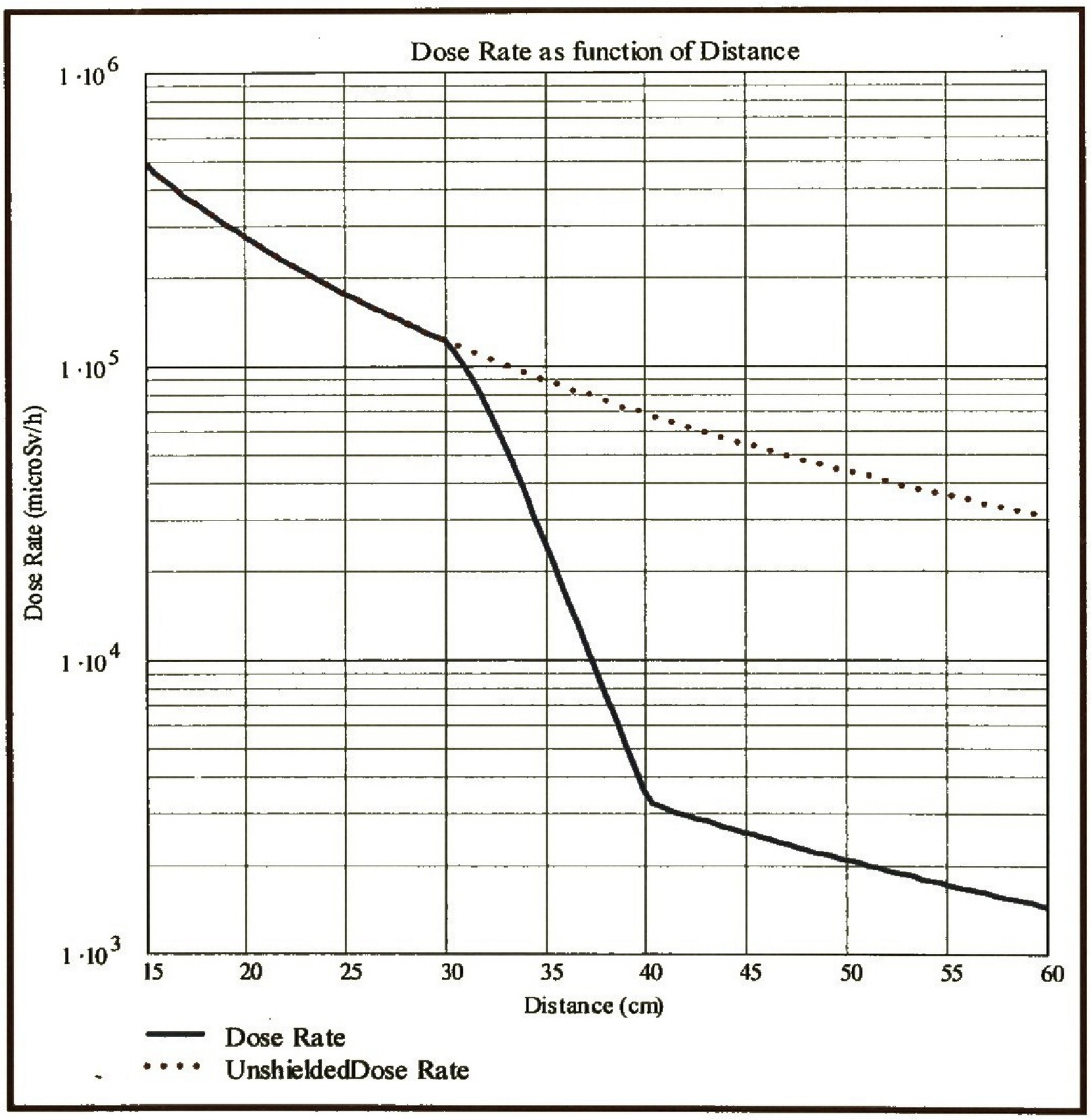


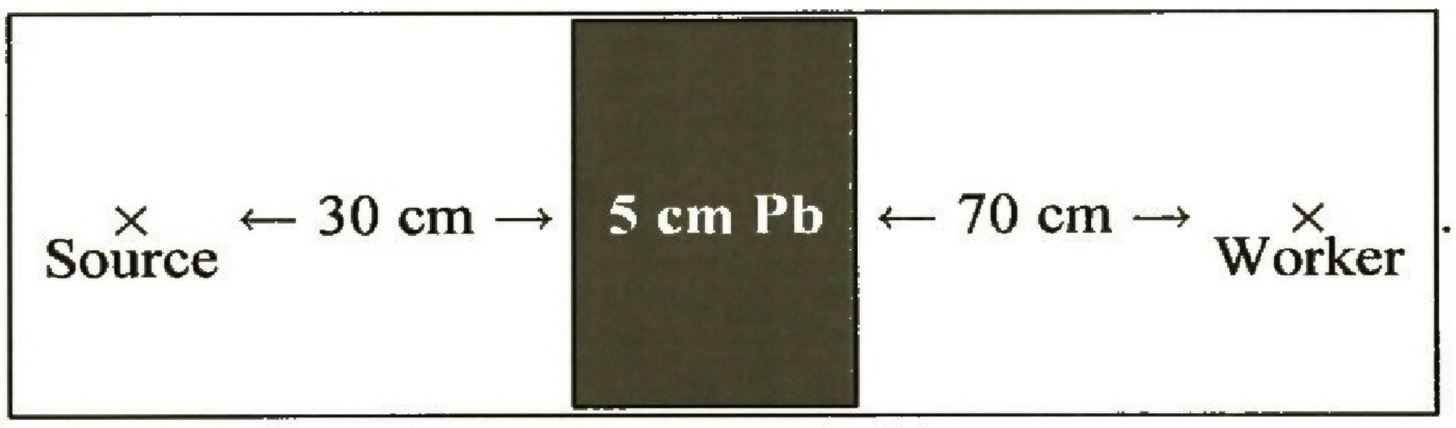
Figure 4.19: *With a 1 Ci ^{22}Na source inside the pharmaceutical dispensing hotcell, the maximum realistic dose rate at the body-position of a worker inside the radio-pharmaceutical dispensing laboratory, is calculated to be 1.1 mSv/h.*

The dose attenuation factor for the ^{22}Na source and the 10 cm thick steel shield, is 21. This means that the steel lowers the dose rate on the other side of the shield to a level 21 times lower than it would be if there was no shield. A dose attenuation factor of 21 is, generally, not nearly good enough for strong radioactive sources.

Scenario 2: Source inside pharmaceutical dispensing hotcells, above track section 1 — dose rate in passage outside radio-pharmaceutical dispensing laboratory

Suppose a source with maximum realistic activity is placed inside the pharmaceutical dispensing hotcell (which is above track section 1). There is 5 cm Pb between the source and somebody standing or walking in the passage (display posters have been put up there).

With the following source-shield-worker configuration,



and maximum realistic activity source if activity 1 Ci ^{22}Na, is inside the pharmaceutical dispensing hotcell. Then the maximum realistic dose rate at the body-position of a worker in the passage outside the radio-pharmaceutical dispensing laboratory, is calculated with the MathCAD worksheet to be $\boxed{\dot{D}_{mr} = 400\ \mu Sv/h}$.

Figure 4.20 shows how the dose rate is lowered by the 5 cm thick Pb shield.

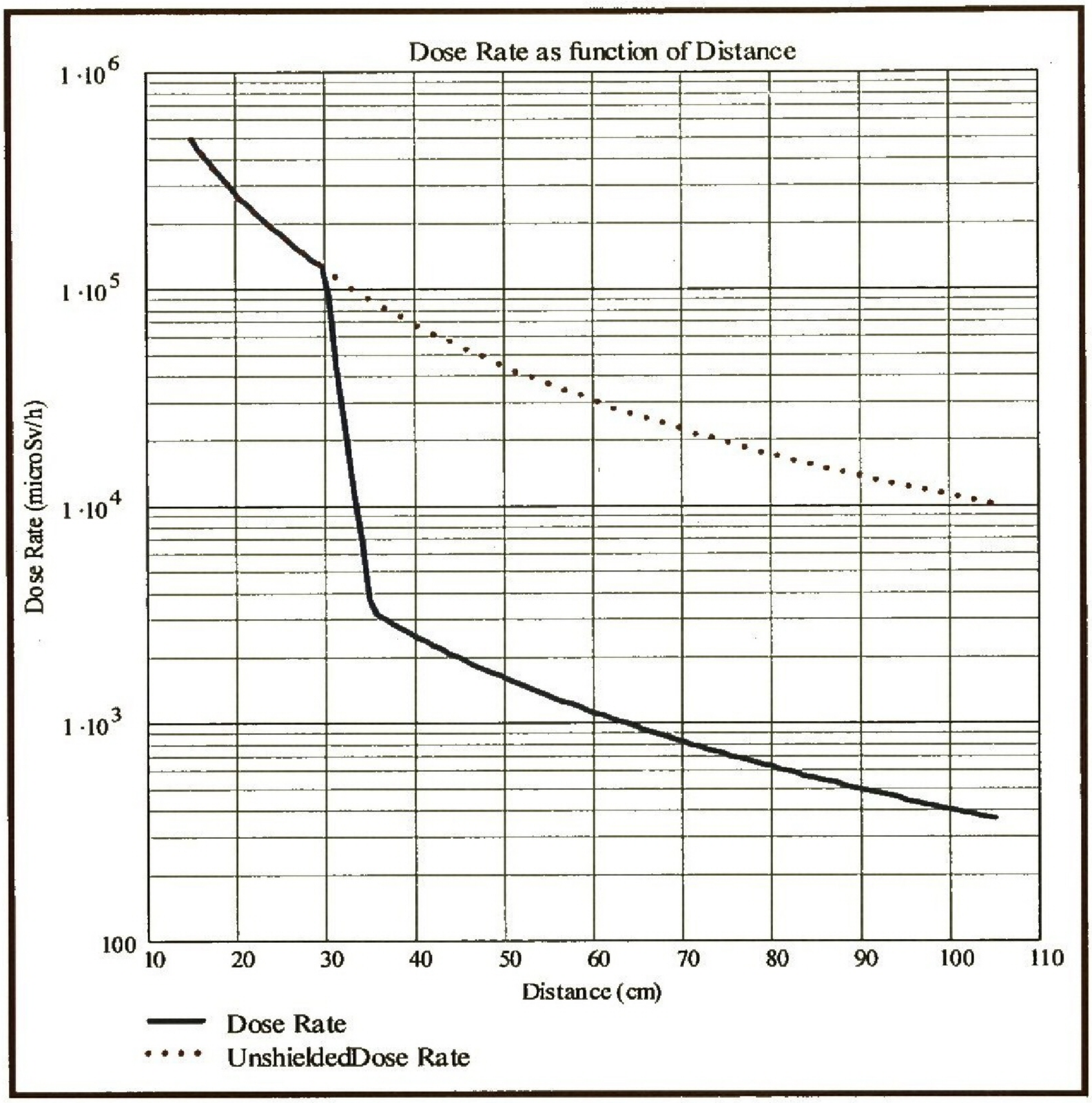
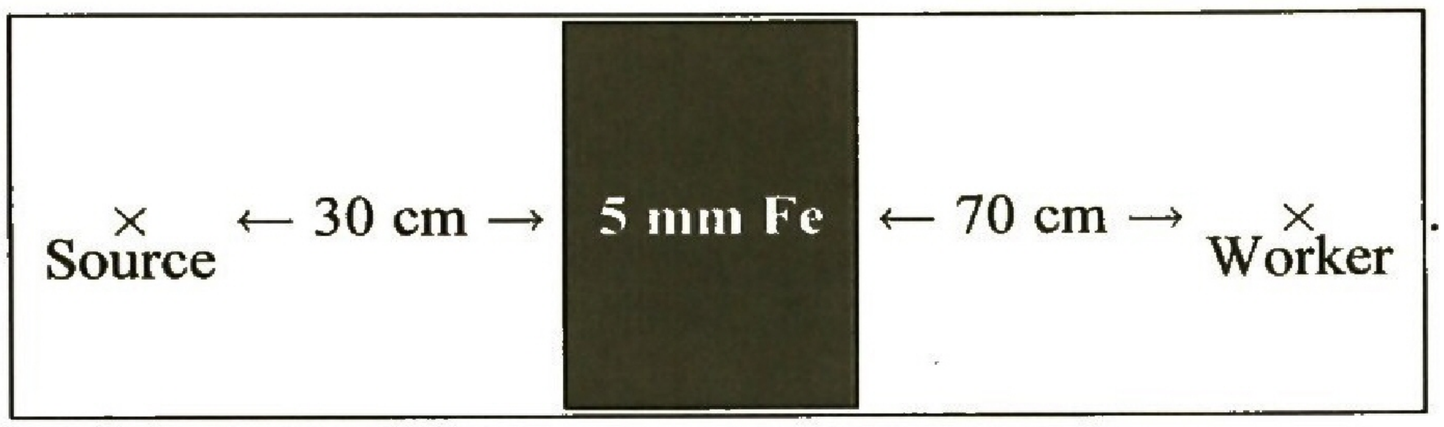


Figure 4.20: *Dose rate in passage on the outside of the radio-pharmaceutical dispensing laboratory, opposite the pharmaceutical dispensing hotcell. A source of maximum realistic activity is inside the pharmaceutical dispensing hotcell. The radiation is attenuated by the 5 cm Pb shield. The maximum realistic dose-rate in the passage is 400 μSv/h, which is excessively high. The dose attenuation factor for the above source-shield-worker configuration is 27.*

Scenario 3: Source inside track section 2 — dose rate in passage opposite this side

Suppose a source with maximum realistic activity is inside track section 2 — see Figure 4.14 on page 51 as well as Figure 4.18 on page 53. There is only 5 mm Fe between the source and somebody standing or walking in the passage (display posters have been put up there).

With the following source-shield-worker configuration,



and with a maximum realistic activity source 1 Ci ^{22}Na, inside Track Section 2 enclosure, the maximum realistic dose rate at the body-position of a person in the passage outside the nearest wall, is calculated with the MathCAD worksheet to be

$$\dot{D}_{mr} = 10 \text{ mSv/h}$$

Figure 4.21 shows how the dose rate is lowered by the prefabricated wall panel, which is assumed to be equivalent to 5 mm steel.

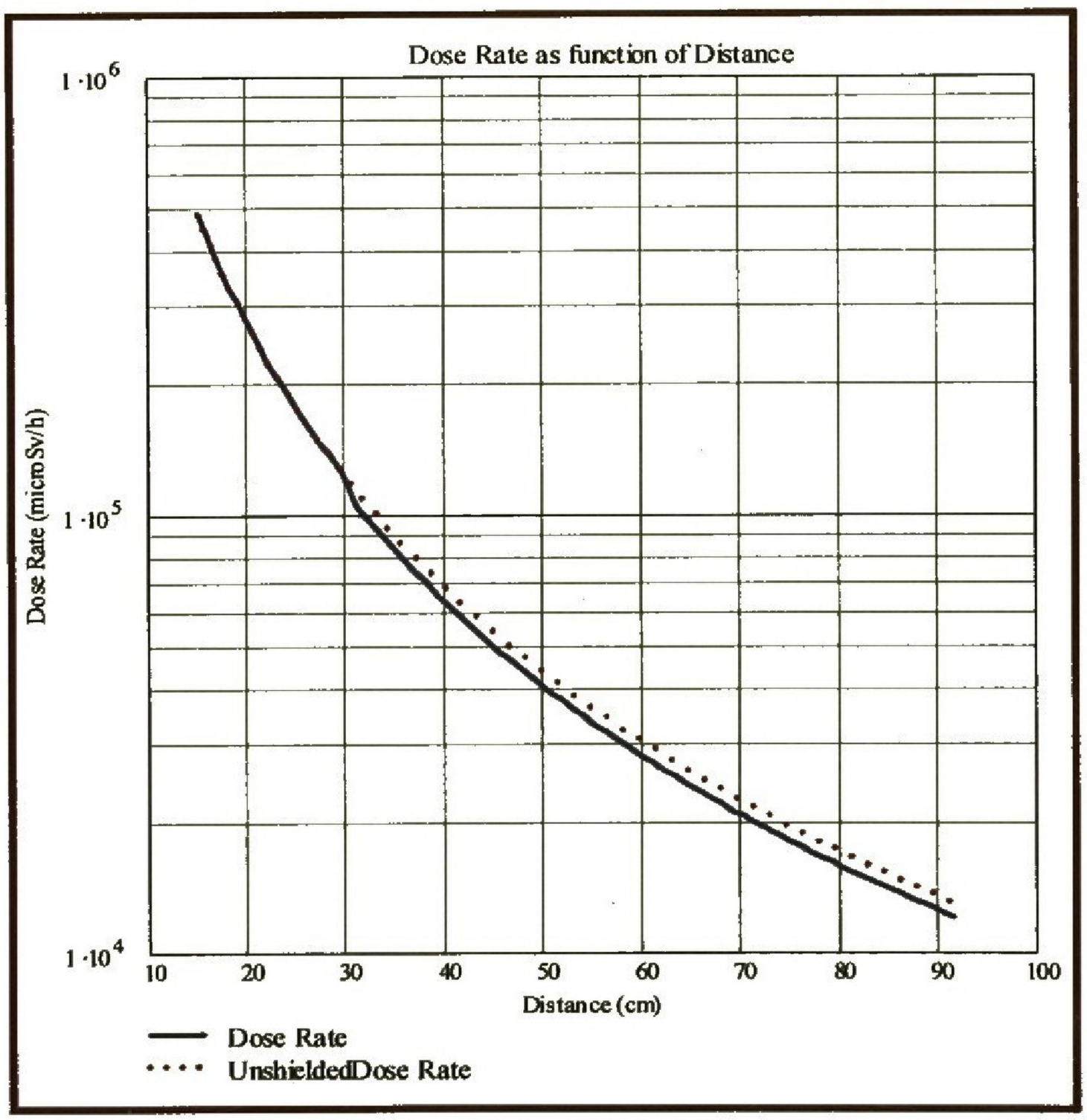


Figure 4.21: *Dose rate in passage on the outside of the radio-pharmaceutical dispensing laboratory, opposite track section 2. A source of maximum realistic activity is inside track section 2. The radiation is insignificantly attenuated by the prefabricated wall, assumed to have a shielding efficiency the same as 5 mm steel. The maximum realistic dose-rate in the passage is 10 mSv/h, which is excessively high. The dose attenuation factor for the above source-shield-worker configuration is insignificantly low.*

Conclusion

The radio-pharmaceutical dispensing laboratory lacks proper shielding. Maximum realistic dose-rates are extremely high and dangerous. This laboratory should be completely redesigned, as it is *potentially very dangerous* at present.

Development of shield design criteria for the radio-pharmaceutical dispensing laboratory

- **Design-base dose**

The design-base dose for work inside radio-pharmaceutical dispensing laboratory is 2 mSv per year.

The design-base dose for passing by outside the radio-pharmaceutical dispensing laboratory and standing at poster display areas is 0.3 mSv per year.

- **Maximum realistic staytime for workers inside radio-pharmaceutical dispensing laboratory**

The maximum realistic staytime inside the radio-pharmaceutical dispensing laboratory is 200 hours per year.

- **Maximum realistic staytime for workers just outside the radio-pharmaceutical dispensing laboratory**

The maximum realistic staytime just outside the radio-pharmaceutical dispensing laboratory, walking by and watching display posters, *while strong sources are in critical positions, leading to high dose rates outside laboratory,* is 10 hours per year.

- **Maximum tolerable dose rate inside radio-pharmaceutical dispensing laboratory**

According to Eq. (4.1) on page 37, the maximum tolerable dose rate will be

$$\begin{aligned} \text{Maximum tolerable dose rate} &= \frac{\text{Design-base dose}}{\text{Annual staytime}} \\ &= \frac{2\ \text{mSv}}{200\ \text{h}} \\ &= 10\ \mu\text{Sv/h} \end{aligned} \tag{4.5}$$

- **Maximum tolerable dose rate outside the radio-pharmaceutical dispensing laboratory**

According to Eq. (4.1) on page 37, the maximum tolerable dose rate will be

$$\begin{aligned}\text{Maximum tolerable dose rate} &= \frac{\text{Design-base dose}}{\text{Annual staytime}} \\ &= \frac{0.3\ \text{mSv}}{10\ \text{h}} \\ &= 30\ \mu\text{Sv/h}\end{aligned} \tag{4.6}$$

Projected annual doses with present design of the radio-pharmaceutical dispensing laboratory

Scenario 1: Source inside pharmaceutical dispensing hotcell and worker shielded by 10 cm steel shield.

According to Eq. (4.2) on page 37, the projected annual dose with the present thickness of steel of the hotcells will be as high as

$$\begin{aligned}\begin{pmatrix}\text{Projected}\\ \text{annual dose}\end{pmatrix} &= \begin{pmatrix}\text{Maximum realistic}\\ \text{dose rate}\end{pmatrix} \times \begin{pmatrix}\text{Maximum realistic}\\ \text{annual staytime}\end{pmatrix} \\ &= \dot{D}_{\text{mr}} \times t_{\text{yr}} \\ &= 1.1\ \text{mSv/h} \times 200\ \text{hours} \\ &= 220\ \text{mSv}\end{aligned}$$

which is far above the legal dose limit and the design-base dose.

Scenario 2: Source inside pharmaceutical dispensing hotcell and worker outside the laboratory, shielded by 5 cm Pb shield.

According to Eq. (4.2) on page 37, the projected annual dose with the present thickness of steel of the hotcells will be as high as

$$\begin{aligned}\begin{pmatrix}\text{Projected}\\ \text{annual dose}\end{pmatrix} &= \begin{pmatrix}\text{Maximum realistic}\\ \text{dose rate}\end{pmatrix} \times \begin{pmatrix}\text{Maximum realistic}\\ \text{annual staytime}\end{pmatrix} \\ &= \dot{D}_{\text{mr}} \times t_{\text{yr}} \\ &= 400\ \mu\text{Sv/h} \times 10\ \text{hour} \\ &= 4\ \text{mSv}\end{aligned}$$

which is more than 10 times higher than the design-base dose.

Scenario 3: Source inside track section 2 and worker outside laboratory, shielded by pre-fabricated wall equivalent to 5 mm steel.

According to Eq. (4.2) on page 37, the projected annual dose with the present thickness of steel of the hotcells will be as high as

$$\begin{pmatrix}\text{Projected}\\ \text{annual dose}\end{pmatrix} = \begin{pmatrix}\text{Maximum realistic}\\ \text{dose rate}\end{pmatrix} \times \begin{pmatrix}\text{Maximum realistic}\\ \text{annual staytime}\end{pmatrix}$$

$$= \dot{D}_{\text{mr}} \times t_{\text{yr}}$$

$$= 10 \text{ mSv/h} \times 10 \text{ hours}$$

$$= 100 \text{ mSv}$$

which is far higher than the design-base dose.

Conclusion

The radio-pharmaceutical dispensing laboratory is dangerously under-shielded. It should be redesigned with sufficiently thick, highly effective shielding materials such as lead.

4.4 Conclusions

The lead shielding of the processing hotcells are not thick enough and must be upgraded.

The shielding inside the target store room is inadequate and must be radically upgraded.

The radio-pharmaceutical dispensing laboratory and the area around it is inherently unsafe. It must be radically redesigned and upgraded.

Chapter 5
Plan for upgrading the production facilities of the Radionuclide Production Group

5.1 Introduction

In this chapter, the planned upgrade to the radionuclide production facilities at *iThemba LABS,* is discussed.

5.2 Planned upgrade to the radionuclide production facilities at *iThemba LABS*

The Radionuclide Production Group (RPG) of *iThemba LABS* currently utilises about 50 hours of 66 MeV proton beam time per week, at a maximum beam intensity of 100 μA, to produce a variety of radionuclides. This is done in the "Elephant" target bombardment station, which can accommodate a beam current not exceeding 100 μA. The installation of a flat-top resonator for the Separated Sector Cyclotron (SSC), will enable *iThemba LABS* to produce 66 MeV proton beams of much higher intensity (i.e. beam current). In order to utilise these beams, the Vertical Beam Target Station (VBTS) and corresponding targetry have to be completed. This new target station and targetry are designed to receive a maximum beam intensity of 300 μA, which is a factor 3 higher than the existing horizontal-beam target station (known as the "Elephant"—see Figure 2.4 on page 18).

There are two ways of delivering the beam for radionuclide production. One option will be chosen, but a final decision has not been made. The one plan is to split the 400 μA 66 MeV proton beam delivered by the SSC cyclotron in the high-energy beamline, so that 100 μA goes to the existing "Elephant" and 300 μA goes to the new VBTS. If this plan is successful, there will be a 4-fold increase in radionuclide production capability at *iThemba LABS*. If it turns out that the first plan does not work, and it is not possible to send a beam to the "Elephant" and the VBTS simultaneously, there will anyhow be a 3-fold increase in the production capability for radionuclides at *iThemba LABS*. In both cases, the current processing hotcell and dispensing facilities are not sufficient to handle the increased load of radioactive material. As seen, these facilities are already inadequate with current production volumes. The hotcell and dispensing facilities therefore have to be upgraded. More targets which are also more radioactive, will be stored in the target store-room, so that the shielding in this room will also have to be upgraded.

The existing hotcell facility consists of two rows of six hotcells each. The first hotcell in each row is a reception hotcell. This means that $12 - 2 = 10$ hotcells are at this time available for chemical processing. The plan is to add 4 new hotcells to the hotcell

complex, i.e. 2 new hotcells in each row. The thickness of the outer lead walls of the existing hotcells will have to be increased since these hotcells have not been designed with the aim of handling the large amounts of activity which will be processed in the future.

The existing radiopharmaceutical dispensing facility contains laminar flow cabinets that have been provided with sliding shielding doors which provide insufficient and only partial radiation protection to staff. These must be replaced with proper dispensing hotcells. The present dispensing facility also occupies the space in the so-called Blue Area of the Radionuclide Production building where the new processing hotcells have to be installed. This means that the entire Radio-pharmaceutical dispensing laboratory has to be moved and rebuilt.

5.3 Methodology for upgrading radiation shielding

As mentioned in Chapter 1, the objectives of this study was to identify inadequate radiation shield designs in the radionuclide production facility of *iThemba LABS* and to re-design these shields for adequate protection. The following methods were used.

Step 1: Identification of inadequate shields

- Estimate realistic annual worktime at positions protected by the shield.
- Allocate a Dose Budget for the task performed there, e.g. 3 mSv per year.
- Calculate maximum tolerable dose rate (MTDR) on personnel side of the shield.
- Measure dose rates AND model the existing shields with (1) a MathCAD worksheet, and (2) the shielding code QAD-CGGP.

If measured and calculated dose rates substantially exceed maximum tolerable dose rate, the shield is inadequate and must be redesigned.

Step 2: Redesigning of inadequate shields

- Model with the MathCAD worksheet to obtain the approximate thickness of chosen shielding material.
- Verify and finalise the improved shield design with QAD-CGGP.
- Present new designs to Radionuclide Production Group management for implementation.

Summary: There are several areas where upgrading of facilities are required in order to safely and optimally use the increased 66 MeV proton beam current that will become available for radionuclide production. Some of these required improvements are to be implemented in:

1. The processing hotcell facility;
2. The target store room.
3. The radio-pharmaceutical dispensing facility;

These areas are now discussed in more detail.

5.4 The processing hotcell facility

It is planned to keep the design of the 4 new processing hotcells very much the same as the existing ones but a few changes will have to be made. Based on the findings reported in Chapter 4, all the lead walls will have to be made thicker. In Chapter 6, the required lead thickness is calculated. The lead-glass windows will also have to be thicker so that they provide close to the same shielding as the thicker lead walls.

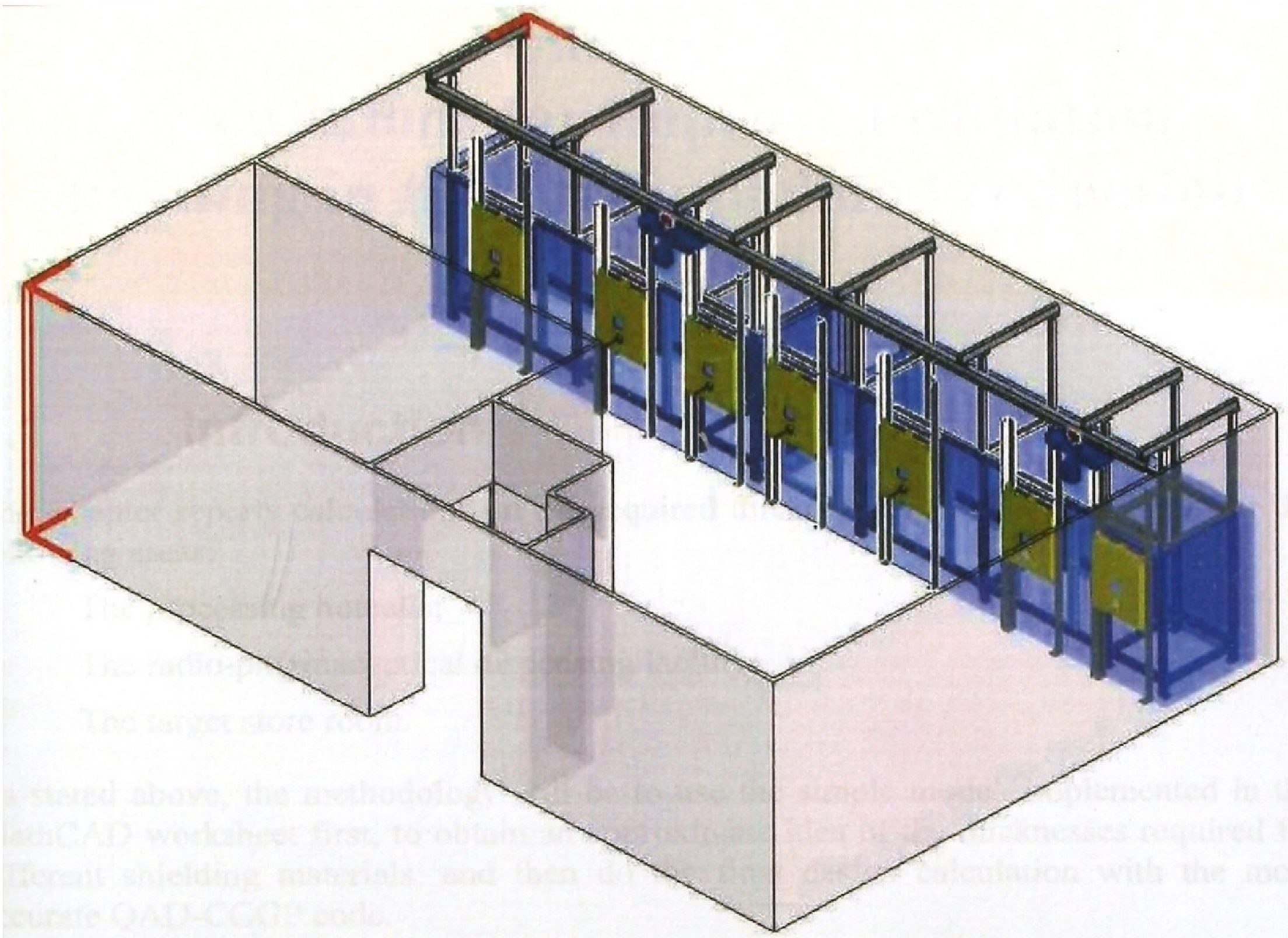
5.5 The target store-room facility

More targets, which will result in a higher radioactivity than ever before, will have to be parked inside the target store room. Decontamination workers will still have to spend up to 12 hours per year cleaning the tracks inside this room. The job of technicians loading new targets into target holders is also done in this room. Shielding in the target store room will clearly have to be upgraded, because it has been shown in Chapter 4 that the present shield performance is wholly inadequate.

5.6 The dispensing facility for radioactive pharmaceuticals

Dedicated dispensing hotcells will have to be built to replace the existing insufficiently shielded flow-cabinets. These hotcells should have front-mounted vertical sliding doors. The required thickness of these shielding doors will be calculated in Chapter 6.

Figure 5.1 is an early design sketch for the new hotcells in the new radio-pharmaceutical dispensing laboratory (McDonagh, 2003).



NWU
LIBRARY

Figure 5.1: *Sketch of planned new hotcells in the planned new radio-pharmaceutical dispensing laboratory.*

5.7 Summary

Calculations must be done to find materials and material thicknesses that will ensure that:

- The processing hotcell facility;
- The radio-pharmaceutical dispensing facility;
- The target store room;

are well-shielded and do not pose an unacceptable risk to workers in the Radionuclide Production Group of *iThemba LABS*.

The task of the scientist designing radiation shielding is to specify materials and their thicknesses; detailed mechanical design work is always left to professional mechanical designers.

Chapter 6
Calculations for improved radiation shielding in the Radionuclide Production Facility

6.1 Introduction

This chapter reports calculations on the required thickness of shielding material, for the following areas:

- The processing hotcells;
- The radio-pharmaceutical dispensing facility;
- The target store room.

As stated above, the methodology will be to use the simple model, implemented in the MathCAD worksheet first, to obtain an approximate idea of the thicknesses required for different shielding materials, and then do the final design calculation with the more accurate QAD-CGGP code.

6.2. Shield design for the processing hotcells

Key assumptions

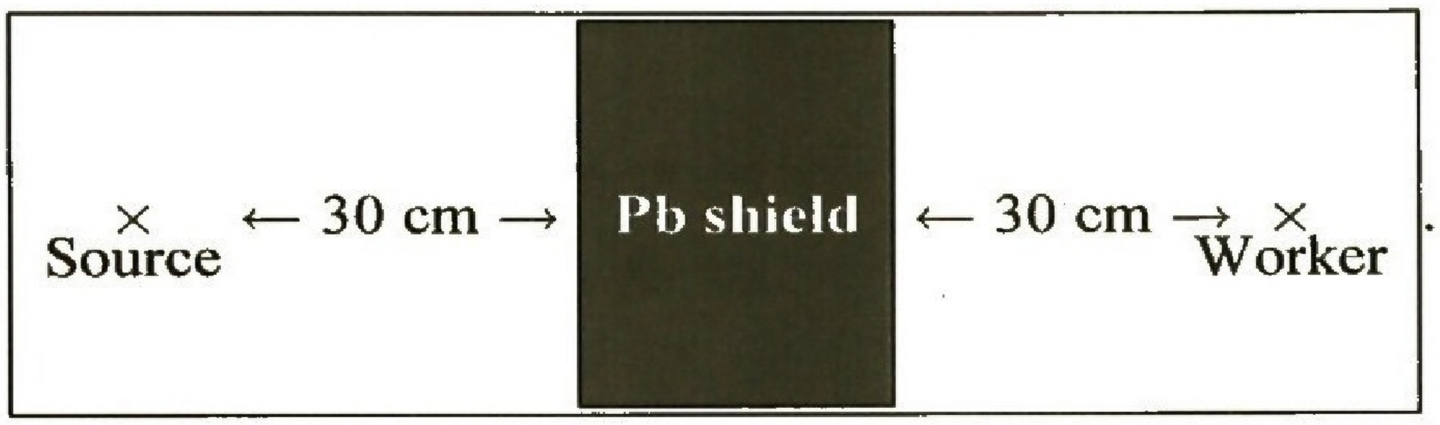
The key assumptions are:

- Design-base dose for hotcell work: 2 mSv per year.
- Maximum realistic staytime for hotcell work: 200 hours per year in front of a hotcell.
- Maximum realistic activity inside a hotcell: equivalent to 10 Ci ^{22}Na.

Shield thickness calculation using a MathCAD worksheet

A motivation for using 10 Ci ^{22}Na as the source term per hotcell, was developed in Chapter 2. As in Chapter 4, it is assumed that this activity is located 30 cm away from the inside surface of the Pb shield on the front side of the hotcell, and that the body of

the radiation worker is located 30 cm outside the outer surface of the hotcell.



Shield performance criteria were developed in Chapter 4. According to Equation (4.4), the maximum tolerable dose rate in front of a hotcell containing the maximum realistic activity of 10 Ci ^{22}Na, is 10 μSv/h.

The results of using the MathCAD worksheet to calculate required shielding thicknesses, are summarised in Table 6.1.

Table 6.1: *Transmitted dose rates and projected maximum realistic annual doses for various thicknesses of the lead shield separating workers in the Blue Area, from the radionuclides present inside a processing hotcell.*
Calculations with simple model implemented in MathCAD worksheet.

Pb Thickness (cm)	**Dose rate** (μSv/h)	**Projected annual dose** (mSv)
10	374	75
11	193	39
12	100	20
13	51	10
14	26	5
15	13.4	2.6
20	0.46	0.1

Lead shields are built from lead bricks that are 5 cm thick. Therefore shields can only jump in thickness by 5 cm jumps. It is clear that 10 cm Pb is inadequate, that 15 cm Pb is an ideal thickness, while 20 cm Pb will be a waste of lead and money because it will be overdesigned in terms of shielding.

Conclusion: Hotcells must have a front shielding wall of 15 cm lead. The shielding walls on the other 5 sides must preferably be 10 cm thick.

For 10 Ci ^{22}Na inside a hotcell, the dose rate in the Blue Area, 30 cm from the outer surface of the shielding wall, will depend on the thickness of the lead as shown in Figure 6.1.

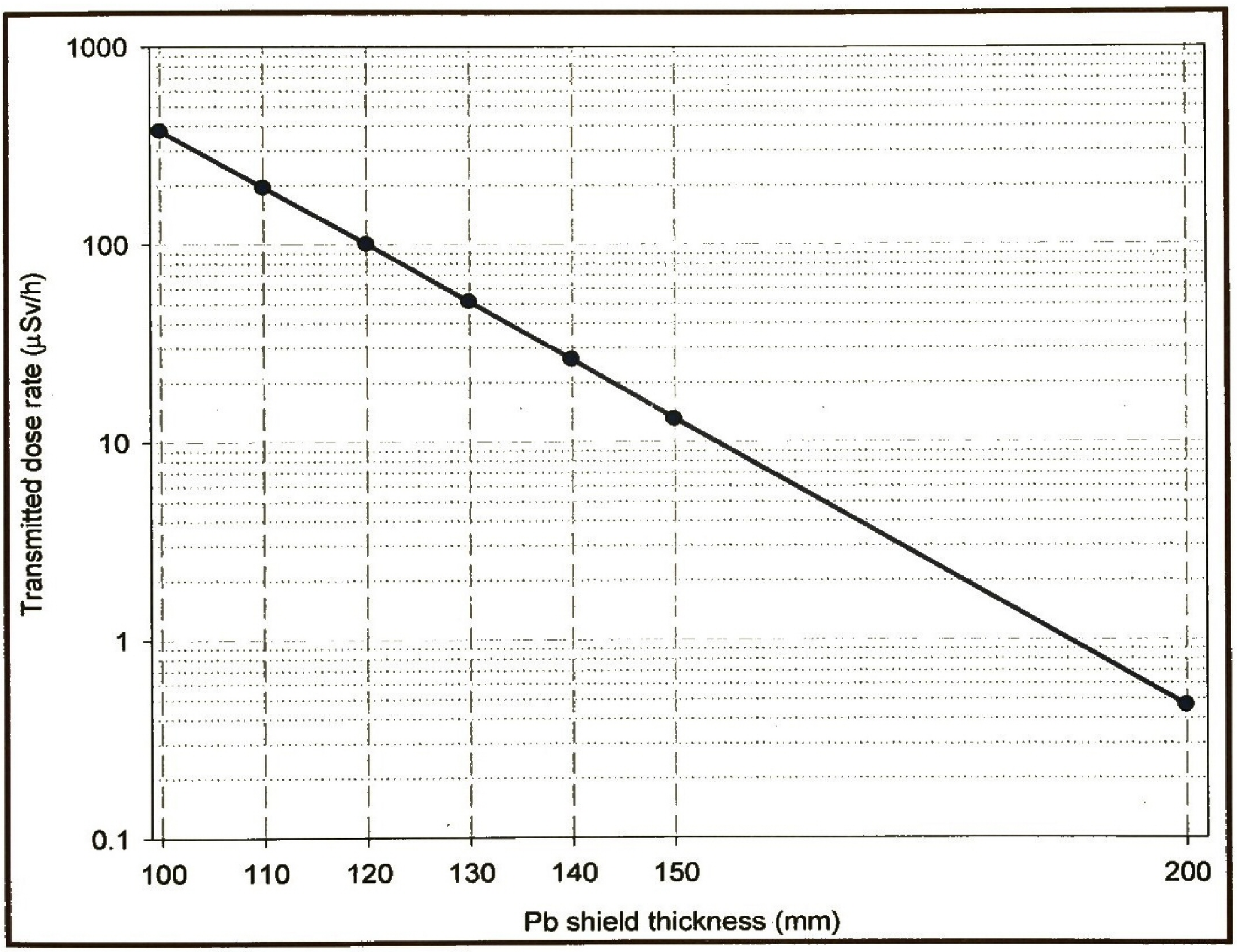


Figure 6.1: *Transmitted dose rate through various thicknesses of Pb shielding. Calculations with simple model implemented in a MathCAD worksheet.*

Projected maximum realistic doses to workers working in front of hotcells containing 10 Ci of ^{22}Na, are shown in Figure 6.2.

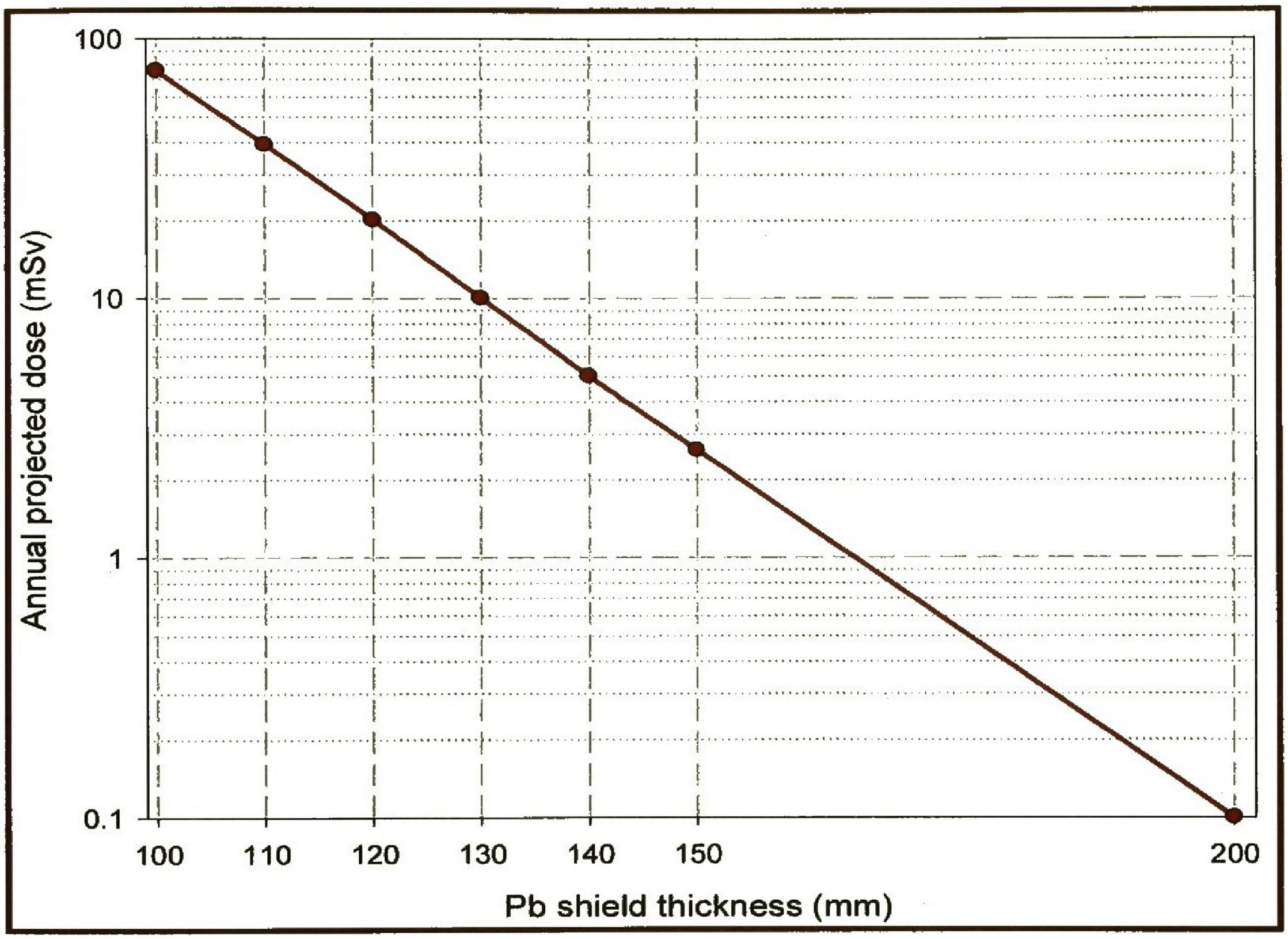


Figure 6.2: *Projected annual dose values to an operator spending 1 hour per day, 200 working days per year, 30 cm from hotcells in the Blue Area of the Radionuclide Production building, for different thicknesses of the Pb shielding wall, when there is 10 Ci ^{22}Na in the hotcell. Calculations were performed with the simple point-kernel radiation shielding model implemented in the MathCAD worksheet of Appendix A (page 86).*

Some facts and results of scientific interest, calculated with and displayed in the MathCAD worksheet of Appendix A (page 86), for the attenuation of 10 Ci ^{22}Na by a 15 cm Pb shield, are reported next.

The attenuation coefficient of the Pb as a function of photon energy is shown in Figure 6.3. The upward change in slope at photon energies above about 4 MeV, is the result of the strong contribution of pair production to the attenuation of photons in this energy region, by Pb. The high attenuation coefficient at low energies is the result of photo-electric absorption.

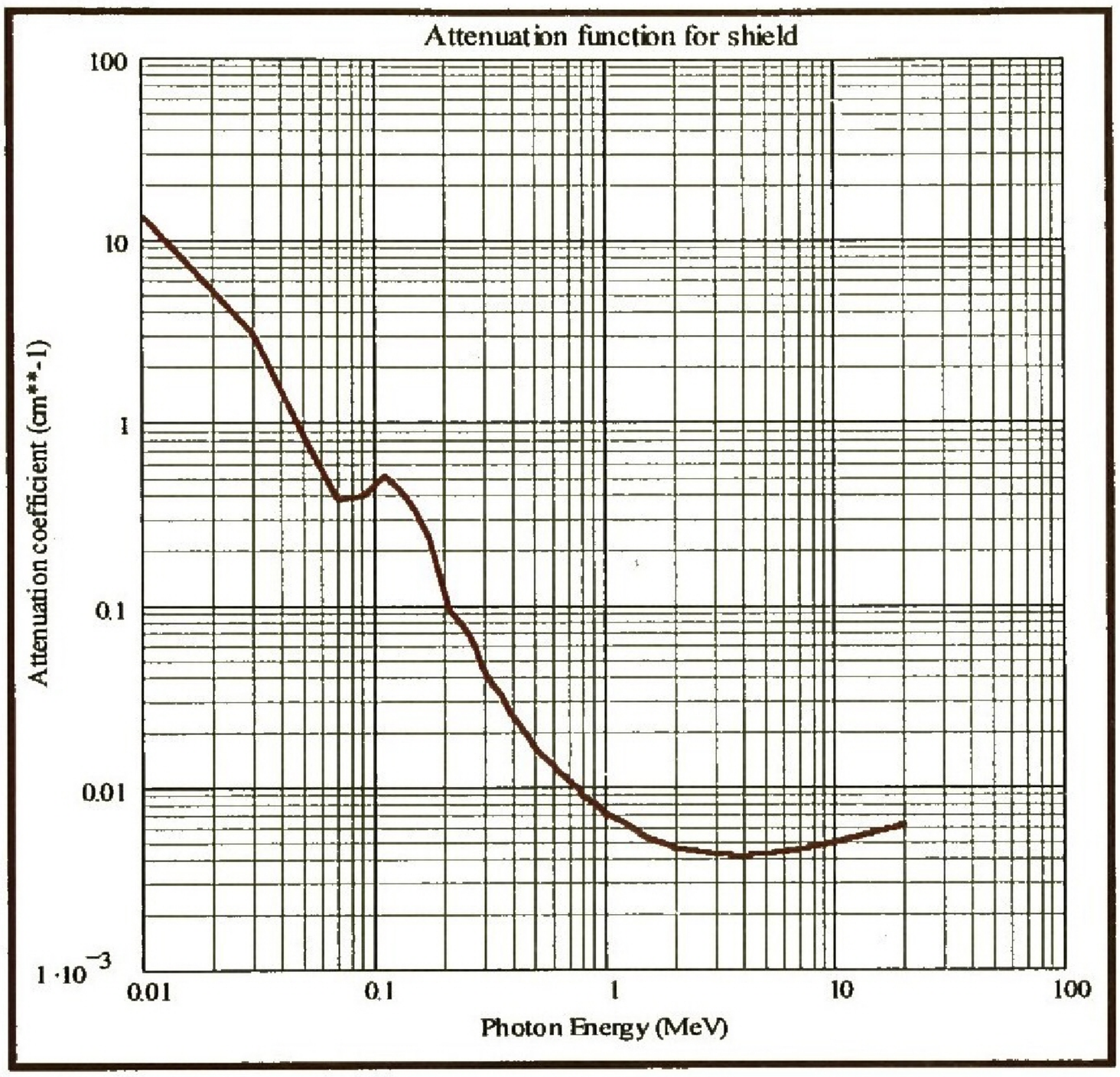


Figure 6.3: *Linear attenuation coefficient of lead as a function of incident photon energy.*

Some important properties of the biological harmfulness of ionising photons, as well as the properties of Pb as a shielding material, at the two photon energies radiated by ^{22}Na, as calculated with the MathCAD worksheet, is summarised in Table 6.2.

Table 6.2: *Important results reported by the MathCAD worksheet used to analyse the shielding requirements of the hotcells.*
Shielding material is Pb; Radionuclide is ^{22}Na.

	$E\gamma = 0.511$ MeV	$E\gamma = 1.27$ MeV
Fluence to Dose Conversion factor, R (ANS, 1991)	$9.33 \times 10^{-9} \left(\frac{\text{Sv/h}}{\text{cm}^{-2}\text{s}^{-1}}\right)$	$1.98 \times 10^{-8} \left(\frac{\text{Sv/h}}{\text{cm}^{-2}\text{s}^{-1}}\right)$
Linear Attenuation Coefficient, μ	$1.79\ \text{cm}^{-1}$	$0.69\ \text{cm}^{-1}$
Mean free path (mfp)	0.56 cm	1.45 cm
Number of mfp in 15 cm Pb	26.8	10.4
Dose buildup in 15 cm Pb	3.0	4.1

Figure 6.4 shows how the dose rate will decrease through the lead for a 15 cm thick lead shield.

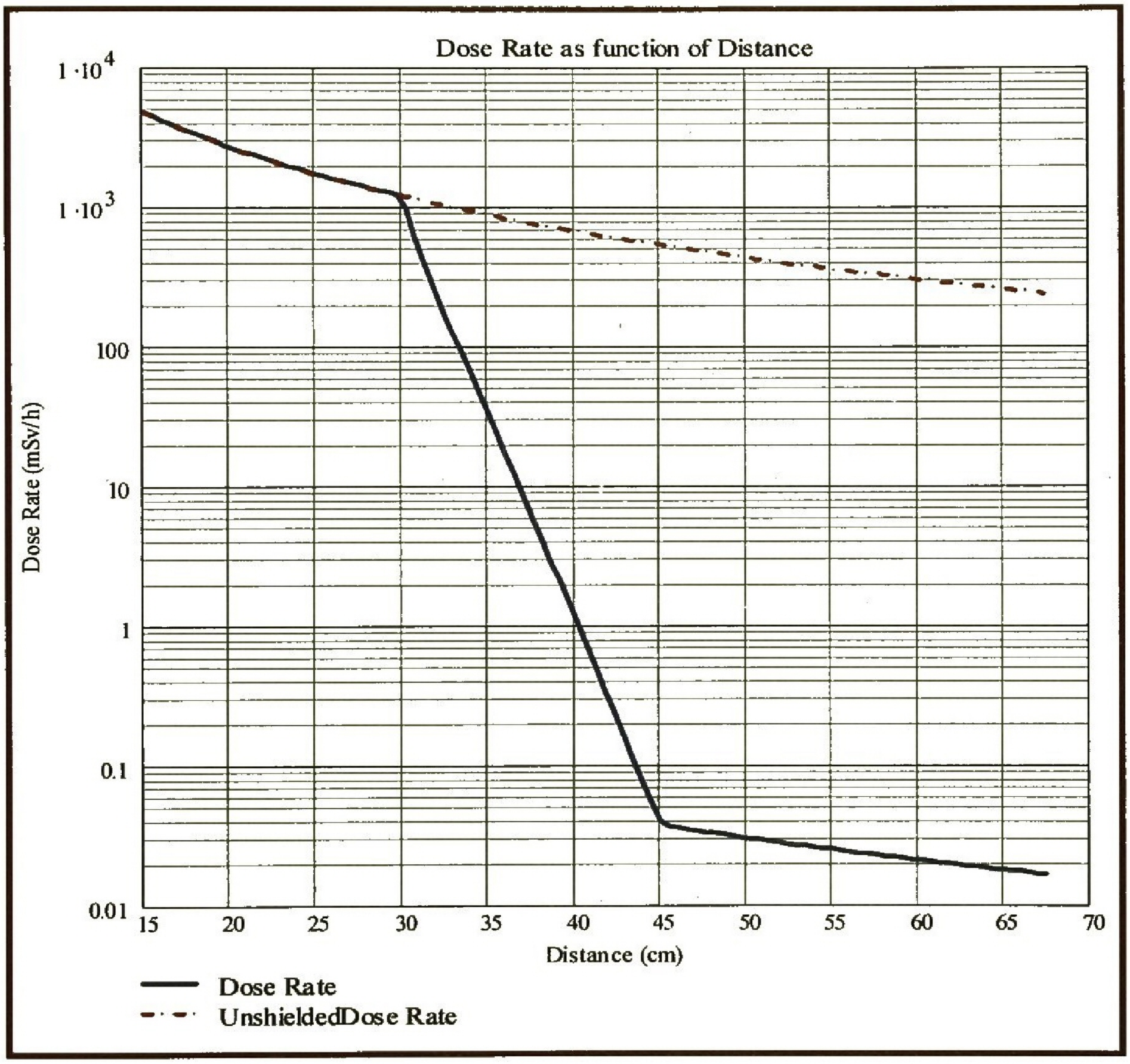


Figure 6.4: *Decrease of dose as photons radiated by ^{22}Na is attenuated by 15 cm Pb. The dotted line shows what the dose would have been if there was no shielding at all. The 15 cm thick Pb shield starts at 30 cm and stops at 45 cm. It is clear that the 15 cm Pb is a very effective shield. The dose attenuation factor is about 14 000.*

When the photons interact, they are not purely absorbed. Secondary photons are produced. These secondary photons also contribute to the dose rate. This contribution is known as "buildup." The MathCAD worksheet calculated the contribution of buildup to be as shown in Figure 6.5, and the dose attenuation factor as a function of shield thickness, as shown in Figure 6.6.

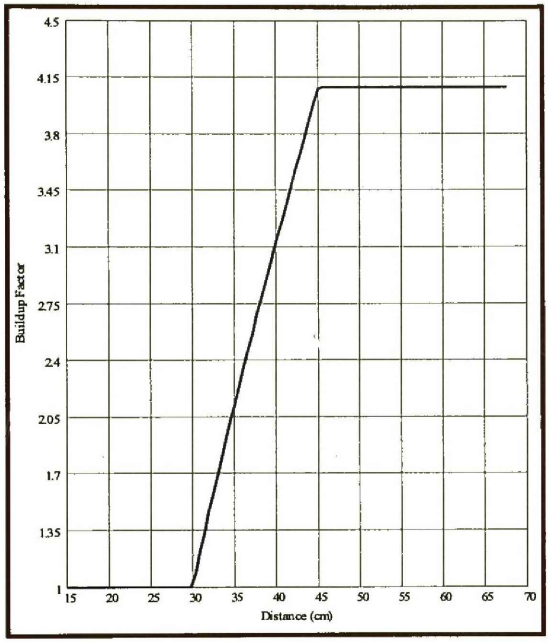


Figure 6.5: *Dose buildup as function of passage through shield. This represents the contribution of secondary photons to the dose-rate.*

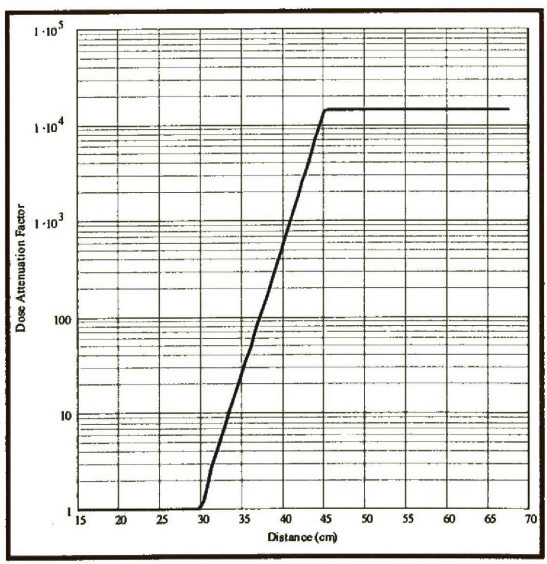


Figure 6.6: *The dose reduction factor of a Pb shield against the ionising photons radiated by ^{22}Na. A thickness of 15 cm Pb has a dose attenuation factor of 14 000, i.e. it reduces the transmitted dose rate by this factor.*

Shield design calculations for the processing hotcells with the code QAD-CGGP

The above calculations were done with a MathCAD worksheet which was developed "in-house." The code QAD-CGGP was subsequently used to perform accurate final design calculations and to ascertain whether the MathCAD scoping calculations were reasonably accurate. QAD-CGGP is internationally used and accepted as an accurate photon shielding code. The QAD-CGGP input data set is for the processing hotcell shield design calculation, is shown in Table 6.3.

Table 6.3: *QAD-CGGP input data set for the processing hotcell shield design calculation.*

```
iThemba LABS Processing Hotcell Shield Design Calculation
10  10   10   3   2   1   2   0  0  3  1  0  0  0  0  0
3.7E+11 0.0 0.0 0.0 0.0 0.0 0.0
  0.000E+00   1.000E-01   2.000E-01   3.000E-01   4.000E-01   5.000E-01
  6.000E-01   7.000E-01   8.000E-01   9.000E-01   1.000E+00
  0.000E+00   2.000E-01   4.000E-01   6.000E-01   8.000E-01   1.000E+00
  1.200E+00   1.400E+00   1.600E+00   1.800E+00   2.000E+00
  0.000E+00   6.283E-01   1.257E+00   1.885E+00   2.513E+00   3.142E+00
  3.770E+00   4.398E+00   5.027E+00   5.655E+00   6.283E+00
   0    0          Hotcell shielding calculation
RPP    1   -9999.0   +9999.0   -9999.0   +9999.0   -9999.0   +9999.0
RPP    2   -9990.0   +9990.0   -9990.0   +9990.0   -9990.0   +9990.0
RCC    3       0.0       0.0       0.0       0.0       0.0      +2.0
                 1.0
RPP    4      -50.0      +50.0      -70.0      +30.0       0.0    +100.0
RPP    5      -60.0      +60.0      -80.0      +45.0     -10.0    +110.0
END
Z01   10      +1      -2
Z02   10      +2      -3      -4      -5
Z03   10      +3
Z04   10      +4      -3
Z05   10      +5      -4      -3
END
1     2   3    4     5
0  1000   1    1     2
99    7    8     82
LEAD ABS
1.03E-3   2.58E-4    0.00
0.0       0.0       11.35
1.27      0.511
0.999     1.8292
1.983E-8  9.331E-9
0.0  0.0
_0.5-1.3
```

_1.27	_1.116	_0.511				
pho/(cm2.s)			Sv/h			w/g
0.0	0.0	20.0	1	0	0	0
0.0	0.0	22.0	1	0	0	0
0.0	0.0	25.0	1	0	0	0
0.0	0.0	26.0	1	0	0	0
0.0	0.0	27.0	1	0	0	0
0.0	0.0	28.0	1	0	0	0
0.0	0.0	29.0	1	0	0	0
0.0	0.0	30.0	1	0	0	0
0.0	0.0	31.0	1	0	0	0
0.0	0.0	32.0	1	0	0	0
0.0	0.0	33.0	1	0	0	0
0.0	0.0	34.0	1	0	0	0
0.0	0.0	35.0	1	0	0	0
0.0	0.0	36.0	1	0	0	0
0.0	0.0	37.0	1	0	0	0
0.0	0.0	38.0	1	0	0	0
0.0	0.0	39.0	1	0	0	0
0.0	0.0	40.0	1	0	0	0
0.0	0.0	41.0	1	0	0	0
0.0	0.0	42.0	1	0	0	0
0.0	0.0	43.0	1	0	0	0
0.0	0.0	44.0	1	0	0	0
0.0	0.0	45.0	1	0	0	0
0.0	0.0	46.0	1	0	0	0
0.0	0.0	50.0	1	0	0	0
0.0	0.0	55.0	1	0	0	0
0.0	0.0	60.0	1	0	0	0
0.0	0.0	65.0	1	0	0	0
0.0	0.0	70.0	1	0	0	0
0.0	0.0	75.0	1	0	0	0
0.0	0.0	0.0	-1	0	0	0

Table 6.4 summarises and compares the numerical results obtained with the MathCAD and QAD-CGGP calculations. It can be concluded that the calculations with the MathCAD worksheet are reasonably accurate, but tend to underestimate the transmitted dose rate by up to a factor 3. The MathCAD worksheet also gives lower dose buildup values than QAD-CGGP. It is important that final designs must, accordingly, always be performed with an internationally acceptable, benchmarked code such as QAD-CGGP.

Table 6.4: *Dose rates in and outside hotcell with wall thickness of 15 cm calculated with a MathCAD worksheet and with the code QAD-CGGP. Dose buildup calculated with QAD-CGGP.*

Distance from Source (cm)	**Dose Rate (QAD-CGGP)** (μSv/h)	**Dose Rate (MathCAD)** (μSv/h)	**Dose Buildup**
20.00	2.7×10^6		1.00
25.00	1.74×10^6		1.00
26.00	1.61×10^6		1.00
28.00	1.39×10^6		1.00
29.00	1.29×10^6		1.00
30.00	1.21×10^6	1.21×10^6	1.00
32.00	3.34×10^5	2.36×10^5	1.95
34.00	9.80×10^4	6.24×10^4	2.62
35.00	5.33×10^4	3.25×10^4	2.94
36.00	2.88×10^4	1.68×10^4	3.23
38.00	8.21×10^3	4.43×10^3	3.80
39.00	4.44×10^3	2.26×10^3	4.08
40.00	2.29×10^3	1.14×10^3	4.35
42.00	632	292	4.88
44.00	173	74	5.42
45.00	90	37	5.69
46.00	87	36	5.69
50.00	73	30	5.69
55.00	61	25	5.69
70.00	37	15	5.69
75.00	33	13	5.69

The dose rate as a function of the distance from the source, calculated with QAD-CGGP, is given in Figure 6.7.

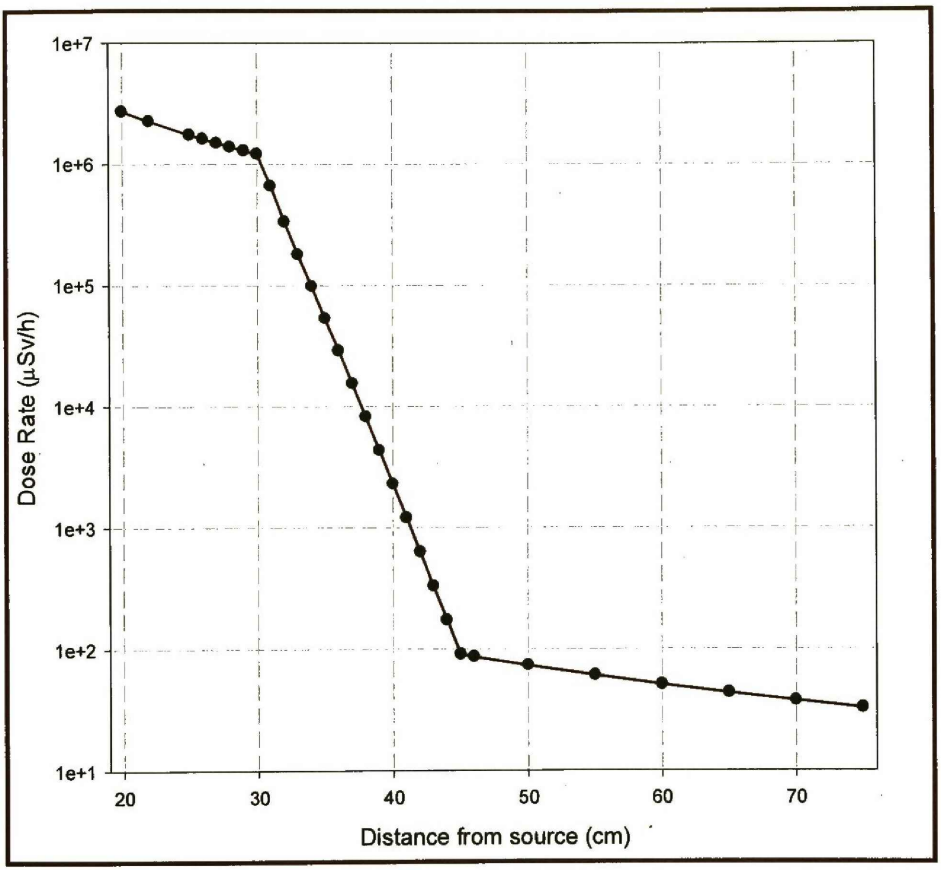


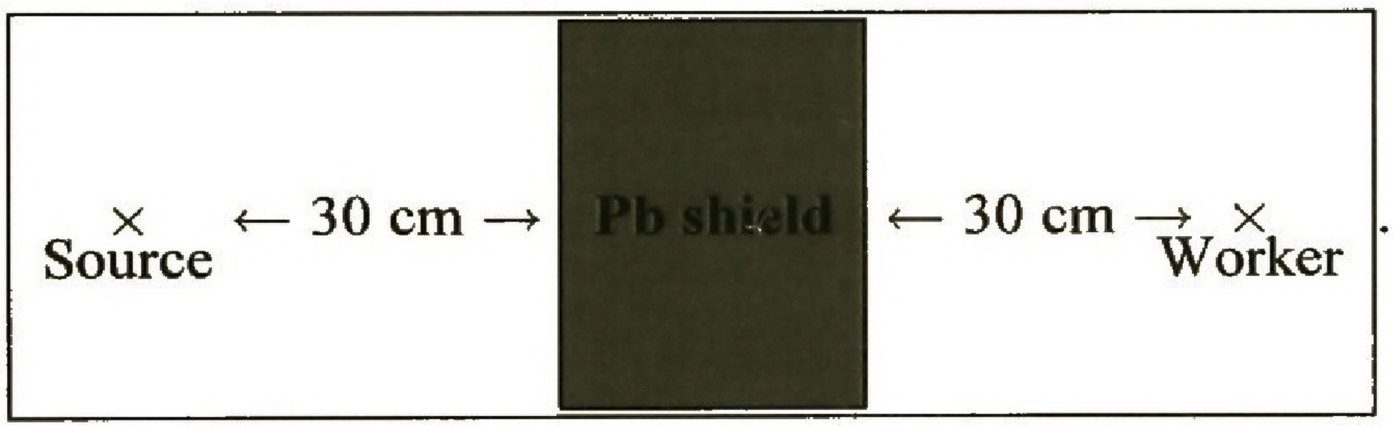
Figure 6.7: *Dose rates at different distances from the source inside the hotcell, calculated with QAD-CGGP. The lead wall thickness is 15 cm. It starts at 30 cm and ends at 45 cm from the source.*

It is concluded that the thickness of the front side of the processing hotcell shielding wall that protects workers from the source inside, must be 15 cm Pb. The other 5 sides of the hotcell box, should have wall thicknesses of 10 cm — the present thicknesses of these other walls are 5 cm each, and this should be upgraded to 10 cm to prevent excessive radiation dose rates. The required thickness of these other 5 walls is lower than the 15 cm required for the front wall, because human occupancy is considerably lower in these other 5 directions, and because the rear side of the hotcells face into the Red Area of the Radionuclide Production building, where higher dose rates are tolerated than in the Blue Area, into which the front sides of the hotcells face.

6.3 Shield design calculations for the Radio-pharmaceutical dispensing laboratory

Design goals

A motivation for using 1 Ci ^{22}Na as the maximum realistic source term per hotcell in the pharmaceutical dispensing laboratory, was developed in Chapter 2. It was assumed that this activity is located 30 cm away from the inside surface of the Pb shield on the front side of the hotcell, and that the body of the radiation worker is located 30 cm outside the outer surface of the hotcell.



Shield performance criteria were developed in Chapter 4; Equation (4.4) was used to set the criterion that 10 μSv/h would be the maximum tolerable dose rate in front of a dispensing hotcell containing the maximum realistic activity of 1 Ci ^{22}Na.

Shield design calculations for the Radio-pharmaceutical dispensing laboratory, using the MathCAD worksheet

The dose rates calculated with the MathCAD worksheet are summarised in Table 6.5. It can be concluded that the hotcell doors in the radio-pharmaceutical dispensing laboratory must have a shielding thickness of 10 cm lead, while the shielding walls on the other 5 sides of these hotcells must be 5 cm Pb.

Table 6.5: *Transmitted dose rates and projected maximum realistic annual doses for various thicknesses of the lead shield separating workers from the radionuclides present inside a hotcell in the radiopharmaceutical dispensing laboratory. The assumed activity in the hotcell is 1 Ci ^{22}Na.*

Pb Thickness (cm)	Dose rate (μSv/h)	Projected annual dose (mSv)
5	940 μSv/h	190
7	190 μSv/h	38
10	37 μSv/h	7
12.5	7 μSv/h	1.4
15.0	1.3 μSv/h	0.26

Shield design calculations for the Radio-pharmaceutical dispensing laboratory, using the code QAD-CGGP

The above calculations were done with a MathCAD worksheet developed "in-house." The code QAD-CGGP was subsequently used to perform accurate final design calculations and to verify that the scoping calculations performed with the MathCAD worksheet, were reasonably accurate. QAD-CGGP is internationally used and accepted as an accurate photon shielding code.

The QAD-CGGP input data set use for this calculation, was very similar to the one listed in Table 6.3 on page 72, so that it is not necessary to reproduce it.

Table 6.6 lists the dose rates calculated with QAD-CGGP. As before, results calculated with QAD-CGGP are about 2 to 3 times higher than the dose rates obtained with the MathCAD worksheet.

Table 6.6: *Dose rates in and around radiopharmaceutical hotcell, calculated with QAD-CGGP.*

Distance from source (cm)	Dose Rate (μSv/h)	Dose Buildup	
20	271157	1.0	
25	173703	1.0	
29	129152	1.0	
30	120697	1.0	← Shield starts
31	65915	1.6	
32	33353	2.0	
33	17934	2.3	
34	9797	2.6	
35	5333	2.9	
36	2880	3.2	
37	1542	3.5	
38	821	3.8	
39	435	4.1	
40	229	4.3	← Shield ends
41	218	4.3	
45	181	4.3	
50	147	4.3	
55	121	4.3	
60	102	4.3	
65	87	4.3	
70	75	4.3	← Operator's body
75	65	4.3	

The dose rate as a function of the distance from the source, is illustrated in Figure 6.8, which again corresponds well with the MathCAD results.

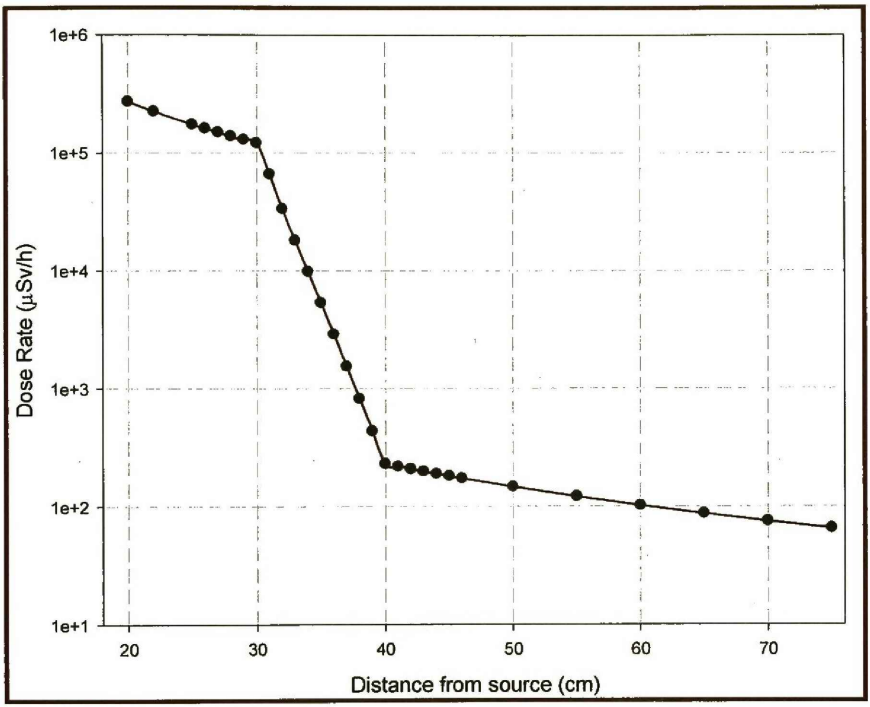


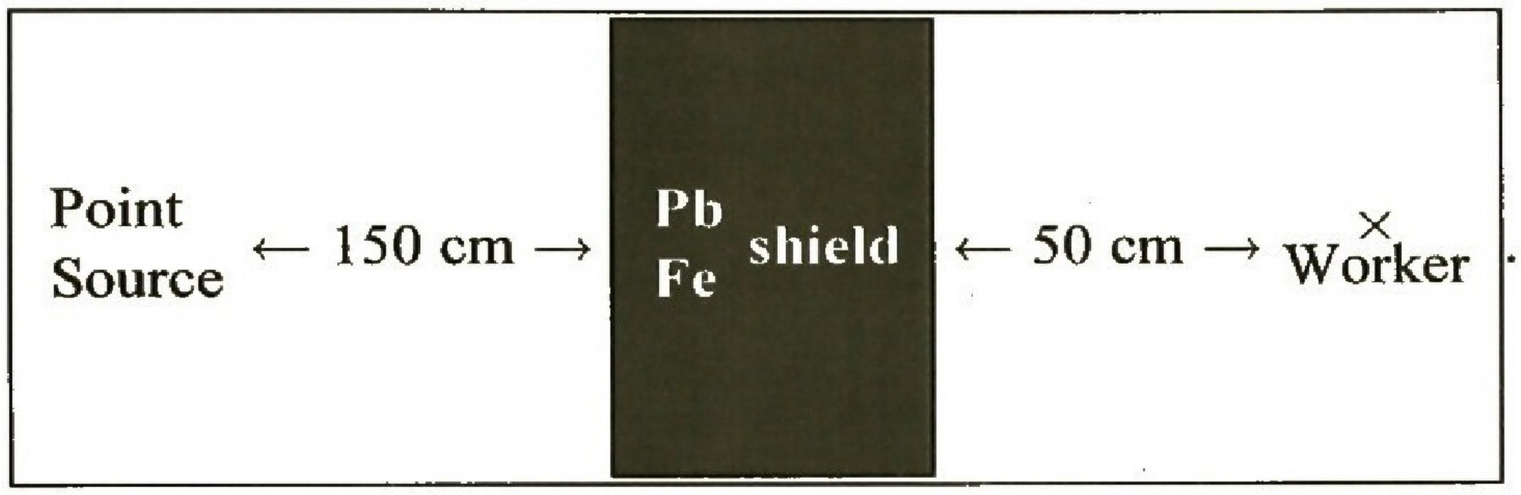
Figure 6.8: *Dose rates at different distances from the source inside the radio-pharmaceutical hotcell. Calculation with QAD-CGGP. The lead wall thickness is 10 cm. It starts at 30 cm and ends at 40 cm from the source.*

6.4 Shield design calculations for the Target Store room

Approximate shield design calculations for the Target Storage room, using a MathCAD worksheet

A motivation for using 100 Ci ^{22}Na as the source term inside the target store shield, was developed in Chapter 2. In Chapter 4, it was assumed that this activity is located at a point 150 cm from the inside surface of the shielding walls, and that the body of the radiation worker cleaning the tracks in this room, is located 50 cm outside the outer

surface of the shielding wall.



Shield performance criteria were developed in Chapter 4. It was calculated on page 47 that 80 μSv/h is the maximum tolerable dose rate outside the shielding around the target carousel containing the maximum realistic activity of 100 Ci ^{22}Na. Table 6.7 gives dose rates around the source if lead shielding is used. Table 6.8 gives the dose rates around the source if steel shielding is used.

Table 6.7: *Transmitted dose rates and projected maximum realistic annual doses for various thicknesses of the lead shield separating workers in target store room, from the radionuclides present inside the targets in the carousel wheel.*

Pb Thickness (cm)	**Dose rate** (μSv/h)	**Projected annual dose** (mSv)
10	415	5
15	16	0.2
20	0.6	0.007

Table 6.8: *Transmitted dose rates and projected maximum realistic annual doses for various thicknesses of steel shield separating workers in target store room, from the radionuclides present inside the targets in the carousel wheel.*

Steel Thickness (cm)	**Dose rate** (μSv/h)	**Projected annual dose** (mSv)
15	1900	23
20	290	3.5
25	43	0.5

The provisional MathCAD calculations indicate that one must either use 15 cm of Pb or 25 cm of steel as local shielding around the target store wheel in the target store room. Concrete can not be used, because there is no available space for the required concrete shield thickness.

The above MathCAD calculations are not satisfactory. The main reason is that the assumption of a point source at the centre of the volume bounded by the shielding walls, is inaccurate, so that it is necessary to run the code QAD-CGGP to be able to simulate the source-shield-geometry more accurately.

Accurate shield design calculations for the Target Storage room, using the code QAD-CGGP

The assumption of a point source for the irradiated targets, is very simplistic and inaccurate. The QAD-CGGP input data set shown in Table 6.9 models the source region as a cylinder with height 10 cm and radius 50 cm. The 100 Ci ^{22}Na is assumed to be spread uniformly throughout this volume, and the absorption of ionising photons inside the target material is ignored. The gap between the outer surface of the target carousel and the inside surface of the shielding walls is taken as 10 cm — this choice is based on a quick visual inspection. Input data set for calculation with 30 cm Fe as shield:

Table 6.9: *QAD-CGGP input data set for the target storeroom shield design calculation.*

```
iThemba LABS Target Store Room Shielding: Fe 30 cm
100  100  100  4   3   1   2   0  0  3  1  0  0  0  0  0
3.7E+12 0.0 0.0 0.0 0.0 0.0 0.0
   0.000E+00   5.000E-01   1.000E+00   1.500E+00   2.000E+00   2.500E+00
   3.000E+00   3.500E+00   4.000E+00   4.500E+00   5.000E+00   5.500E+00
   6.000E+00   6.500E+00   7.000E+00   7.500E+00   8.000E+00   8.500E+00
   9.000E+00   9.500E+00   1.000E+01   1.050E+01   1.100E+01   1.150E+01
   1.200E+01   1.250E+01   1.300E+01   1.350E+01   1.400E+01   1.450E+01
   1.500E+01   1.550E+01   1.600E+01   1.650E+01   1.700E+01   1.750E+01
   1.800E+01   1.850E+01   1.900E+01   1.950E+01   2.000E+01   2.050E+01
   2.100E+01   2.150E+01   2.200E+01   2.250E+01   2.300E+01   2.350E+01
   2.400E+01   2.450E+01   2.500E+01   2.550E+01   2.600E+01   2.650E+01
   2.700E+01   2.750E+01   2.800E+01   2.850E+01   2.900E+01   2.950E+01
   3.000E+01   3.050E+01   3.100E+01   3.150E+01   3.200E+01   3.250E+01
   3.300E+01   3.350E+01   3.400E+01   3.450E+01   3.500E+01   3.550E+01
   3.600E+01   3.650E+01   3.700E+01   3.750E+01   3.800E+01   3.850E+01
   3.900E+01   3.950E+01   4.000E+01   4.050E+01   4.100E+01   4.150E+01
   4.200E+01   4.250E+01   4.300E+01   4.350E+01   4.400E+01   4.450E+01
   4.500E+01   4.550E+01   4.600E+01   4.650E+01   4.700E+01   4.750E+01
   4.800E+01   4.850E+01   4.900E+01   4.950E+01   5.000E+01
   0.000E+00   1.000E-01   2.000E-01   3.000E-01   4.000E-01   5.000E-01
   6.000E-01   7.000E-01   8.000E-01   9.000E-01   1.000E+00   1.100E+00
   1.200E+00   1.300E+00   1.400E+00   1.500E+00   1.600E+00   1.700E+00
   1.800E+00   1.900E+00   2.000E+00   2.100E+00   2.200E+00   2.300E+00
   2.400E+00   2.500E+00   2.600E+00   2.700E+00   2.800E+00   2.900E+00
   3.000E+00   3.100E+00   3.200E+00   3.300E+00   3.400E+00   3.500E+00
   3.600E+00   3.700E+00   3.800E+00   3.900E+00   4.000E+00   4.100E+00
   4.200E+00   4.300E+00   4.400E+00   4.500E+00   4.600E+00   4.700E+00
   4.800E+00   4.900E+00   5.000E+00   5.100E+00   5.200E+00   5.300E+00
   5.400E+00   5.500E+00   5.600E+00   5.700E+00   5.800E+00   5.900E+00
   6.000E+00   6.100E+00   6.200E+00   6.300E+00   6.400E+00   6.500E+00
   6.600E+00   6.700E+00   6.800E+00   6.900E+00   7.000E+00   7.100E+00
   7.200E+00   7.300E+00   7.400E+00   7.500E+00   7.600E+00   7.700E+00
   7.800E+00   7.900E+00   8.000E+00   8.100E+00   8.200E+00   8.300E+00
   8.400E+00   8.500E+00   8.600E+00   8.700E+00   8.800E+00   8.900E+00
   9.000E+00   9.100E+00   9.200E+00   9.300E+00   9.400E+00   9.500E+00
   9.600E+00   9.700E+00   9.800E+00   9.900E+00   1.000E+01
   0.000E+00   6.283E-02   1.257E-01   1.885E-01   2.513E-01   3.142E-01
   3.770E-01   4.398E-01   5.027E-01   5.655E-01   6.283E-01   6.912E-01
   7.540E-01   8.168E-01   8.796E-01   9.425E-01   1.005E+00   1.068E+00
   1.131E+00   1.194E+00   1.257E+00   1.319E+00   1.382E+00   1.445E+00
   1.508E+00   1.571E+00   1.634E+00   1.696E+00   1.759E+00   1.822E+00
   1.885E+00   1.948E+00   2.011E+00   2.073E+00   2.136E+00   2.199E+00
   2.262E+00   2.325E+00   2.388E+00   2.450E+00   2.513E+00   2.576E+00
   2.639E+00   2.702E+00   2.765E+00   2.827E+00   2.890E+00   2.953E+00
   3.016E+00   3.079E+00   3.142E+00   3.204E+00   3.267E+00   3.330E+00
   3.393E+00   3.456E+00   3.519E+00   3.581E+00   3.644E+00   3.707E+00
   3.770E+00   3.833E+00   3.896E+00   3.958E+00   4.021E+00   4.084E+00
```

```
 4.147E+00   4.210E+00   4.273E+00   4.335E+00   4.398E+00   4.461E+00
 4.524E+00   4.587E+00   4.650E+00   4.712E+00   4.775E+00   4.838E+00
 4.901E+00   4.964E+00   5.027E+00   5.089E+00   5.152E+00   5.215E+00
 5.278E+00   5.341E+00   5.404E+00   5.466E+00   5.529E+00   5.592E+00
 5.655E+00   5.718E+00   5.781E+00   5.843E+00   5.906E+00   5.969E+00
 6.032E+00   6.095E+00   6.158E+00   6.220E+00   6.283E+00
  0    0          Target Storeroom Shielding
RPP    1   -9999.0   +9999.0   -9999.0   +9999.0   -9999.0   +9999.0
RPP    2   -9990.0   +9990.0   -9990.0   +9990.0   -9990.0   +9990.0
RCC    3       0.0       0.0       0.0       0.0       0.0     +10.0
              +50.0
RPP    4     -60.0     +60.0     -60.0     +60.0       0.0     +100.0
RPP    5     -90.0     +90.0     -90.0     +90.0       0.0     +100.0
END
Z01   10      +1      -2
Z02   10      +2      -3      -4      -5
Z03   10      +3
Z04   10      +4      -3
Z05   10      +5      -4      -3
END
1      2    3    4     5
0   1000    1    1     3
99     7           8       26        82
IRON ABS
1.03E-3    2.58E-4     0.00      0.00
0.00       0.00        0.00     11.35
0.00       0.00        7.86      0.00
1.27       0.511
0.999      1.8292
1.983E-8   9.331E-9
0.0  0.0
_0.5-1.3
_1.27   1.116   _0.511
_pho/(cm2.s)        Sv/h          w/g
0.0    0.0    20.0        1    0   0   0
0.0    0.0    25.0        1    0   0   0
0.0    0.0    30.0        1    0   0   0
0.0    0.0    40.0        1    0   0   0
0.0    0.0    50.0        1    0   0   0
0.0    0.0    55.0        1    0   0   0
0.0    0.0    59.0        1    0   0   0
0.0    0.0    60.0        1    0   0   0
0.0    0.0    61.0        1    0   0   0
0.0    0.0    62.0        1    0   0   0
0.0    0.0    63.0        1    0   0   0
0.0    0.0    64.0        1    0   0   0
0.0    0.0    65.0        1    0   0   0
0.0    0.0    66.0        1    0   0   0
0.0    0.0    67.0        1    0   0   0
0.0    0.0    68.0        1    0   0   0
0.0    0.0    69.0        1    0   0   0
0.0    0.0    70.0        1    0   0   0
0.0    0.0    71.0        1    0   0   0
0.0    0.0    72.0        1    0   0   0
0.0    0.0    73.0        1    0   0   0
0.0    0.0    74.0        1    0   0   0
0.0    0.0    75.0        1    0   0   0
0.0    0.0    76.0        1    0   0   0
0.0    0.0    77.0        1    0   0   0
0.0    0.0    78.0        1    0   0   0
0.0    0.0    79.0        1    0   0   0
0.0    0.0    80.0        1    0   0   0
0.0    0.0    81.0        1    0   0   0
0.0    0.0    82.0        1    0   0   0
0.0    0.0    83.0        1    0   0   0
0.0    0.0    84.0        1    0   0   0
0.0    0.0    85.0        1    0   0   0
0.0    0.0    86.0        1    0   0   0
0.0    0.0    87.0        1    0   0   0
0.0    0.0    88.0        1    0   0   0
0.0    0.0    89.0        1    0   0   0
0.0    0.0    90.0        1    0   0   0
0.0    0.0    91.0        1    0   0   0
0.0    0.0    95.0        1    0   0   0
0.0    0.0   100.0        1    0   0   0
0.0    0.0   150.0        1    0   0   0
0.0    0.0     0.0       -1    0   0   0
```

The dose rates obtained with the QAD-CGGP calculation are summarised in Table 6.10. Direct comparison with MathCAD worksheet results is not meaningful, because the source geometries differ greatly.

Table 6.10: *Dose rates calculated with QAD-CGGP for two thicknesses of Pb shields and two thicknesses of Fe shields around the target store room carousel.*

Distance (cm)	Dose rate 15 cm Pb (μSv/h)	Dose rate 20 cm Pb (μSv/h)	Dose rate 20 cm Fe (μSv/h)	Dose rate 30 cm Fe (μSv/h)
20	2.16E+07	2.16E+07	2.16E+07	2.16E+07
30	2.03E+07	2.03E+07	2.03E+07	2.03E+07
40	1.78E+07	1.78E+07	1.78E+07	1.78E+07
50	1.11E+07	1.11E+07	1.11E+07	1.11E+07
59	5.21E+06	5.21E+06	5.20E+06	5.20E+06
60	4.91E+06	4.91E+06	4.90E+06	4.90E+06
61	2.44E+06	2.44E+06	4.42E+06	4.42E+06
62	1.17E+06	1.17E+06	3.37E+06	3.37E+06
63	6.04E+05	6.04E+05	2.40E+06	2.40E+06
64	3.17E+05	3.17E+05	1.64E+06	1.64E+06
65	1.67E+05	1.67E+05	1.11E+06	1.11E+06
66	8.73E+04	8.73E+04	7.41E+05	7.41E+05
67	4.57E+04	4.57E+04	4.94E+05	4.94E+05
68	2.38E+04	2.38E+04	3.29E+05	3.29E+05
69	1.24E+04	1.24E+04	2.19E+05	2.19E+05
70	6.45E+03	6.45E+03	1.46E+05	1.46E+05
71	3.35E+03	3.35E+03	9.75E+04	9.75E+04
72	1.74E+03	1.74E+03	6.53E+04	6.53E+04
73	9.06E+02	9.06E+02	4.37E+04	4.37E+04
74	4.71E+02	4.71E+02	2.93E+04	2.93E+04
75	2.45E+02	2.45E+02	1.96E+04	1.96E+04
76	2.40E+02	1.28E+02	1.32E+04	1.32E+04
77	2.36E+02	6.64E+01	8.85E+03	8.85E+03
78	2.31E+02	3.45E+01	5.95E+03	5.95E+03
79	2.27E+02	1.80E+01	3.99E+03	3.99E+03
80	2.22E+02	9.35E+00	2.68E+03	2.68E+03
81	2.18E+02	9.20E+00	2.63E+03	1.80E+03
82	2.14E+02	9.04E+00	2.57E+03	1.21E+03
83	2.10E+02	8.89E+00	2.52E+03	8.11E+02
84	2.06E+02	8.74E+00	2.47E+03	5.44E+02
85	2.02E+02	8.59E+00	2.42E+03	3.65E+02
86	1.99E+02	8.45E+00	2.37E+03	2.44E+02
87	1.95E+02	8.31E+00	2.33E+03	1.64E+02
88	1.91E+02	8.17E+00	2.28E+03	1.10E+02
89	1.88E+02	8.04E+00	2.24E+03	7.34E+01
90	1.84E+02	7.91E+00	2.20E+03	4.91E+01
91	1.81E+02	7.78E+00	2.15E+03	4.82E+01
95	1.69E+02	7.29E+00	2.00E+03	4.52E+01
100	1.55E+02	6.74E+00	1.83E+03	4.17E+01
150	7.54E+01	3.43E+00	8.63E+02	2.09E+01

The dose rates calculated by QAD-CGGP are illustrated in Figure 6.9

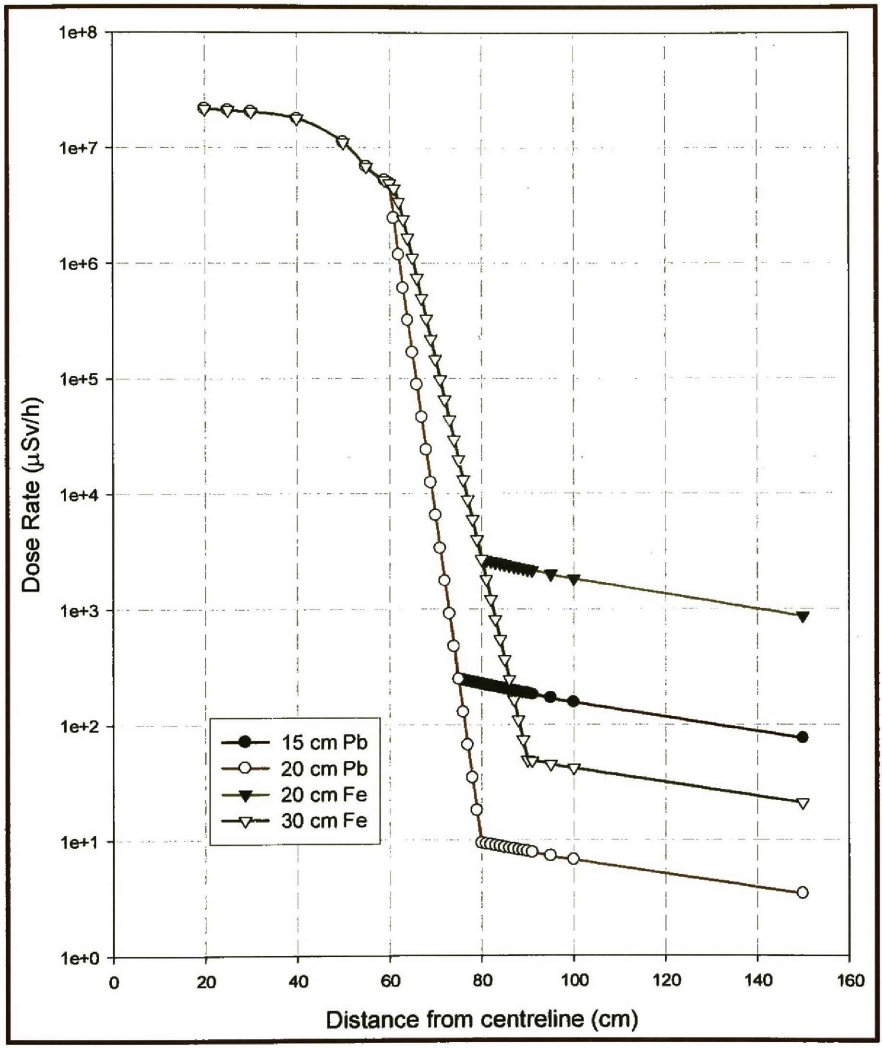


Figure 6.9: *Results of shield design calculation for the target store room. Two thicknesses of Pb shielding and 2 thicknesses of Fe shielding, are considered.*

On page 47 it was calculated that 80 μSv/h was the maximum tolerable dose rate outside the shielding in the target store room. From Figure 6.9 and Table 6.10, it follows that it is necessary to use 20 cm Pb or 30 cm steel as shielding material for the total activity of 100 Ci ^{22}Na assumed to be present in the irradiated targets kept in the storage wheel in the target store room.

-

Chapter 7
Conclusions and recommendations

In this chapter, conclusions and recommendations are made for the investigation.

Conclusions

The aim of this study was to evaluate and redesign radiation shielding in the radionuclide production facility of iThemba LABS. It was found that there are shields in the radionuclide production facility of iThemba that do not adequately protect workers against ionising radiation. To identify the inadequate shields, dose rates outside existing shields were measured; existing shields were then modelled with (1) a MathCAD worksheet, and (2) the point-kernel shielding code QAD-CGGP.

It was found that there are several areas where upgrading of facilities are required. Calculations were performed to determine the materials and thicknesses required to provide adequate radiation shielding. Initial scoping calculations were performed with a MathCAD worksheet. The improved shield designs were then verified and finalised with calculations using the internationally used and accepted code QAD-CGGP. The radiation shielding provided by the shields with the stipulated materials and thicknesses, will ensure that personnel doses are kept ALARA — As Low As Reasonably Achievable.

It is believed that this project has contributed significantly to radiation protection at *iThemba LABS.*

Recommendations

Shielding in the processing hotcells, the target store room and the radiopharmaceutical dispensing laboratory of the Radionuclide Production facilities at *iThemba LABS* are inadequate. Combinations of shielding materials and thicknesses that will ensure adequate radiation protection, have been obtained. The management of the Radionuclide Production Group of *iThemba LABS* is advised to implement the shield redesigns recommended in this work, as soon as possible, in the interest of maintaining personnel exposures to ionising radiation as ALARA.

-

Appendix A:
MathCAD worksheet for simple point-kernel shielding calculations

Point kernel shielding calculations for a point source

Worksheet compiled by:
Johann van Rooyen
johanvr@tlabs.ac.za
+27-82-829-8734

Problem specification

Shield_Material ≡ "Pb"

Buildup_Material ≡ "Pb"

Shield_Thickness := 15·cm

Starting z-coordinate of the shield relative to the source at the origin:

$Shield_1 := 30cm$

Calculate z-coordinate of exterior surface of shield:

$Shield_2 := Shield_1 + Shield_Thickness$ $\quad Shield_2 = 45\,cm$

Radionuclide source: Radionuclide := Na_22

Reference activity of source on reference date: $Act_0 := 10 \cdot Ci$

Specify reference date in vector format (year, month, day):

$$Reference_date := \begin{pmatrix} 2003 \\ 07 \\ 22.5 \end{pmatrix} \qquad Today := \begin{pmatrix} 2003 \\ 07 \\ 22.5 \end{pmatrix}$$

Reference_date := Today

Actions

Go to Number Mean Free Paths (mu*x)

Go to Health GP BU Formalism

Go to Value of BU

Go to Calculated Dose Rate

Go to Dose Rate Attenuation Factor

Hidden section starts here

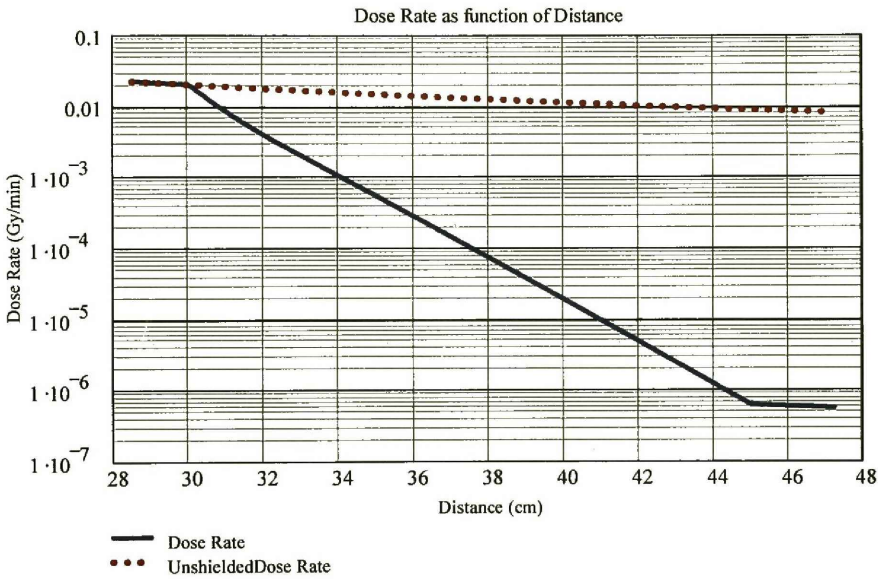


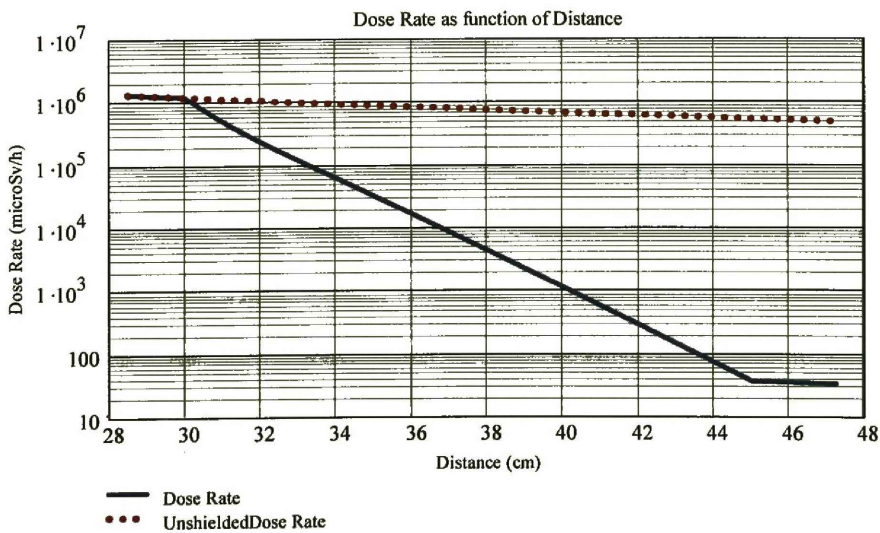




Hidden section ends here

Spatial dependence of dose-rate





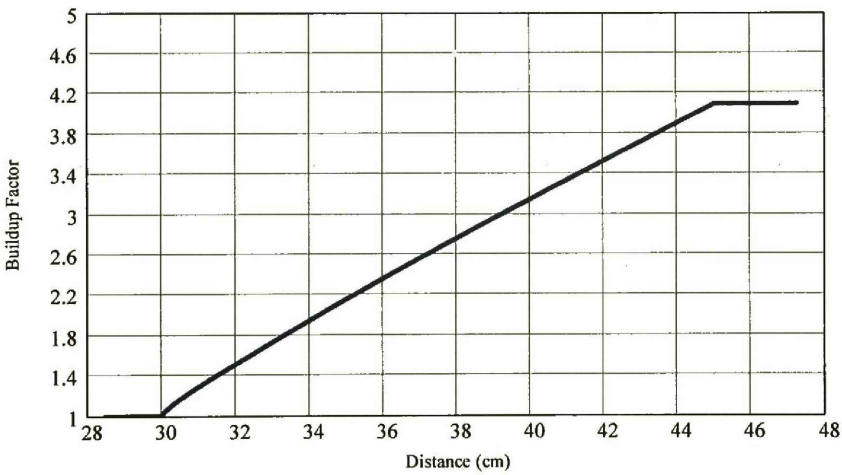
Dose rate calculation at specified radial coordinates

$\text{Dose_Rate}(\text{Shield}_2) = 6.2 \times 10^{-7}\ \text{Sv}\cdot\text{min}^{-1}$

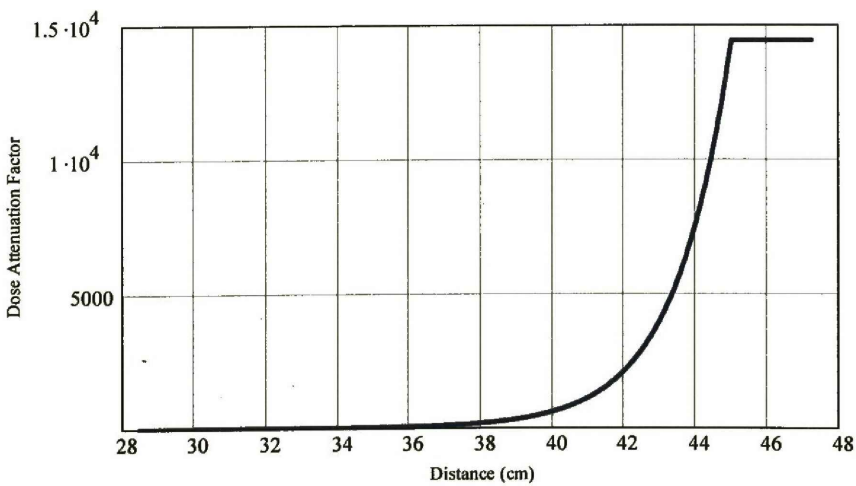
Go to List of Actions

Go to Problem Specs

Spatial dependence of build-up



Spatial dependence of dose attenuation factor



Dose attenuation factor

$$\text{Dose_Reduction_Factor}(r) := \left(\frac{\text{Dose_Rate}(r)}{\text{Dose_Rate_No_Shield}(r)}\right)^{-1}$$

For the shielding materia: $\text{Shield_Material} = \text{"Pb"}$

having a thickness of $\text{Shield_Thickness} = 15\,\text{cm}$

The dose reduction factor is: $\text{Dose_Reduction_Factor}(\text{Shield}_2) = 1.44 \times 10^4$

Go to List of Actions

Bibliography

AMERICAN NUCLEAR SOCIETY (ANS). 1991. *Neutron and gamma-ray fluence-to-dose Factors.* Report ANSI/ANS-6.1.1-1991. La Grange Park, Illinois: American Nuclear Society. 19 p.

CLOUGH, RL & SHALABY, SW. 1991. *Radiation Effects on Polymers.* Washington DC. American Chemical Society. ISBN 0-8412-2165-0.

ICRP. 1983. *ICRP Publication 38—Radionuclide Transformations: Energy and Intensity of Emissions.* Annals of the ICRP (International Commission on Radiological Protection. Pergamon Press.

ICRP. 1991. *ICRP Publication 60: The 1990 Recommendations of the ICRP.* Pergamon Press. ISBN 0-08-041144-4.

ICRP. 1997. *ICRP Publication 75: General Principles for the Radiation Protection of Workers.* Oxford, UK: Elsevier Science Ltd. ISBN 0-08-042741-3.

KNOLL, G.F. 2000. *Radiation Detection and Measurement.* New York: John Wiley & Sons. 802 p. ISBN 0-471-07338-5.

MACKRIEL, DEG. 2003. Personal communication by the supervisor of the decontamination workers on 2 September 2003.

MARMIER, P. & SHELDON, E. 1969. *Physics of Nuclei and Particles.* Vol. I. New York: Academic Press. 809 p. ISBN 0-12-473101-5.

McDONAGH, J. 2003. Personal communication. Design Office, Technical Services Group, *iThemba LABS,* PO Box 722, Somerset West, 7129, South Africa.

RSICC DATA LIBRARY DLC-119. 1986. *HILO86: 66 Neutron, 22 Gamma-Ray Group Cross Sections for Radiation Transport for Neutron Energies up to 400 MeV.* Radiation Safety Information Computational Center. Oak Ridge National Laboratory, USA.

RSICC CODE CCC-493. 1988. *QAD-CGGP: Point Kernel Code System for Neutron and Gamma-Ray Shielding Calculations Using the GP Buildup Factor.* Radiation Safety Information Computational Center, Oak Ridge National Laboratories, USA.

SHULTIS, JK & FAW, RE. 1996. *Radiation Shielding.* Upper Saddle River, NJ: Prentice Hall. ISBN 0-13-125691-2.

STEYN, GF. 2003a. Personal communication via e-mail received on 14 February 2003. Radionuclide Production Group (RPG), *iThemba LABS,* PO Box 722, Somerset West, 7129, South Africa.

STEYN, GF. 2003b. Personal communication via e-mail received on 11 March 2003. Radionuclide Production Group (RPG), *iThemba LABS,* PO Box 722, Somerset West, 7129, South Africa.

NWU
LIBRARY